

# The electrocatalysis of dioxygen reduction on transition metal chelates

**Citation for published version (APA):**

Putten, van der, A. M. T. P. (1986). *The electrocatalysis of dioxygen reduction on transition metal chelates*. [Phd Thesis 1 (Research TU/e / Graduation TU/e), Chemical Engineering and Chemistry]. Technische Universiteit Eindhoven. <https://doi.org/10.6100/IR255164>

**DOI:**

[10.6100/IR255164](https://doi.org/10.6100/IR255164)

**Document status and date:**

Published: 01/01/1986

**Document Version:**

Publisher's PDF, also known as Version of Record (includes final page, issue and volume numbers)

**Please check the document version of this publication:**

- A submitted manuscript is the version of the article upon submission and before peer-review. There can be important differences between the submitted version and the official published version of record. People interested in the research are advised to contact the author for the final version of the publication, or visit the DOI to the publisher's website.
- The final author version and the galley proof are versions of the publication after peer review.
- The final published version features the final layout of the paper including the volume, issue and page numbers.

[Link to publication](#)

**General rights**

Copyright and moral rights for the publications made accessible in the public portal are retained by the authors and/or other copyright owners and it is a condition of accessing publications that users recognise and abide by the legal requirements associated with these rights.

- Users may download and print one copy of any publication from the public portal for the purpose of private study or research.
- You may not further distribute the material or use it for any profit-making activity or commercial gain
- You may freely distribute the URL identifying the publication in the public portal.

If the publication is distributed under the terms of Article 25fa of the Dutch Copyright Act, indicated by the "Taverne" license above, please follow below link for the End User Agreement:

[www.tue.nl/taverne](http://www.tue.nl/taverne)

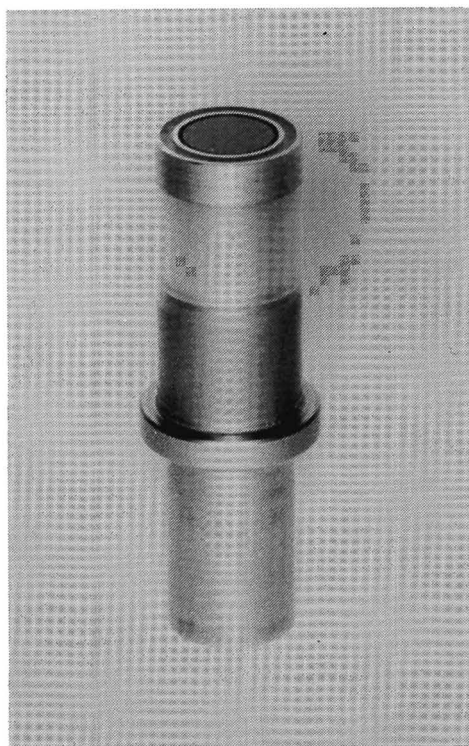
**Take down policy**

If you believe that this document breaches copyright please contact us at:

[openaccess@tue.nl](mailto:openaccess@tue.nl)

providing details and we will investigate your claim.

THE ELECTROCATALYSIS OF DIOXYGEN REDUCTION  
ON  
TRANSITION METAL CHELATES



ANDRE VAN DER PUTTEN

THE ELECTROCATALYSIS OF DIOXYGEN REDUCTION ON TRANSITION METAL CHELATES

Cover: a rotating ring-disc electrode with a pyrolytic graphite disc and platinum ring.



# THE ELECTROCATALYSIS OF DIOXYGEN REDUCTION ON TRANSITION METAL CHELATES

PROEFSCHRIFT

ter verkrijging van de graad van doctor aan  
de Technische Universiteit Eindhoven, op gezag  
van de rector magnificus, prof. dr. F.N. Hooge,  
voor een commissie aangewezen door het college  
van dekanen in het openbaar te verdedigen op  
vrijdag 19 december 1986 om 16.00 uur

door

ANDREAS MARTINUS THEODORUS PAULUS VAN DER PUTTEN

geboren te Helmond

Dit proefschrift is goedgekeurd door de promotoren:

Prof. E. Barendrecht

Prof. dr. J. Reedijk

copromotor: Dr. W. Visscher

*Aan mijn ouders.*

## Contents

page

1. The reduction of dioxygen and its application in fuel cells.	1
2. Short review of previous work on the reduction of dioxygen on transition metal chelates.	
2.1 Introduction	5
2.2 Activity	5
2.3 Selectivity	7
2.4 Stability	8
2.5 References	8
3. Methodology of the measurement of dioxygen reduction on transition metal chelates.	
3.1 Activity	11
3.2 Selectivity	15
3.3 Stability	15
3.4 Characterization	16
3.5 References	17
4. The cathodic reduction of dioxygen at cobalt phthalocyanine: Influence of electrode preparation on electrocatalysis.	
4.1 Introduction	18
4.2 Theoretical aspects	19
4.3 Experimental	20
4.4 Results and discussion	22
4.5 Conclusions	29
4.6 References	30
5. Dioxygen reduction on vacuum deposited and adsorbed transition metal phthalocyanine films.	
5.1 Introduction	31
5.2 Experimental	31
5.3 Results	32
5.4 Discussion	41
5.5 References	44
6. Redox potential and electrocatalysis of dioxygen reduction on transition metal chelates.	
6.1 Introduction	45
6.2 pH and thermodynamics of O <sub>2</sub> reduction	46
6.3 Experimental	47
6.4 Results	49
6.5 Discussion	52
6.6 Concluding remarks	54
6.7 References	
7. The four electron reduction of dioxygen to water on a planar dicobalt chelate.	56

8. Increased valence theory and the four-electron reduction of dioxygen to water.	
8.1 Introduction	62
8.2 Increased valence theory	63
8.3 Increased valence theory and O <sub>2</sub> adducts	66
8.4 Application of the increased valence theory to O <sub>2</sub> reduction on dimeric O <sub>2</sub> adducts	68
8.5 Concluding remarks	72
8.6 References	72
9. A new method of preparing a rotating ring-disc electrode for the study of carbon-supported catalysts.	
9.1 Introduction	74
9.2 Preparation technique	74
9.3 The hydrodynamic behaviour	76
9.4 Results of some preliminary experiments	77
9.5 Concluding remarks	80
9.6 References	81
10. Dioxygen reduction on pyrolyzed carbon-supported transition metal chelates.	
10.1 Introduction	82
10.2 Developed theories for activity enhancement	84
10.3 Experimental	86
10.4 Results	87
10.5 Discussion	91
10.6 References	94
11. Concluding remarks and outlines for future research.	95
Acknowledgements	99
List of symbols and abbreviations	100
Summary	102
Samenvatting	104
Curriculum vitae	106
Dankwoord	107

## Chapter 1 The reduction of dioxygen and its application in fuel cells.

The reduction of dioxygen is an important reaction occurring in fuel cells, devices in which the chemical energy of a fuel (hydrogen or hydrogen-rich gas) is directly converted into electrical energy<sup>1-3</sup>. The principle of the fuel cell was already described by Grove in 1839 and is most easily explained as reversed water electrolysis. According to reactions (1) and (2), hydrogen and dioxygen are combined to water. At the anode the fuel, in this case H<sub>2</sub>, is oxidized:



At the cathode, dioxygen is reduced:



Due to these spontaneously proceeding reactions a potential difference is developed over the electrodes, i.e. electricity is produced. Similar to a battery, this electricity is produced by means of electrochemical reactions; the difference is that a fuel cell can be operated as a continuous process; a battery - by definition - operates batchwise.

Contrary to the oxidation of hydrogen, O<sub>2</sub> reduction is a slow process. High current densities can only be obtained if suitable electrocatalysts and a special electrode configuration are used<sup>3</sup>. Therefore, fuel cells were not developed until the beginning of space travel. For this special purpose, price is relatively unimportant. Both for the oxidation and reduction reactions platinum was used as the catalyst<sup>3</sup>. In principle also batteries can be used as a current supply but this is unattractive due to their high weight and the occurrence of self discharge. Since the energy crisis of the early seventies, fuel cells are also considered for the large scale production of electricity. Fuel cells for terrestrial applications can be divided into three classes:

- low temperature fuel cells. The electrolyte consists of an aqueous solution of for instance phosphoric acid, sulphuric acid or potassium hydroxide. At the moment phosphoric acid fuel cells are commercially available<sup>4</sup>.
- molten carbonate fuel cells. The electrolyte is a mixture of lithium and potassium carbonate at ca. 650°C. This type of fuel cell is developed upto pilot plant scale<sup>4</sup>.
- high temperature fuel cells. The electrolyte consists of a mixture of yttrium and zirconium oxide at ca. 1000°C. This solid oxide is an excellent ionic conductor at these temperatures. This fuel cell is still in the laboratory phase<sup>4</sup>.

The major advantage of fuel cells, compared to conventional systems for producing electricity, is their high efficiency with which they convert chemical energy into electricity. In conventional devices like turbines, the chemical energy is first converted into heat and then into electricity. Under practical conditions, the efficiency of such a Carnot cycle is only about 40%<sup>4</sup>. Fuel cells avoid the Carnot cycle and much higher efficiencies (upto 65% for the molten carbonate cells) can be obtained. Other advantages are:<sup>5</sup>

- The conversion process is clean. Of course, if fossil fuels are used, impurities like sulfur also have to be removed because they poison the electrocatalyst, but since fuel cells have a higher efficiency, as a whole less pollution is released.
- The system is modular. Via series connections of separate fuel cell elements, so-called stacks with the desired voltage can be manufactured; the desired power can simply be realized by increasing the number of stacks.
- The system has a low noise production, allowing the in situ generation of electricity. The part of the chemical energy that is converted into heat can be used efficiently, because the heat is generated at the same location where it is needed.
- The system has a short response time. Moreover, the energy efficiency is virtually independent of the delivered power output. These properties make fuel cells very suitable for peak shaving and load levelling.

Whether fuel cells will be used for the large scale production of electricity, is largely a matter of prize. As a consequence only cheap fuels can be used like coal, fossil fuels, methanol or natural gas. In most cases the fuel will have to be processed first to a mixture of carbon oxides ( $\text{CO}$ ,  $\text{CO}_2$ ) and hydrogen, before it is supplied to the anode. In molten-carbonate and solid oxide fuel cells the temperature is so high that the electrochemical reactions proceed with sufficient rates. The cells are more a problem of materials science than of electrocatalysis. From an electrocatalytic point of view, low-temperature fuel cells are the most interesting. If carbon-containing fuels are used only acid electrolytes come into consideration. Cleaning the fuel from carbon oxides is technologically very difficult and even traces of these impurities will lead to carbonization of alkaline electrolytes with loss of activity. In acid media, the best studied electrocatalyst for the  $\text{O}_2$  reduction and the only one which has been used in practical systems is platinum. Due to its high prize and low availability, an alternative for this catalyst has to be found if this type of fuel cell is to be applied for utility

purposes<sup>4</sup>. An alternative was developed by looking at the way nature reduces dioxygen. Both the active centres of O<sub>2</sub>-transporting enzymes (like haemoglobin) and O<sub>2</sub>-reducing enzymes (like cytochrome c oxidase), contain porphyrin groups, a transition metal ion surrounded by four nitrogen atoms which are part of an aromatic organic skeleton. In 1965, Jasinski reported O<sub>2</sub> reduction on cobalt phthalocyanine<sup>6</sup>, a molecule that closely resembles the porphyrin structure. Indeed this molecule appeared to be a good catalyst for the reduction of dioxygen, although not as efficient as the enzymes nature uses. The source of the activity is the high interaction of O<sub>2</sub> with these molecules. The O-O bond is weakened and therefore more easily split. After this publication, a lot of work has been performed on transition metal macrocycles; a short review is given in chapter 2. The N<sub>4</sub> chelates of Fe and Co were found to be the most promising ones; therefore the work, described in this thesis is focussed on such species. A critical examination of the published data shows that the obtained results are to a large extent influenced by the electrode-preparation method. Most of the work has been performed using porous gas-diffusion electrodes. This method, however, has a drawback of rather ill-defined mass-transport properties. Electrocatalytic properties like activity, selectivity and stability are to a large extent influenced by the morphology of the electrode system, rather than the properties of the electrocatalyst itself. Well-defined mass-transport properties can be attained using the rotating ring-disc electrode technique (chapter 3). Moreover, contrary to gas-diffusion electrodes, this technique allows the determination of the selectivity: The reduction of O<sub>2</sub> not always proceeds to water as the final product; in some cases only hydrogen peroxide is formed.

The first approach therefore was to develop a well-defined electrode system, using the rotating ring-disc electrode technique, in order to find a system which enables a good characterization of the electrocatalyst, both in a qualitative and quantitative sense (chapters 4 and 5). In the case of irreversibly adsorbed monolayers, the activity of iron phthalocyanine (FePc), cobalt phthalocyanine (CoPc) and cobalt tetraazaannulene (CoTAA) was investigated as a function of the electrolyte pH. Since also the redox potentials of these chelates (i.e. the potential at which the central metal ion changes its valency) are a function of the solution pH, the relation between these redox potentials and the potential where O<sub>2</sub> reduction is occurring, was investigated (chapter 6).

One of the most interesting recent developments is the dicofacial dicobalt porphyrin of Collman and Anson<sup>7</sup>: two amide bridged cobalt porphyrins, with



the two Co centres at a distance of ca. 4 Å. While the corresponding monomers only yield hydrogen peroxide as reduction product, this dicobalt porphyrin reduces dioxygen directly to water in acid media. This unique selectivity is obtained because the O<sub>2</sub> molecule is able to adsorb on two Co atoms simultaneously. The O-O bond is even more weakened than in the case of monomeric adsorption. Chapter 7 shows that this condition can also be fulfilled by a planar dicobalt chelate, with two Co centres in the plane of the molecule.

A theoretical explanation for the behaviour of these dicobalt complexes with the aid of the "increased valence theory" is presented in chapter 8. The chapters 9-11 have a more technological importance. In practical fuel cells, the electrocatalyst is dispersed on a porous carbon support and processed to gas-diffusion electrodes. Early work had already shown that pyrolysis (heating in an inert atmosphere) improves both the stability and the activity of carbon-supported transition metal chelates. Nevertheless, there is still disagreement in the literature about the origin of this improvement. This disagreement appears to be related to ill-defined mass-transport properties, associated with use of gas-diffusion electrodes. Therefore, a method was developed to study carbon-supported catalysts with the rotating ring-disc technique. With this technique the effect of pyrolysis was investigated on Norit BRX supported FePc, CoPc, CoTAA and their metal-free analogues. Finally, in chapter 11 a number of concluding remarks and some outlines for future research are presented.

### References

1. W. Vielstich, "Fuel Cells", Wiley Interscience (1970).
2. J.O'M. Bockris, S. Srinivasan, "Fuel cells; Their Electrochemistry", McGraw Hill Book Company (1969).
3. K. Kordesch, "Brennstoffbatterien", Springer Verlag, Wien (1984).
4. "Assessment of Research Needs for Advanced Fuel Cells", U.S. Department of Energy Advanced Fuel Cell Working Group, 1984-85, edited by S.S. Penner, also published as Energy 11 (1986) 1.
5. "Handbook of Fuel Cell Performance", prepared by T.G. Benjamin, E.H. Camara and L.G. Marianowski, Institute of Gas Technology, Chicago, U.S.A. (1980).
6. R. Jasinski, J. Electrochem. Soc. 112 (1965) 526.
7. J.P. Collman, M. Marocco, P. Denisevich, C. Koval and F.C. Anson, J. Electroanal. Chem. 101 (1979) 117.

Chapter 2 Short review of previous work on the reduction of dioxygen on transition metal chelates.

2.1. Introduction

An extensive review of the work on the reduction of dioxygen on transition metal chelates up to 1981 has been published by van den Brink et al.<sup>1</sup>. In this chapter a survey of the most important conclusions of that work will be given, updated with more recent developments.

2.2. Activity

The most extensively studied chelates as O<sub>2</sub>-reduction catalysts are transition metal phthalocyanines (MePc), tetrasubstituted porphyrins (MeTRP) and dihydrodibenzotetraazaannulenes (MeTAA):

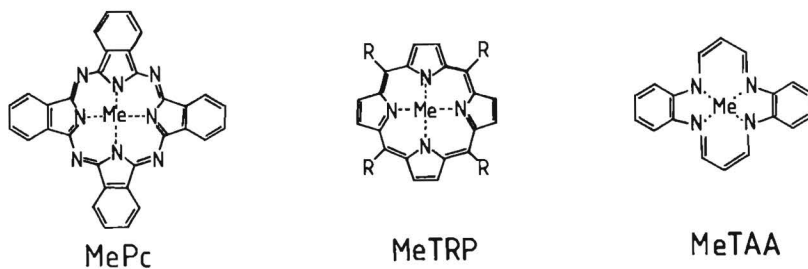


Fig. 2.1: Molecular structure of the most extensively studied chelates.

For the determination of the activity of the various complexes, different electrode-preparation techniques were used. Initially these studies were performed using porous electrodes<sup>2-4</sup>: the chelates are dispersed on a porous carbon support. Thereafter either slurry electrodes or gas-diffusion electrodes are manufactured. In the first case a stirred suspension is prepared from the carbon powder. Electrons are supplied via a feeder electrode: the O<sub>2</sub> is dissolved in the electrolyte and is transported to the catalyst via the liquid phase. In the latter case, the modified carbon is mixed with teflon as a binder and pressed onto a metal screen. The O<sub>2</sub> is supplied from the gas phase. The disadvantages of these electrode systems is that the transport of O<sub>2</sub> is ill-defined. This problem can be solved using more sophisticated hydrodynamic methods such as the rotating disc electrode (see chapter 3). In some cases the catalyst is applied to the disc as a paste<sup>5,6</sup>, but the obtained results are to a large extent influenced by the wetting behaviour of the electrode<sup>7</sup>. Alternatives are spraying of catalyst particles onto the disc<sup>8</sup>, electrophoretic deposition of carbon particles<sup>9</sup>, precipitation of the catalyst onto the disc through evaporation of a suitable solvent<sup>10,11</sup>,

vacuum deposition<sup>12,13</sup> or irreversible adsorption<sup>14,15</sup>. Recently, even more methods have been reported: incorporation into a (conducting<sup>16</sup>) polymer<sup>17,18</sup>, electrodeposition<sup>19</sup>, chemical modification<sup>20</sup> and in situ synthesis on a metal substrate<sup>21</sup>. Also chelates, dissolved in the electrolyte have been studied<sup>22-24</sup>.

Unfortunately, the various electrode-preparation techniques give rise to different results with respect to the activity: a good example is the comparison of cobalt phthalocyanine (its water-soluble sulphonate derivative) adsorbed on pyrolytic graphite<sup>14</sup>, with cobalt phthalocyanine, deposited in high loadings on active carbon<sup>3</sup>. In the first case, in acid media no current is observed at potentials higher than 300 mV vs. a reversible hydrogen electrode (RHE); in the second case the reduction starts at 900 mV vs. RHE. Although in a quantitative sense different results are obtained with the various electrode systems, some general conclusions with respect to the activity can be drawn:

- From the 3d transition metals, the  $N_4$  chelates of Fe and Co exhibit the highest activity<sup>3</sup>. Chelates with other hetero atoms like O and S were shown to be less active.
- With respect to the macrocyclic structure, TAA shows the highest activity followed by Pc and TRP<sup>3</sup>. Experiments with porous electrodes however, show that the effect of the ring structure is much less than that of the central metal ion and ligands.
- The activity is higher in alkaline than in acid solution.

These observations clearly show that the central metal ion is the catalytically active site.

For the description of the catalytic activity, different concepts have been developed. According to the MO theory, the origin of the activity is the strong interaction of  $O_2$  with the central metal ion, decreasing the O-O bond strength<sup>4</sup>. In a free transition metal ion, the five d-orbitals are degenerate, i.e. they have the same energy. Due to the presence of four nitrogen ligands and (possibly) the electrode surface supplying a fifth ligand, the levels will split. The position of the levels will depend on the ligand field strength and symmetry. The adsorption of  $O_2$  is explained with the formation of a  $\sigma$ -bond between a lone pair of the  $O_2$  molecule and the empty  $3d_z^2$  orbital, and back-bonding due to overlap of an empty  $\pi^*$  antibonding orbital of  $O_2$  with a filled  $3d_{xz}$  or  $3d_{yz}$  orbital. According to this description, a good catalyst should have an empty  $3d_z^2$  orbital and filled  $3d_{xz}$  and  $3d_{yz}$  orbitals. The strongest interaction of  $O_2$  will therefore be obtained with Fe(II), which fulfills both preconditions. In the case of Co(II) the interaction will be weaker since Co(II) has one electron in its  $3d_z^2$  orbital<sup>4</sup>. Different ligands

change the location of the energy levels of the 3d orbitals: with TAA the highest overlap between the 3d orbitals of the central metal ion and the molecular orbitals of  $O_2$  is obtained. A different model was developed by Ulstrup<sup>25</sup>. In this model, the transition of electrons from the electrode towards the  $O_2$  is improbable because the corresponding energy levels lie too far apart. The catalyst acts as a mediator, supplying intermediate levels, increasing the probability of electron transfer. A third description is that of redox catalysis, developed by Beck<sup>26</sup>. In this model, during  $O_2$  adsorption the central metal ion is oxidized, thereby reducing the  $O_2$  molecule. At the end of the catalytic cycle, the oxidized central metal ion is reduced to its initial state. Therefore, the observed  $O_2$  reduction is closely related to the redox potential of the central metal ion. Just like in gas-phase catalysis, this relation can be expressed as so-called volcano plots<sup>27,28</sup>: The activity will exhibit a maximum as a function of the redox potential of the central metal atom.

With respect to the mechanism of the  $O_2$  reduction, most authors assume that the rate determining step (RDS) is the formation of superoxide<sup>29,30</sup>:  $O_2 + e^- \rightarrow O_2^-$ . The standard electrode potential of this redox couple is  $-0.33$  V vs. normal hydrogen electrode (NHE). Since this redox process is pH independent, the reduction is likely more reversible in alkaline than in acid solution. Although this conclusion has been reported in the literature, in our view its importance has not been fully recognized.

### 2.3. Selectivity

The study of  $O_2$  reduction is complicated by the fact that  $O_2$  can be either directly reduced to  $H_2O$ , or to  $H_2O_2$ , which is the stable end product or is subsequently reduced to  $H_2O$ . Studies of the  $O_2$  reduction on noble metals like Au and Pt have shown that the selectivity is determined by the way the  $O_2$  is adsorbed on the catalyst<sup>31</sup>. If the  $O_2$  molecule interacts with only one metal atom (end-on or side-on adsorption), then (at least initially)  $H_2O_2$  is produced (Au); if the  $O_2$  molecule is adsorbed at two metal atoms (bridge adsorption), direct  $4e^-$  reduction to  $H_2O$  becomes possible (Pt). This model is corroborated by recent observations, viz. the effect of interatomic spacing<sup>32</sup>, underpotential deposited layers (UPD) of Pb<sup>33</sup>, Tl<sup>34</sup> or Bi<sup>35</sup> on Au, and  $O_2$  reduction at dicofacial dicobalt porphyrins<sup>36,37</sup>. A decrease of the interatomic Pt-Pt distance lowers the activation energy. This indicates that the optimum distance for bridge adsorption is not yet reached;

with pure Pt, this distance is too high <sup>32</sup>. In the presence of adsorbed Bi atoms on an Au single crystal <sup>35</sup>, O<sub>2</sub> was reduced to H<sub>2</sub>O instead of H<sub>2</sub>O<sub>2</sub> at pure Au or a surface, completely covered with Bi. This change in selectivity is explained with a bimetal bridge adsorption, i.e. the formation of Bi-O-O-Au adducts. The importance of bridge adsorption on transition metal complexes was shown by Collman and Anson <sup>36,37</sup>. They synthesized dicofacial dicobalt porphyrins, two Co porphyrin units linked so that the planar macrocycles are held in a face to face orientation. Complexes with different interplanar distances were synthesized showing that reduction to water only occurred if the two Co centres were located at a distance of ca. 4 Å, apparently to enable bridge adsorption of dioxygen <sup>38</sup>.

#### 2.4. Stability

For the application of transition metal chelates in fuel-cell electrodes, a good stability is of prime importance. Unfortunately, the most active Fe complexes are less stable than their Co analogues. The deterioration of the electrode performance can have various causes:

- degradation of the carbon support, or oxidation of the macrocyclic structure by H<sub>2</sub>O<sub>2</sub> or intermediately formed radicals;
- dissolution of the central metal ion due to hydrolysis <sup>39,40</sup>.

The most promising way of improving the stability of carbon-supported transition metal chelates is pyrolysis, i.e. heat treatment in an inert gas atmosphere <sup>3</sup>. With respect to the increase in stability there is agreement in the literature: during pyrolysis the most reactive parts of the chelates react with the carbon support and are no longer liable to irreversible oxidation. A more interesting phenomenon is that the pyrolysis not only increases the stability, but also the activity and selectivity. For the explanation of this phenomenon, conflicting opinions have been reported in the literature <sup>41-43</sup>. The increased selectivity results in a lower H<sub>2</sub>O<sub>2</sub> concentration in the pores of the catalyst and this also has a beneficial effect on the stability. Pyrolyzed cobalt tetramethoxyphenyl porphyrin has been shown to maintain its activity upto 10000 hours <sup>44</sup>.

#### 2.5. References

1. F. van den Brink, E. Barendrecht and W. Visscher, Recl. Trav. Chim. Pays-Bas 99 (1980) 253.
2. R. Jasinski, J. Electrochem. Soc. 112 (1965) 526.

3. H. Jahnke, M. Schönborn and G. Zimmermann, *Topics in current chemistry* 61 (1976) 133.
4. H. Alt, H. Binder and G. Sandstede, *J. Catal.* 28 (1973) 8.
5. A.J. Appleby and M. Savy, *Electrocatalysis on non metallic surfaces*. NBS special publication (1976) 455.
6. M.R. Tarasevich, K.A. Radiyschkina and S.I. Androuseva, *Bioelectrochem. Bioenergetics* 4 (1977) 18.
7. J.A.R. van Veen, *Electrochim. Acta* 27 (1982) 1403.
8. R.J. Brodd, V.Z. Leger, R.F. Scarr and A. Kozawa, *Electrocatalysis on non metallic surfaces*. NBS special publication (1976) 253.
9. M. Savy, P. Andro and C. Bernard, *Electrochim. Acta* 19 (1974) 403.
10. H. Behret, W. Clauberg and G. Sandstede, *Ber. Bunsenges. Phys. Chem.* 81 (1977) 54; *Z. Phys. Chem. NF* 113 (1978) 97.
11. K. Shigehara and F.C. Anson, *J. Phys. Chem.* 86 (1982) 2776.
12. M. Savy, C. Bernard and G. Magner, *Electrochim. Acta* 20 (1975) 383.
13. F. van den Brink, Thesis, Eindhoven University of Technology, Eindhoven (1981).
14. J. Zagal-Moya, Thesis, Case Western Reserve University, Cleveland (1978).
15. B. Simic-Glavaski, S. Zecevic and E. Yeager, *J. Electroanal. Chem.* 150 (1983) 469.
16. R.A. Bull, F.R. Fan and A.J. Bard, *J. Electrochem. Soc.* 130 (1983) 1636.
17. O. Hirabaru, T. Nakase, K. Hanabusa, J. Shirai, K. Takemoto and N. Hojo, *J. Chem. Soc., Chem. Comm.* (1983) 481.
18. D.A. Buttry and F.C. Anson. *J. Am. Chem. Soc.* 106 (1984) 59.
19. M. Yamana, R. Darby, H.P. Dhar and R.E. White, *J. Electroanal. Chem.* 152 (1983) 261.
20. M. Yamana, R. Darby and R.E. White, *Electrochim. Acta* 29 (1984) 329.
21. D. Wöhrle, R. Bannehr, B. Schumann and N. Jaeger, *Angew. Makromol. Chem.* 117 (1983) 103; *J. Mol. Catal.* 21 (1983) 255.
22. W. Beyer and F. von Sturm, *Angew. Chem.* 84 (1972) 154.
23. P.A. Forshey and T. Kuwana, *Inorg. Chem.* 22 (1983) 699.
24. N. Kobayashi and Y. Nishiyama, *J. Phys. Chem.* 89 (1985) 1167.
25. J. Ulstrup, *J. Electroanal. Chem.* 79 (1977) 191.
26. F. Beck, *Ber. Bunsenges. Phys. Chem.* 77 (1973) 353; *J. Appl. Electrochem.* 7 (1977) 239.
27. J.P. Randin, *Electrochim. Acta* 19 (1974) 83.
28. J.A.R. van Veen, *Ber. Bunsenges. Phys. Chem.* 85 (1981) 693.

29. D.T. Sawyer and E.T. Seo, *Inorg. Chem.* 16 (1977) 499.
30. E. Yeager, *Electrochim. Acta* 29 (1984) 1527.
31. P. Fischer and J. Heitbaum, *J. Electroanal. Chem.* 112 (1980) 231.
32. V. Jalan and E.J. Taylor, *J. Electrochem. Soc.* 130 (1983) 2299.
33. K. Jüttner, *Electrochim. Acta* 29 (1984) 1597.
34. R. Amadelli, N. Markovic, R. Adzic and E. Yeager, *J. Electroanal. Chem.* 159 (1983) 391.
35. S.M. Sayed, K. Jüttner, *Electrochim. Acta* 28 (1983) 1635.
36. J.P. Collman, M. Marocco, P. Denisevich, C. Koval and F.C. Anson, *J. Electroanal. Chem.* 101 (1979) 117.
37. J.P. Collman, P. Denisevich, Y. Konai, M. Marocco, C. Koval and F.C. Anson, *J. Am. Chem. Soc.* 102 (1980) 6027.
38. R.R. Durand Jr., C.S. Bencosme, J.P. Collman and F.C. Anson, *J. Am. Chem. Soc.* 105 (1983) 2710.
39. H. Meier, U. Tschirwitz, E. Zimmerhackl, W. Albrecht and G. Zeiler, *J. Phys. Chem.* 81 (1977) 712.
40. J. Blomquist, U. Helgeson, L.C. Moberg, L.Y. Johansson and R. Larsson, *Electrochim. Acta* 27 (1982) 1453.
41. J.A.R. van Veen and H.A. Colijn. *Ber. Bunsenges. Phys. Chem.* 85 (1981) 700.
42. G. Gruenig, K. Wiesener, S. Gamburgzev, I. Iliev and A. Kaisheva, *J. Electroanal. Chem.* 159 (1983) 155.
43. D.A. Scherson, S.L. Gupta, C. Fierro, E.B. Yeager, M.E. Kordesch, J. Eldridge, R.W. Hoffman and J. Blue, *Electrochim. Acta* 28 (1982) 1205.
44. V.S. Bagotskii, M.R. Tarasevich, O.A. Levina, K.A. Radyushkina and S.I. Andruseva, *Dokl. Akad. Nauk SSSR* 233 (1977) 889.

Chapter 3 Methodology of the measurement of dioxygen reduction on transition metal chelates.

3.1. Activity

In catalysis, the normal procedure for studying a new catalyst is measurement of its activity, selectivity and stability, in combination with a characterization of the catalyst under similar conditions. The activity can be expressed as the increase in rate of a reaction in the presence of the catalyst. The catalyst does not change the thermodynamics of a reaction: it increases the reaction rate by lowering the activation energy. In catalysis, the parameter that is varied is the temperature. The temperature influences the thermodynamics of the reaction by changing the Gibbs free energy  $\Delta G = \Delta H - T\Delta S$ . For a reaction  $A \rightarrow B$  with positive  $\Delta H$  and  $\Delta S$ , the temperature determines whether the reaction can proceed to the right or to the left. In electrocatalysis, the potential is the equivalent of the temperature in catalysis. For a redox system  $ox + ne \rightleftharpoons red$ , the potential determines whether the occurring reaction will be a reduction or an oxidation. For the rate (= current) of electrochemical reactions the following equation has been derived:

$$i = i_0 \left[ \frac{C_{red}^{\sigma}}{C_{red}^s} \exp \frac{(1-\alpha) F\eta}{RT} - \frac{C_{ox}^{\sigma}}{C_{ox}^s} \exp \frac{-\alpha F\eta}{RT} \right] \quad (1)$$

with  $i$  the current density,  $i_0$  the exchange current density,  $\eta = E - E_{eq}$  the overpotential and  $E_{eq}$  the equilibrium potential according to the Nernst equation,  $C$  the concentration (superscripts  $\sigma$  and  $s$  mean surface or bulk respectively),  $\alpha$  the transfer coefficient (lowering of the activation energy divided by the lowering of the Gibbs free energy due to application of the electric field),  $F$  the Faraday,  $R$  the gas constant and  $T$  the temperature. In the case of an irreversible reduction, no anodic reaction is taking place and (1) is simplified to

$$i = -i_0 \frac{C_{ox}^{\sigma}}{C_{ox}^s} \exp \frac{-\alpha F\eta}{RT} \quad (2)$$

In general the surface concentration deviates from the bulk concentration if a current is flowing and therefore the obtained current density is determined both by mass transport and the kinetics. The kinetic parameters  $\alpha$  and  $i_0$



therefore cannot be determined with equation (2) since the actual surface concentration is unknown. This problem can be solved using hydrodynamic methods such as the rotating ring-disc electrode technique<sup>2</sup> (RRDE). This electrode consists of a disc equipped with a concentric (platinum) ring (Fig. 3.1). The ring is only used if selectivity measurements have to be performed

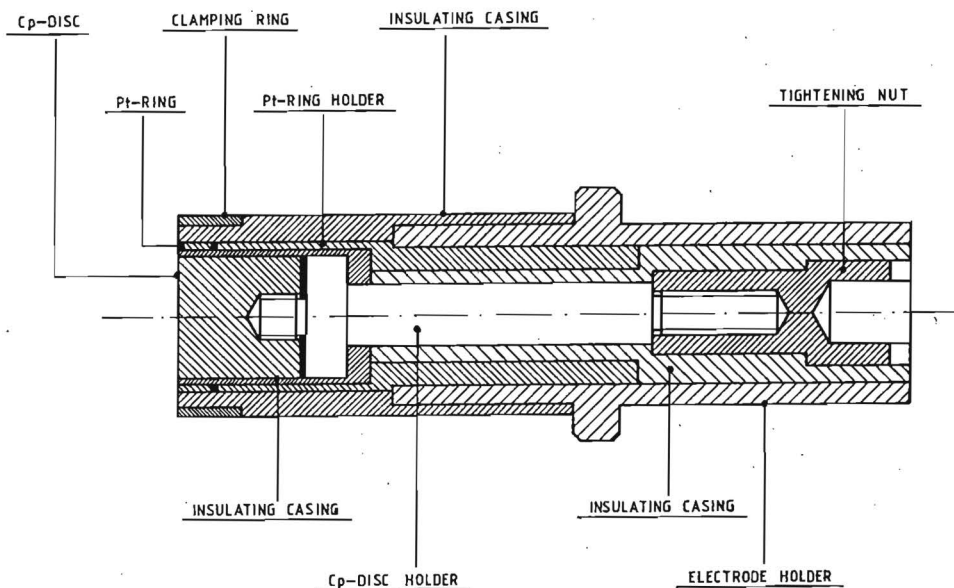


Fig. 3.1: Cross section of a rotating ring-disc electrode

(see section 3.2). Rotation of this electrode in the solution (face-down) causes a radial flow to the disc surface. In fact the whole system acts as a pump, sucking fluid towards it, spinning it around and flinging it out sideways<sup>3</sup>. Next to the electrode surface, a stagnant layer is formed. At the outside of this diffusion layer the solution is well-stirred and no deviations from the bulk concentration of the reactant occurs. If the electrode is so active that every ox molecule that reaches the disc is directly reduced, a mass-transport limited current density  $i_L$  will be reached:

$$i_L = -0.61 nF D_{ox}^{2/3} \nu^{-1/6} C_{ox}^s \omega^{1/2} = -nFk_d \quad (3)$$

with  $D_{ox}$  the diffusion coefficient,  $\nu$  the kinematic viscosity,  $\omega$  the angular velocity and  $k_d$  the rate constant of diffusion. The advantage of this method is that mass transport is well defined. It can be shown that

$$\frac{C_{\text{ox}}^{\sigma}}{C_{\text{ox}}^s} = \frac{i_L - i}{i_L} \quad (4)$$

i.e. the surface concentration is known as a function of the current density and therefore  $\alpha$  and  $i_0$  can be determined if  $i$  is measured as a function of potential. This  $i$ - $E$  curve is recorded using the three electrode principle<sup>4</sup>. The cell in which the measurements were performed is given in figure 3.2.

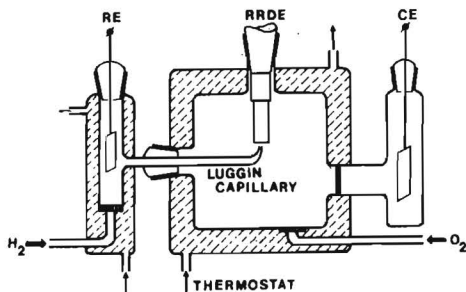


Fig. 3.2. The electrochemical cell.

The working electrode (RRDE) is attached to a holder (figure 3.3) which is connected with an electromotor (Motomatic, Electrocraft Corporation). The holder perfectly fits in the glass cell so that the disc electrode is immersed in the electrolyte.

With a control unit (Electrocraft Corporation) the rotation frequency can be varied from 0 - 64 s<sup>-1</sup>. Both the holder and RRDE's were machined in our own workshop. As the reference electrode (RE) a reversible hydrogen electrode (RHE) was used; the counter electrode (CE) was a platinum foil. All three electrodes are connected with a potentiostat (Tacussel, type Bipad). This apparatus maintains a fixed potential difference between the WE and the RE, by passing a current through the circuit of the WE and the CE. If a scan generator (Wenking VSG 72) is connected to the input of the potentiostat, any desired voltage program can be run. In this work only triangular sweep voltammetry was used: starting at a value where O<sub>2</sub> reduction does not proceed, the potential is linearly decreased in cathodic direction until the set minimum value is reached. Then the sweep is reversed and the potential is increased up to the initial value. During such a scan,  $\omega$  is held constant. The experiment can be repeated at different rotation frequencies. Both  $i$  and  $E$  were recorded on a XY recorder (Hewlett Packard 7046 A). In the case of an irreversible reduction, at constant  $\omega$  this  $i$ - $E$  curve has the form of a wave (Fig. 3.4).

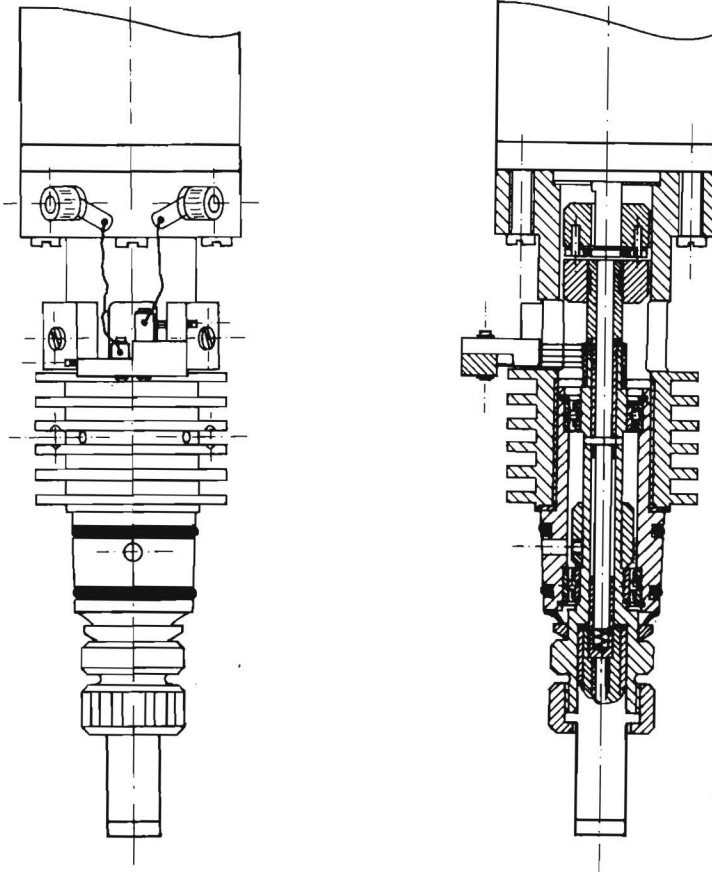


Fig. 3.3. Cross-section of a rotating ring-disk electrode assembly.

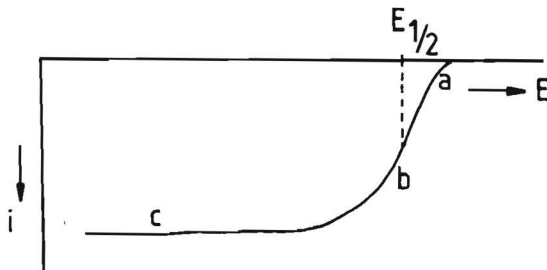


Fig. 3.4.  $i$ - $E$  curve for an irreversible reduction at a rotating disc electrode

At low overpotential (region a) the surface concentration does not deviate from the bulk concentration and  $i$  is purely kinetically limited. At high overpotential (region c) the diffusion-limited current is reached; the kinetic information is lost. In region b mixed kinetics is occurring: the current density is determined both by mass transport and the kinetics. The wave can be characterized by the half-wave potential  $E_{1/2}$ , the potential where  $i = \frac{1}{2} i_L$ . For a slow electrochemical reaction <sup>3</sup>

$$E_{1/2} = E_{eq} - \frac{RT}{\alpha F} \ln \frac{k_d}{k_o} \quad (5)$$

with  $k_o$  being the heterogeneous rate constant ( $= i_o/nF$ ). Note that, in that case  $E_{1/2}$  is a kinetic parameter.

### 3.2. Selectivity

The selectivity for the  $O_2$  reduction can be defined as the fraction of the supplied oxygen that is reduced to hydrogen peroxide. The magnitude of  $i_L$  already contains some information about the selectivity since this quantity is proportional to  $n$ , the number of transferred electrons per oxygen molecule ( $n = 2$  for the  $O_2$  production; 4 for reduction to  $H_2O$ ). A more sophisticated method is the rotating ring-disc technique. The potential of the ring is set at a value where every  $H_2O_2$  molecule that diffuses to the ring is quantitatively oxidized to  $O_2$  and  $H_2O$ . Only a fraction  $N$  (the collection efficiency) of the amount of  $H_2O_2$  that is produced at the disc, will be able to reach the ring; the rest will be swept into the solution. If the rotation frequency increases, two opposing effects regarding  $N$  will occur. The formed  $H_2O_2$  is more easily swept into the solution. At the same time, the thickness of the diffusion layer decreases, thereby increasing the rate of diffusion of  $H_2O_2$  to the ring. Mathematical analysis has shown that these effects exactly compensate each other, so  $N$  is independent of  $\omega$ . Therefore the measured ring current, divided by  $N$ , yields the amount of  $H_2O_2$  that is produced at the disc. For rotating ring-disc experiments a bipotentiostat has to be used in combination with a 'XYY' recorder.

### 3.3. Stability

The stability has only been checked on the time scale of a rotating disc experiment. For this purpose the stability was found to be sufficient. For the study of the long term stability, rotating disc electrodes are not suitable

and gas-diffusion electrodes have to be prepared. Therefore, the long term stability has not been studied extensively in this thesis.

### 3.4. Characterization

The purpose of the characterization is to obtain both quantitative and qualitative information of the catalyst that is applied onto the disc. Since all experiments are performed in the solution phase, only in situ techniques can be used for a reliable characterization. Unfortunately, this severely limits the number of applicable techniques. From the arsenal of spectroscopic techniques only UV-VIS (reflectance) spectroscopy and ellipsometry can be used in combination with rotating disc electrodes. For high vacuum techniques the electrode has to be removed from the solution; it is questionable whether the obtained results are representative for the condition of the electrode in the solution phase. An alternative is electrochemical characterization via cyclic voltammetry in oxygen-free solution. Transition metal chelates contain a metal ion, which valency can change at a certain potential, the so-called redox potential. If the potential is swept through the potential region where this redox potential is situated, a peak in the measured current will arise. In the reverse sweep, the metal centers will be restored in their initial condition, so a similar peak will be observed. The result is a cyclic voltammogram, depicted in figure 3.5.

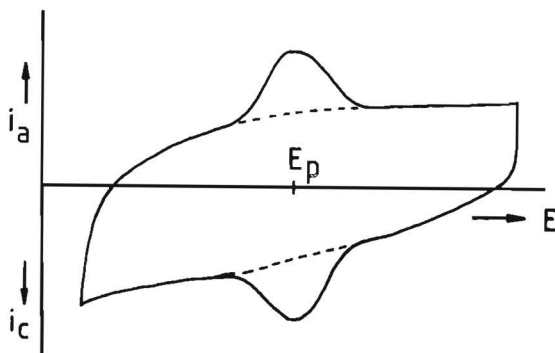


Fig. 3.5. Cyclic voltammogram in  $O_2$ -free solution, in order to detect redox peaks of the applied catalyst.

The background current (dashed line) is caused by the electric double layer: if an electrode is charged, a charge of opposite sign is induced in the electrolyte system. The system can be regarded as a capacitor. If the potential is varied the capacitor is charged or discharged, depending on the direction of the sweep. In triangular sweep voltammetry the potential varies linearly and

this "double layer current" should have a constant value. The contribution of the current due to the metal centers is superimposed on the double layer current. The peak potential  $E_p$  is equal to the redox potential. This  $E_p$  is the same in anodic and cathodic direction if the species are irreversibly adsorbed on the surface; in that case no mass-transport problems will occur. From the surface area under the peak the amount of catalyst molecules present can be calculated.

#### References

1. J.O'M. Bockris, A.K.N. Reddy, "Modern Electrochemistry", Plenum Press, New York (1970).
2. W.J. Albery, M.L. Hitchmann, "Rotating ring disc electrodes", Clarendon Press, Oxford (1971).
3. J. Albery, "Electrode Kinetics", Clarendon Press, Oxford (1975).
4. A.J. Bard, L.R. Faulkner, "Electrochemical Methods", Wiley, New York (1980).

Chapter 4 The cathodic reduction of dioxygen at cobalt phthalocyanine:  
Influence of electrode preparation on electrocatalysis.

4.1 Introduction

In recent years a considerable number of papers have been published on dioxygen reduction. In many of these investigations a metal chelate is used as a catalyst. These catalysts are attached to the electrode with the aid of different methods, such as irreversible adsorption<sup>1</sup>; vacuum deposition<sup>2</sup>; incorporation into a conducting polymer, as polypyrrole<sup>3</sup>; impregnation of porous carbon<sup>4</sup>; evaporation of the solvent<sup>5</sup>. All these preparation techniques result in electrodes with different activity even if the same catalyst and the same amount of catalyst is used. One of the most striking examples is the difference in activity between an electrode prepared by vacuum deposition of cobalt phthalocyanine (CoPc) and by incorporation of water-soluble tetra(sulfonate)phthalocyanato cobalt(II), abbreviated as CoTSPc, in polypyrrole<sup>3</sup>. Especially in acid media, the catalyst incorporated in polypyrrole is much more active than the vacuum-deposited one, while in both cases a thick layer containing the catalyst is present. To explain the difference in activity, we have to take into account the conductivity of the catalyst layer and the possibility of the diffusion of O<sub>2</sub> through this layer. Both the conductivity of, and the dioxygen diffusion velocity in, the catalyst/polypyrrole layer is so high, that all attached catalyst molecules can take part in the electrocatalysis, which is not the case for the vacuum-deposited film, as will be shown later in this chapter. A comprehensive theoretical description of this phenomenon is given in a paper by Saveant et al.<sup>6</sup>

The purpose of the present chapter is to demonstrate how preparation conditions affect the activity. This will be illustrated for the reduction of O<sub>2</sub> on CoPc or, in some cases, the water-soluble modification CoTSPc. The following preparation methods were investigated: a. Irreversible adsorption; b. Vacuum deposition; c. Incorporation in polypyrrole; d. Impregnation of porous carbon; e. Evaporation of the solvent. For a precise description see the section 'experimental'.

## 4.2 Theoretical aspects

CoPc (or CoTSPc) gives under all circumstances a first reduction wave of dioxygen to hydrogen peroxide. The kinetics for the reaction is in general much faster in alkaline solutions than in acid solutions. The main reason is that the probable intermediate  $O_2^-$ , or an  $O_2^-$ -like species, is relatively more stable in alkaline solutions than in acid solutions, as was stressed by Yeager<sup>7</sup>. With this in mind, we expect the effect of the preparation method on the activity to be more dramatic in acid than in alkaline solutions, therefore, for comparison, measurements were carried out in both electrolytes.

Clearly, the number of active sites is an important parameter determining the  $i$ - $E$  relationship, characterized by the half-wave potential  $E_{1/2}$ , as determined with the rotating disc electrode technique. It can be shown that this half-wave potential shifts when the number of active sites at an electrode is increased. Suppose, we have an irreversible electrochemical reaction with a rate-determining electron transfer as the first step. For the current density measured with a rotating disc electrode the following relation has been derived by Albery<sup>8</sup> for a first-order reaction:

$$\frac{i}{i_L} = \frac{1}{1 + k_d/k} \quad (1)$$

$i$  : current density ( $\text{mA}/\text{cm}^2$ )

$i_L$  : transport-limited current density ( $\text{mA}/\text{cm}^2$ )

$k_d$  : heterogeneous rate constant describing mass transport ( $\text{cm}/\text{s}$ )

$k$  : observed heterogeneous rate constant of the electron transfer ( $\text{cm}/\text{s}$ )

At the half-wave potential ( $i = \frac{1}{2} i_L$ ),  $k_d = k$ . Rate constant  $k$  corresponds with a surface with a certain amount of active sites. If this amount of active sites on the surface increases with a factor  $p$ , then also the rate constant  $k$  increases with this factor, because  $k$  is based on the geometric surface area. Increasing the number of active sites neither affects the size of this geometric area nor the diffusion to this surface. Therefore, for the original and the new surface (1 and 2, respectively), we have, in the case of a cathodic reaction, the following relations:



$$\text{surface 1: } k_d = k_o \exp \frac{-\alpha F \eta_1}{RT} \quad (2)$$

$$\text{surface 2: } k_d = p \cdot k_o \exp \frac{-\alpha F \eta_2}{RT} \quad (3)$$

with  $k_o$  : the value of  $k$  at  $E = E_{eq}$   
 $E_{eq}$  : the equilibrium electrode potential  
 $\eta_1, \eta_2$  =  $(E_{1/2})_1 - E_{eq}, (E_{1/2})_2 - E_{eq}$ : overpotential for surface 1 and 2, respectively.  
 $(E_{1/2})_1, (E_{1/2})_2$  : half-wave potential of surface 1 and 2, respectively.

The difference between the two half-wave potentials is:

$$(E_{1/2})_2 - (E_{1/2})_1 = \Delta E_{1/2} = \frac{RT}{\alpha F} \ln p \quad (4)$$

For  $\alpha = 1/2$  the lowering of the half-wave overpotential is 118 mV for a ten-fold increase of the number of active sites. Generally, the shift of the half-wave potential for a ten-fold increase of the number of active sites is equal to the Tafel slope.

### 4.3 Experimental

CoPc was obtained from Eastman Kodak. The sodium salt of CoTSPc was synthesized according to the method described by Weber and Busch<sup>9</sup>. All other chemicals were commercially available and used without further purification, except the pyrrole which was distilled before use. As will be explained below, five different electrode systems (a-e) were prepared. For electrode system b and d, a gold disc with a surface area of 0.50 cm<sup>2</sup> and for system a, c and e, a pyrolytic graphite (C<sub>p</sub>) disc with a surface area of 0.52 cm<sup>2</sup> was used. Before the preparation of the electrode systems the electrodes were polished with 0.3 μm alumina, rinsed with doubly distilled water and cleaned in an ultrasonic water bath for one minute.

a. Irreversible adsorption. A pyrolytic graphite electrode (C<sub>p</sub>) is dipped into a solution of CoPc or CoTSPc, resulting in the irreversible adsorption of the complex on the electrode<sup>1</sup>. A (sub)monolayer of catalyst is obtained. Characterization by cyclic voltammetry is possible with these electrodes, so the exact number of active sites can be determined. It is also possible to

produce electrodes with different surface coverages by dipping the  $C_p$  electrode in solutions of CoPc in pyridine (or CoTSPc in water) with concentrations ranging from  $10^{-3}$  to  $10^{-5}$  mol/l. The time of exposure (dipping time) appeared to be unimportant.

b. Vacuum deposition. This technique has already been previously employed in our laboratory<sup>2</sup>. In this way, it is possible to produce an electrode, which is covered with a high amount of catalyst. The thickness of the layer was determined spectroscopically, as described in the same paper.

c. Incorporation in polypyrrole. The sodium salt of CoTSPc is soluble in water. The electrooxidation of pyrrole gives a polymer with positive charges, which must be compensated by negatively charged ions<sup>8</sup>. When the polymerization is carried out in the presence of the CoTSPc<sup>4-</sup> anion, incorporation of this ion in the film is obtained. For the preparation of this type of electrode systems, a  $10^{-3}$  M CoTSPc solution in water, containing 1 vol % pyrrole, was used. The electrooxidation was carried out galvanostatically with a current of 0.2 mA. By varying the time, layers of different thickness can be produced.

d. Impregnation of porous carbon. The impregnation of the carbon support (Norit BRX) was realized by dissolving 10 mg of CoPc in 20 ml THF, adding 40 mg of the carbon, then refluxing and stirring for 30 minutes. The carbon particles were attached to the Au disc of the electrode via incorporation in a polypyrrole film, according to a previously described procedure<sup>11</sup>. The carbon support has a high conductivity, and a high specific surface area, so many catalyst molecules can be adsorbed on the surface.

e. Evaporation of the solvent. A drop (several microliters) of a CoPc solution in pyridine is placed on a  $C_p$  electrode; thereafter, the solvent is allowed to evaporate, yielding electrodes with relatively thick layers of catalyst. By changing the concentration of the solution from  $10^{-3}$  to  $10^{-5}$  mol/l, the thickness of the layer can be regulated.

The electrochemical experiments were carried out in a standard three-compartment electrochemical cell, filled with 100 ml electrolyte. As electrolyte both acid (0.5 M  $H_2SO_4$  or 0.05 M  $H_2SO_4$ ) and alkaline (1 M KOH or 0.1 M KOH) solutions were used. The polypyrrole electrodes were not tested in 0.1 M KOH and in 1 M KOH, because of the lack of stability of polypyrrole in alkaline solutions<sup>12</sup>. For characterization of the electrode, cyclic voltammetry was conducted in dioxygen-free solutions. The  $O_2$  reduction was measured in dioxygen-saturated solutions, with the rotating disc-electrode

technique. The electrochemical measurements were carried out using a Tacussel bipotentiostat (Bipad). As reference electrode a reversible hydrogen electrode (RHE) was used. All potentials in this paper are given versus the RHE. The reduction curves of electrode systems in which polypyrrole was used, are corrected for the high capacitive current of the polypyrrole itself.

#### 4.4 Results and discussion

##### a. Acid media

Figure 4.1 gives the result for the dioxygen reduction on the electrode systems (a-e). In table 4.1 the amounts of attached catalyst for the different

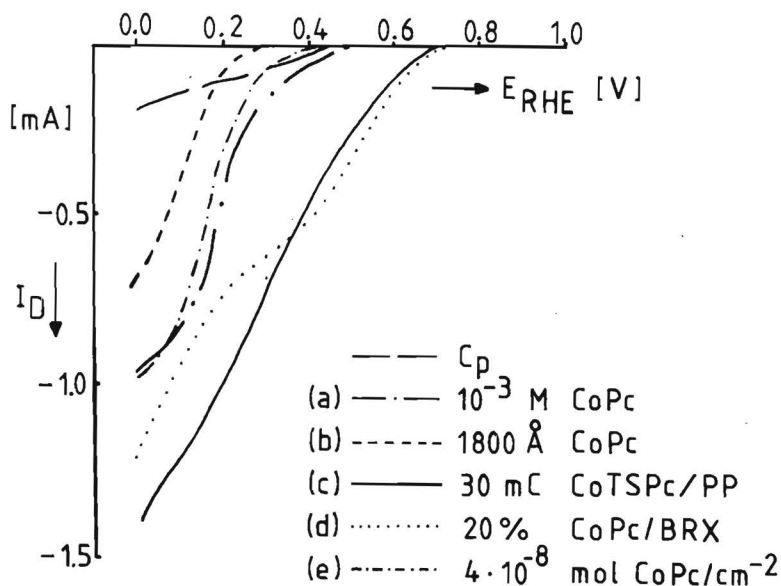


Fig. 4.1: Effect of electrode preparation on the  $O_2$  reduction. For notation see table 1. Electrolyte: 0.5 M  $H_2SO_4$ ,  $O_2$  saturated; scan rate: 50 mV/s; rotation frequency: 16/s.

electrode systems are given. It is obvious that each electrode system catalyses the reduction of  $O_2$ , however, to a different extent, indicating that the amount of active sites is not automatically the same as the total number of catalyst molecules present; an electrode prepared via irreversible adsorption is even more active than a thick vacuum-deposited film.

To illustrate the shift in half-wave potential due to a change in active sites, as derived in equation (4), the  $O_2$  reduction was investigated as a

**Table 4.1:** The amounts of attached catalyst for the electrode systems of figure 4.1.

Electrode type	Description	Amount of catalyst (mol/cm <sup>2</sup> )
a	irreversible adsorption ( $10^{-3}$ M CoPc)	$2.6 \cdot 10^{-10}$
b	vacuum deposition (1800 Å)	$6.3 \cdot 10^{-8}$
c	incorporation in polypyrrole (30 mC)	$1.7 \cdot 10^{-8}$
d	impregnation of porous carbon (20%)	$1.8 \cdot 10^{-7}$
e	evaporation of the solvent	$4.0 \cdot 10^{-8}$

function of the CoTSPc/polypyrrole layer thickness (type c). Since the polymer layer is very thin compared to the thickness of the diffusion layer,  $k_d$  will remain unchanged for all layer thicknesses. In figure 4.2 the  $O_2$  reduction on CoTSPc adsorbed on  $C_p$  (1), and on various CoTSPc/polypyrrole layers (2-6) in 0.05 M  $H_2SO_4$  is shown. In this figure, the thickness of the layer is expressed in the charge passed during the electropolymerization of pyrrole. In order to determine the amount of catalyst in a film, a cyclic voltammogram in an  $O_2$ -free solution was measured for a 30 mC thick layer; see figure 4.3. In

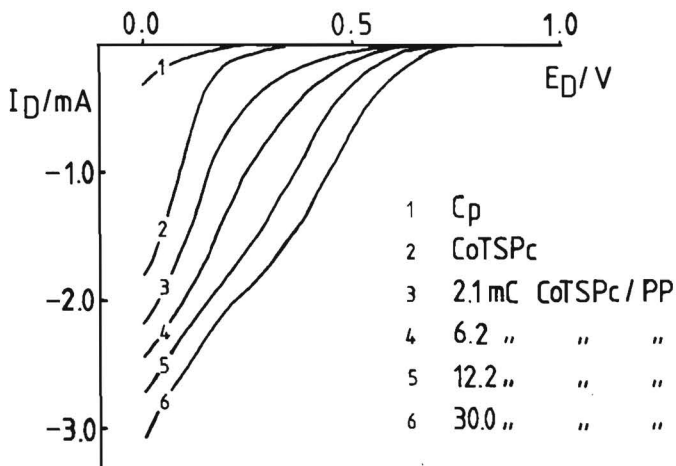


**Fig. 4.2:**  $O_2$  reduction as a function of the CoTSPc/polypyrrole layer thickness. Electrolyte: 0.05 M  $H_2SO_4$ ,  $O_2$  saturated; scan rate: 50 mV/s; rotation frequency: 64/s. For comparison the  $O_2$  reduction on an irreversibly adsorbed layer of CoTSPc on  $C_p$  is also included (curve 2).

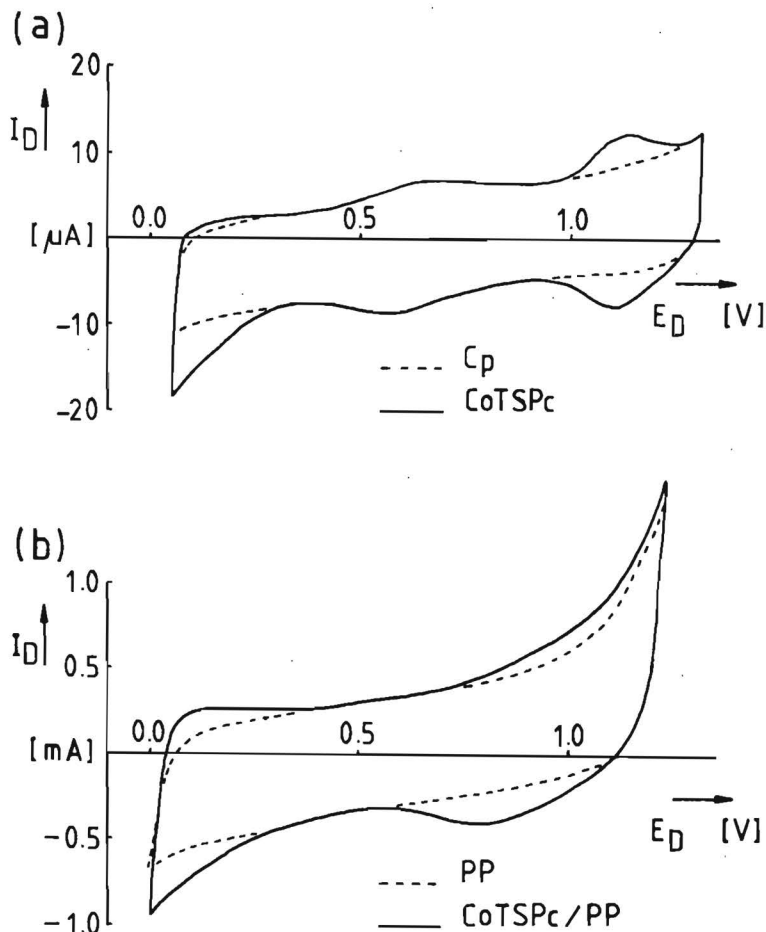


Fig. 4.3: Cyclic voltammograms of CoTSPc adsorbed on  $C_p$  (a) and of a 30 mC CoTSPc/polypyrrole layer (b). Electrolyte: 0.05 M  $H_2SO_4$ ,  $O_2$ -free; scan rate: 100 mV/s.

this figure also the cyclic voltammogram of CoTSPc adsorbed on  $C_p$  is given (a). The characterization of the electrodes is somewhat hampered by the instability of CoTSPc in acid solutions. Moreover, at potentials above 1 volt versus RHE, the polypyrrole degrades rapidly. In spite of these difficulties, for an electrode obtained from irreversible adsorption, a surface coverage of  $1.4 \cdot 10^{-10}$  mol/cm<sup>2</sup> can be determined from the area under the reduction peak at 1.1 V. The 30 mC CoTSPc/ polypyrrole layer (b) gives a coverage of  $7.8 \cdot 10^{-9}$  mol/cm<sup>2</sup>. If it is assumed that for the oxidation of pyrrole to neutral polypyrrole 2 electrons per molecule are involved, and that

in the oxidized form of polypyrrole, every four pyrrole units carry one positive charge <sup>10</sup>, a coverage of  $1.67 \cdot 10^{-8}$  mol/cm<sup>2</sup> can be calculated for a 30 mC CoTSPc/polypyrrole layer. In this chapter this theoretical value will be used.

A limiting current of 2.5 mA is reached below 0 V versus RHE in curve 2, figure 4.2. (The plateau is not shown in the figure). This value equals the theoretical diffusion limiting current for the reaction of oxygen to hydrogen peroxide. Curve 6, in the same figure, shows, although not very clearly, a first wave and the start of a second wave. In our view the first wave corresponds to the reaction of dioxygen to hydrogen peroxide; the second wave is attributed to the further reduction of hydrogen peroxide to water. With this in mind, the half-wave potentials for the curves 2 and 6, can be determined with reasonable accuracy, if only the reaction of O<sub>2</sub> to hydrogen peroxide is considered. The results are respectively 70 mV and 395 mV. With the use of these values, and the surface coverage in the two cases, the shift in halfwave potential as a function of the number of active sites can be calculated. The result is 155 mV/decade of active sites.

For the Tafel slope of the first wave of curve 6 (figure 4.2) a value of -155 mV has been determined. Notwithstanding the difficulty of the determination, this is the same value as reported by Zagal-Moya <sup>7</sup>, for the O<sub>2</sub> reduction on CoTSPc adsorbed on C<sub>p</sub>. The value of the Tafel slope corresponds very well with the observed shift in the half-wave potential. This agreement may be somewhat flattered because of two compensating effects. First, the amount of catalyst in the film is probably taken too high, if we compare this with the results of the cyclic voltammetric measurements; secondly, it is probable not correct to neglect the dioxygen reduction on the polypyrrole matrix completely.

Returning to the results for the five different electrode systems as presented in figure 4.1, we note that a vacuum-deposited layer (b) has a lower activity than an irreversibly adsorbed layer (a), notwithstanding its thickness. Since the film has a relative low conductivity, the reaction must take place mainly at the interface between the substrate and the phthalocyanine film. O<sub>2</sub> must diffuse through the inactive outer parts of the film to reach the active sites at the interface. The electrode obtained by evaporation of the solvent (e) has a comparable physical structure, but probably a somewhat higher porosity and/or conductivity, resulting in a slightly increased activity for this electrode system as compared with system b.

The two other electrode systems consist of a catalyst dispersed on a matrix

with high porosity and high conductivity, so that the whole layer, or at least a major part of it, is involved in the electrocatalysis. The direct incorporation in polypyrrole results in the most efficient utilization of the catalyst.

b. Alkaline media

Electrode systems a, b and e all show about the same activity in 1 M KOH, as can be concluded from the figures 4.4 and 4.5. Due to the greater stability of CoPc (or CoTSPc) in alkaline as compared with acid solutions, a more pre-

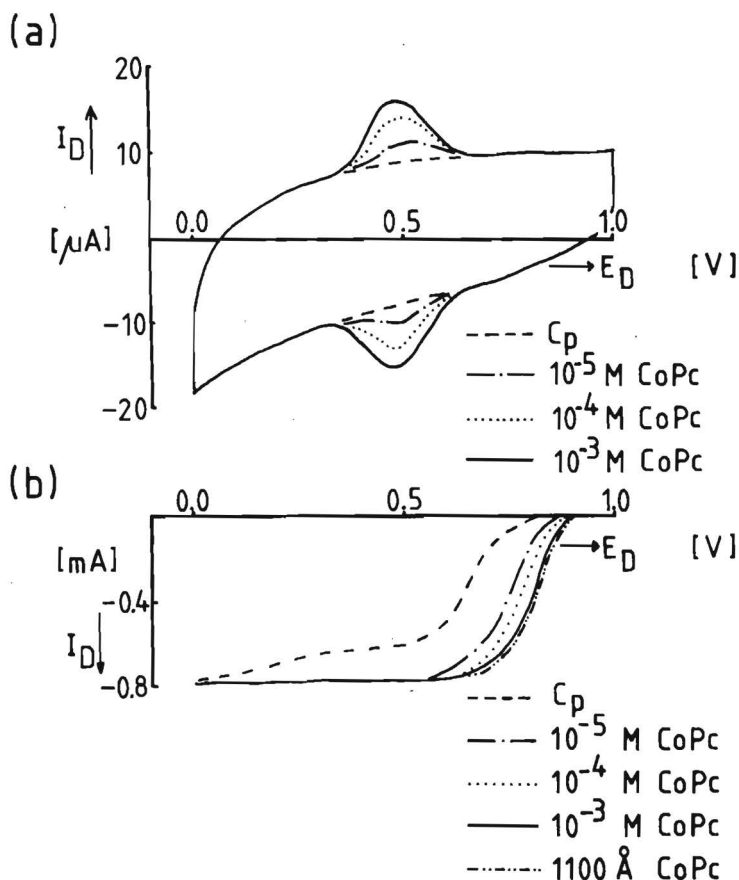


Fig. 4.4: a) Cyclic voltammogram of CoPc adsorbed on  $C_p$ . The concentrations of the dip solutions are given in the figure. Electrolyte: 1 M KOH,  $O_2$ -free; scan rate: 100 mV/s. b)  $O_2$  reduction on the electrodes of figure 4a, compared with a vacuum-deposited layer of CoPc. Electrolyte: 1 M KOH,  $O_2$  saturated; scan rate 50 mV/s; rotation frequency: 16/s.

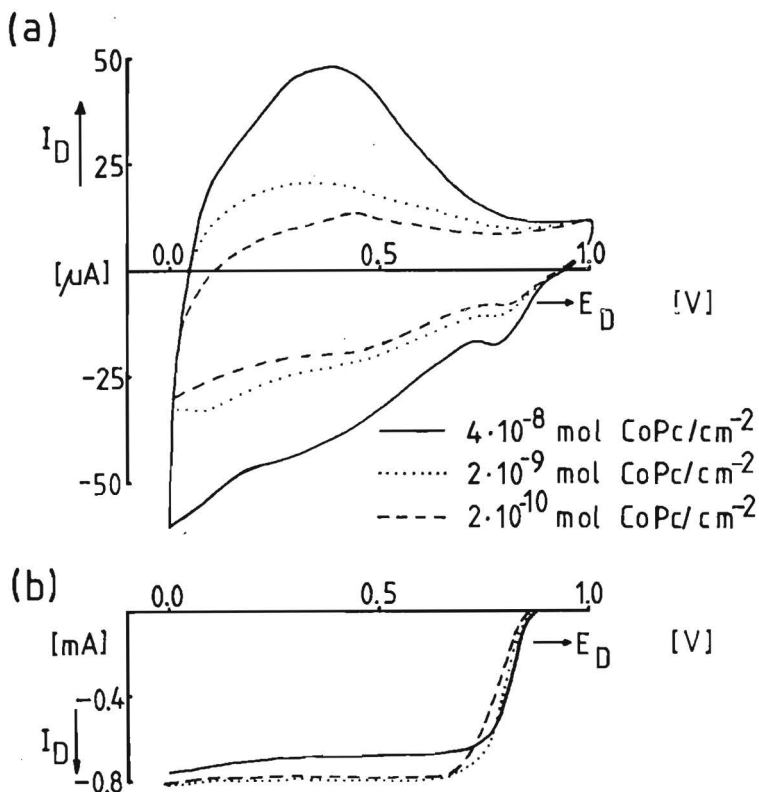


Fig. 4.5 a) Cyclic voltammogram of electrode system e (evaporation of the solvent). The amounts of deposited catalyst are given in the figure. Electrolyte: 1 M KOH,  $O_2$ -free; scan rate: 100 mV/s. b)  $O_2$  reduction on the same electrodes as in figure 5a. Electrolyte: 1 M KOH,  $O_2$  saturated; scan rate: 50 mV/s; rotation frequency: 16/s.

cise characterization of the electrode is now possible. In figure 4.4a, the results are given for an irreversibly adsorbed layer prepared by using solutions of different concentrations. The surface coverage increases from  $6.4 \cdot 10^{-11} \text{ mol/cm}^2$  (for a concentration of  $10^{-5} \text{ M CoPc}$ ) to  $2.6 \cdot 10^{-10} \text{ mol/cm}^2$  (for a concentration of  $10^{-3} \text{ M CoPc}$ ). Figure 4.4b demonstrates that the increased coverage is accompanied only by a slight increase in activity. The vacuum-deposited film (1100 Å) also drawn in figure 4.4b has the same activity as the above mentioned a-type electrode prepared from a  $10^{-3} \text{ M}$  solution.

An electrode with a vacuum-deposited film gives non-reproducible and featureless cyclic voltammograms in  $O_2$ -free solutions. From the measured



activity, it can be concluded that the conductivity and porosity of the layer are such, that about the same activity as that obtained for a monolayer is realized. On comparing figures 4.1 and 4.4b, it appears that the vacuum-deposited films show a relative higher activity in alkaline than in acid solution. In our view, this difference is not caused by the electrolytes themselves, but due to the used preparation method. It is difficult to obtain films with identical physical properties. Different films have a somewhat different conductivity and/or porosity, depending on the exact preparation conditions; these conditions cannot be kept constant with the applied method. Nevertheless, in both electrolytes only one monolayer or even less, is electrochemically active.

With electrode system e (deposition of CoPc by evaporation of the solvent), the characterization also results in a featureless cyclic voltammogram as can be observed in figure 4.5a. The amount of catalyst has almost no effect on the activity as is demonstrated in figure 4.5b.

The  $O_2$  reduction on electrode system c (CoTSPc incorporated in polypyrrole) has been examined in 0.1 M KOH solutions. The result is shown in figure 4.6. For comparison, the dioxygen reduction curve measured on a layer, prepared from irreversible adsorption of CoTSPc (coverage  $1.4 \cdot 10^{-10} \text{ mol/cm}^2$ ) has been drawn in the same figure. As can be seen from these curves, there is almost no difference in activity, in spite of the high catalyst loading in the case of the 30 mC CoTSPc/polypyrrole film ( $1.67 \cdot 10^{-8} \text{ mol/cm}^2$ ). With the CoTSPc/polypyrrole layer again a second wave appears.

This wave can be ascribed, as also done for acid electrolytes, to the further reduction of hydrogen peroxide to water. The appearance of the second wave is due to the great number of active catalyst molecules. For the vacuum-deposited layer, there is no second wave, again suggesting that only part of the vacuum-deposited layer is active. At high overpotential, the current decreases due to the change of polypyrrole to a reduced, non-conducting, form.

It is difficult to determine one unique Tafel slope for the first wave of the  $O_2$  reduction on a 30 mC CoTSPc/polypyrrole layer in 0.1 M KOH: results vary from -60 mV at low overpotentials to -130 mV at higher overpotentials. Tafel slopes of -120 mV have been reported by Zagal-Moya for an irreversibly adsorbed layer of CoTSPc<sup>7</sup>. Figure 4.6 shows that the shift of the halfwave potential as a function of the amount of catalyst, is not equal to the observed Tafel slope. The reason for this is that an adsorbed monolayer already accomplishes a reversible (or quasi-reversible) reduction of dioxygen to hydrogen peroxide in 0.1 M KOH. Any further increase of the number of

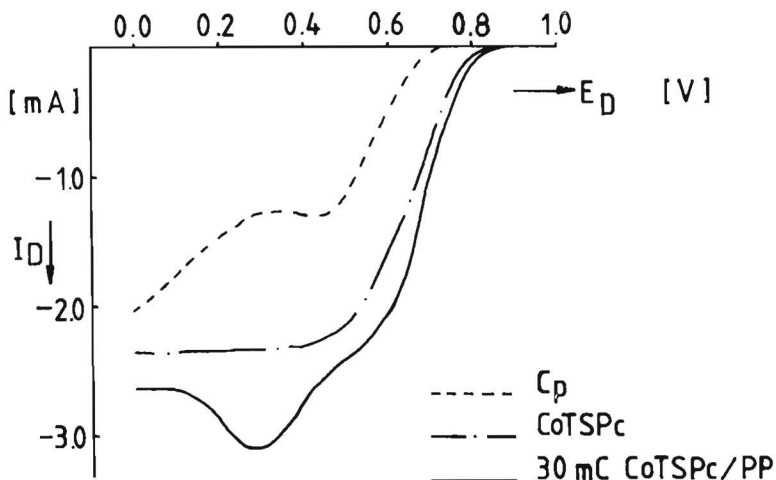


Fig. 4.6:  $O_2$  reduction on CoTSPc, adsorbed on  $C_p$ , compared with a 30 mC CoTSPc/polypyrrole layer. Electrolyte: 0.1 M KOH,  $O_2$ -saturated; scan rate: 50 mV/s; rotation frequency: 64/s.

active sites does not bring about an enhanced activity, as is characteristic for reversible reactions.

#### 4.5 Conclusions

The investigations of five electrode systems demonstrate that the number of active sites is an important factor determining the activity of an electrode. This number is by no means the same as the total amount of catalyst present on the surface. A layer prepared by irreversible adsorption on an inert electrode material is recommended to study electrocatalysis, because of the possibility of determining the exact number of active sites and, moreover, the diffusion to the surface is well defined. The use of this electrode system enables the determination of the "intrinsic catalytic activity" of a catalyst. With "intrinsic catalytic activity" is meant the (catalytic) activity of a surface expressed by an exchange current density and corrected for the number of the active sites on this surface. The obtained quantity can be called turnover number.

The use of this turnover number instead of the exchange current density will not give very different results for metal electrodes, since they all have about the same number of surface atoms per unit surface area. However, this is not the case with large organic molecules as catalyst, containing only one

active site per molecule. For instance, when the catalytic activity of a surface, covered with CoTSPc, is compared with the activity of platinum, the use of exchange current densities gives a false picture. If the same geometric surface area is taken into account, an adsorbed monolayer of CoTSPc contains  $5.10^{13}$  molecules/cm<sup>2</sup>, assuming an area of 200 Å<sup>2</sup> per molecule with the molecules lying parallel to the surface. For platinum, however, a number of  $1.35 \cdot 10^{15}$  atoms/cm<sup>2</sup> can be calculated using a density of 21.45 g/cm<sup>3</sup>. Thus, a platinum electrode has 27 times more active sites than an adsorbed monolayer of CoTSPc. An (imaginary) CoTSPc electrode that would contain the same number of active sites as platinum per unit surface area (and which, therefore, allows a fair comparison), would show in acid electrolytes a half-wave potential, that is shifted 220 mV in anodic direction, compared with the electrode, described by curve 2 in figure 4.2.

#### 4.6 References

1. J. Zagal, R.K. Sen and E. Yeager, J. Electroanal. Chem., 83 (1977) 207.
2. F. van den Brink, W. Visscher and E. Barendrecht, J. Electroanal. Chem., 157 (1983) 283.
3. M.I. Florit, W.E. O'Grady, C.A. Linkous, T. Skotheim and M. Rosenthal, Published, Abstract N415, Extended Abstracts, vol. 84-1, The Electrochem. Soc. (1984).  
R.A. Bull, F.R. Fan and A.J. Bard, J. Electrochem. Soc., 131 (1984) 687.
4. L. Kreja and A. Plewka, Electrochim. Acta, 27 (1982) 251.
5. H. Behret, W. Clauberg and G. Sandstede, Ber. Bunsenges. Phys. Chem., 81 (1977) 54.  
H. Behret, W. Clauberg and G. Sandstede, Zeitschrift für Physikalische Chemie, Neue Folge, Bd 113 (1978) 97.
6. C.P. Andrieux, J.M. Dumas-Bouchiat and J.M. Savéant, J. Electroanal. Chem., 131 (1982) 1.
7. E. Yeager, Electrochim. Acta, 29 (1984) 1527.  
Thesis J.H. Zagal-Moya, Case Western Reserve University, 1978.
8. J. Albery, Electrode Kinetics, Clarendon Press, Oxford 1975.
9. J.H. Weber and D.H. Busch, J. Inorg. Chem. 4 (1965) 469.
10. A.F. Diaz, J.I. Castillo, J.A. Logan and W.Y. Lee, J. Electroanal. Chem., 129 (1981) 115.
11. A. van der Putten, W. Visscher and E. Barendrecht, J. Electroanal. Chem. 195 (1985) 63 (chapter 9 of this thesis).
12. E.M. Genies and A.A. Syed, Synth. Met., 10 (1984) 21.

## Chapter 5 Dioxygen reduction on vacuum-deposited and adsorbed transition metal phthalocyanine films.

### 5.1 Introduction

The transition metal phthalocyanines of iron and cobalt (abbreviated as FePc and CoPc, respectively) have been studied for almost two decades as electrocatalysts for the cathodic reduction of dioxygen<sup>1</sup>. A lot of work has been performed using gas-diffusion electrodes<sup>2</sup>, however, more detailed information about the catalysis can only be obtained with more sophisticated methods, such as the rotating ring-disc electrode (RRDE). The chelates can be applied to the disc via irreversible adsorption<sup>3</sup>, evaporation of the solvent<sup>4</sup>, vacuum deposition<sup>5</sup> or incorporation into a conducting polymer<sup>6</sup>. In previous publications the results of vacuum-deposited iron- and cobalt phthalocyanine films in alkaline solution were reported<sup>7</sup>. This chapter describes the behaviour of these electrodes in acid solution, and compares the results with electrodes onto which a monolayer is irreversibly adsorbed. Because of the significant differences, it was also investigated how the physical properties of the films affect the electrochemical behaviour, both in acid and alkaline solution.

### 5.2 Experimental

The vacuum-deposited phthalocyanine films were prepared according to the described procedure<sup>7a</sup>. The films were deposited onto gold, platinum, and pyrolytic graphite (Cp) disc electrodes, all equipped with a platinum ring. The electrodes have a surface area of 0.5 cm<sup>2</sup> and a collection efficiency  $N$  of 0.27 (Au and Cp) or 0.24 (Pt). The film thicknesses varied from 700–3000 Å, since it was not possible with this technique to produce films with a reproducible thickness. The film thickness was measured using an indirect spectrophotometric method<sup>7a</sup>.

Irreversibly adsorbed monolayers of FePc and CoPc were prepared by dipping a dry, freshly polished (up to 0.3 μm Al<sub>2</sub>O<sub>3</sub>, Buehler) Cp electrode in a 10<sup>-3</sup> M solution of the corresponding phthalocyanine in pyridine for one minute, and flushing it with doubly distilled water.

The following measuring procedure was applied to the electrodes:

- Measurement of the  $O_2$  reduction as a function of potential and rotation frequency. At the disc  $O_2$  is reduced; at the ring the amount of formed hydrogen peroxide is monitored.
- Cyclic voltammetry of the electrodes in  $O_2$ -free electrolyte. The objective is to detect redox peaks corresponding to the central metal ion and to relate these to the observed catalytic properties.
- Measurement of the  $H_2O_2$  reduction in  $O_2$ -free solutions as a function of potential and rotation frequency. Since the  $O_2$  reduction can proceed along two pathways (viz. the direct  $4e^-$  reduction to water, or the  $2e^-$  reduction to  $H_2O_2$  which can be either the stable end product or is subsequently reduced to water), also the reduction behaviour of  $H_2O_2$  on these electrodes is of interest.

All measurements were performed in a standard three-compartment electrochemical cell, filled with 150 ml electrolyte. A reversible hydrogen electrode (RHE) was used as a reference electrode; a platinum foil as a counter electrode. Both the acid (0.5 M  $H_2SO_4$ ) and the alkaline (1 M KOH) electrolytes were prepared from p.a. chemicals (Merck) and doubly distilled water. The  $O_2$  reduction was measured by scanning the disc potential from 1.0 to 0 V vs. RHE, and vice versa with  $50 \text{ mV s}^{-1}$ , at four rotation frequencies: 4, 16, 36 and  $64 \text{ s}^{-1}$ . The platinized ring <sup>7a</sup> was maintained at a potential of 1.2 V to ensure quantitative  $H_2O_2$  detection. Characterization of the electrodes in  $O_2$ -free solutions was performed by also scanning the disc potential from 1.0 to 0 V versus RHE and back again, now with  $100 \text{ mV s}^{-1}$ . The behaviour of peroxide was studied in  $O_2$ -free 4-7 mM  $H_2O_2$  solutions, by scanning the disc potential from 1.0 to 0 V and vice versa with  $50 \text{ mV s}^{-1}$  at rotation frequencies of 4, 16, 36 and  $64 \text{ s}^{-1}$ .

### 5.3 Results

#### 1. Vacuum-deposited phthalocyanine films.

In figure 5.1 the results are given for the  $O_2$  reduction in 0.5 M  $H_2SO_4$  at a  $1800 \text{ \AA}$  CoPc film deposited on pyrolytic graphite. The same results were obtained with Au as substrate. The ratio of ring and disc current shows that  $O_2$  is reduced to  $H_2O_2$  exclusively; the reduction starts at about 200 mV vs. RHE i.e. at high overpotential. Since the diffusion-limited current for

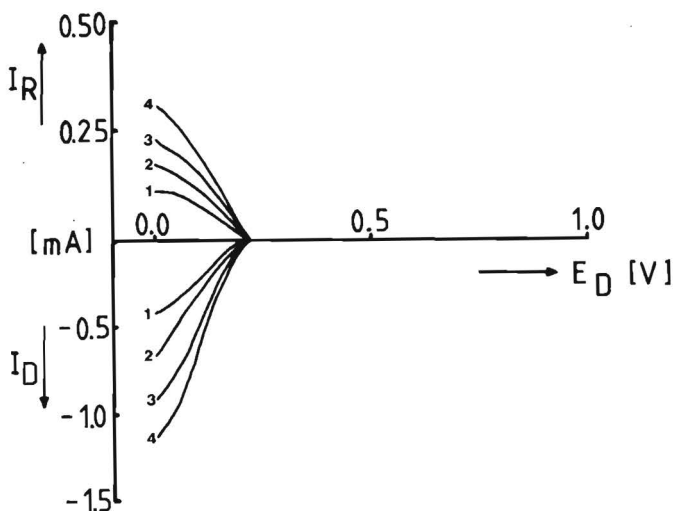


Fig. 5.1  $O_2$  reduction in  $0.5\text{ M H}_2\text{SO}_4$  at a  $1800\text{ \AA}$  CoPc film deposited on Cp; scan rate  $50\text{ mV s}^{-1}$ , rotation frequencies  $4$  (1),  $16$  (2),  $36$  (3) and  $64\text{ s}^{-1}$  (4).

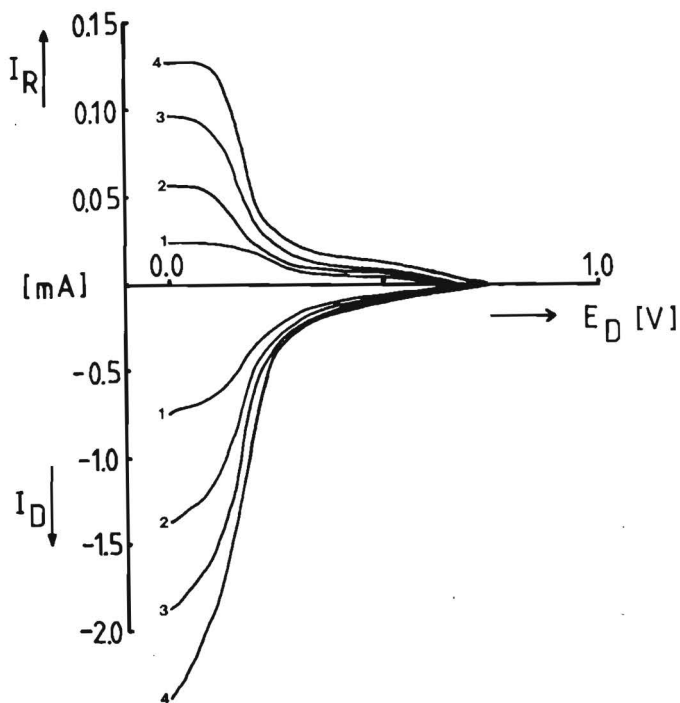


Fig. 5.2  $O_2$  reduction in  $0.5\text{ M H}_2\text{SO}_4$  at a  $2200\text{ \AA}$  FePc film, deposited on Au; scan rate  $50\text{ mV s}^{-1}$ , rotation frequencies  $4$  (1),  $16$  (2),  $36$  (3) and  $64\text{ s}^{-1}$  (4).

reduction of  $O_2$  to  $H_2O_2$  ( $n = 2$ ) is 2 mA at  $64 \text{ s}^{-1}$ , it is clear that the reduction is kinetically limited in this potential region.

In fig. 5.2 the results for a 2200 Å FePc film on Au are depicted under the same conditions. The reduction seems to proceed in two waves. The first wave starts at about 700 mV vs. RHE and is kinetically limited. At 200 mV vs. RHE the current increases rapidly and reaches values exceeding the diffusion-limited current for the reduction of  $O_2$  to  $H_2O_2$ . This, together with the measured ring currents, shows that FePc yields a mixed production of  $H_2O_2$  and  $H_2O$  in acid electrolyte. In order to give a complete picture, the behaviour of the CoPc and FePc films in 1 M KOH under the same experimental conditions is presented in the figures 5.3–5.5. In this electrolyte a substrate effect occurred: a CoPc film (1100 Å) deposited on Cp (fig. 5.3) reduces  $O_2$  in one wave, starting at about 870 mV vs. RHE. At high overpotential the disc current is proportional to the square root of the rotation frequency, so the reduction is pure diffusion limited at these potentials. The magnitude of the limiting current matches the theoretical value in 1 M KOH (1.5 mA at  $64 \text{ s}^{-1}$ ) for reduction to  $H_2O_2$ . The ring currents likewise indicate that  $H_2O_2$  is the sole product. Also the behaviour of  $H_2O_2$  itself at this electrode was studied: the dashed line in fig. 5.3 represents the disc current at  $64 \text{ s}^{-1}$  in a 4 mM  $H_2O_2$  solution, containing no  $O_2$  and shows that, indeed,  $H_2O_2$  is stable at this electrode. If CoPc is deposited on Au (1400 Å, fig. 5.4) the behaviour is different: the reduction now proceeds in two waves. The

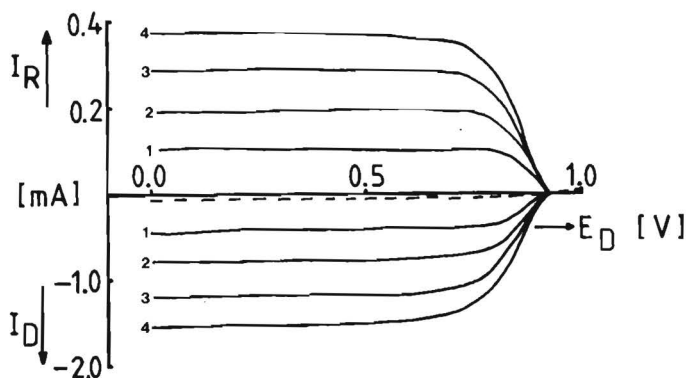


Fig. 5.3  $O_2$  reduction in 1 M KOH at a 1100 Å CoPc film, deposited on Cp (solid lines); scan rate  $50 \text{ mV s}^{-1}$ , rotation frequencies 4 (1), 16 (2), 36 (3) and  $64 \text{ s}^{-1}$  (4). Reduction of  $H_2O_2$  in  $O_2$ -free 4 mM  $H_2O_2$  solution in 1 M KOH (dashed line); scan rate  $50 \text{ mV s}^{-1}$ , rotation frequency  $64 \text{ s}^{-1}$ .

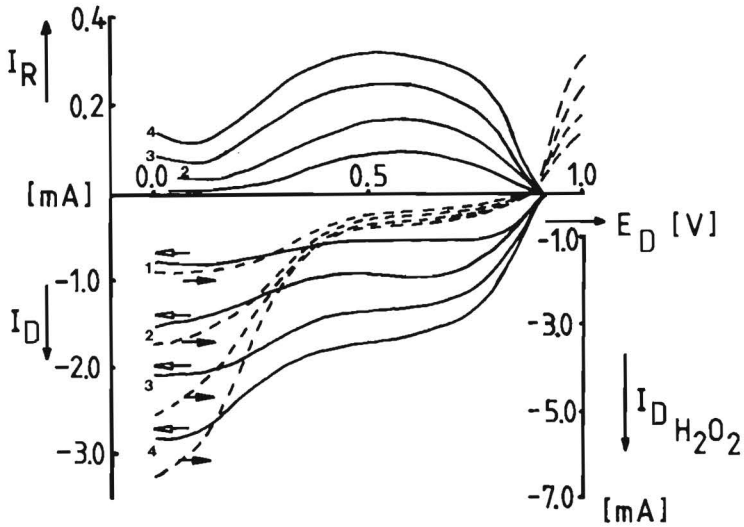


Fig. 5.4  $O_2$  reduction in 1 M KOH at a 1400 Å CoPc film deposited on Au (solid lines); scan rate  $50 \text{ mV s}^{-1}$ , rotation frequencies 4 (1), 16 (2), 36 (3) and  $64 \text{ s}^{-1}$  (4). Reduction of  $H_2O_2$  in  $O_2$ -free 4 mM  $H_2O_2$  solution in 1 M KOH (dashed lines) at the same scan rate and rotation frequencies.

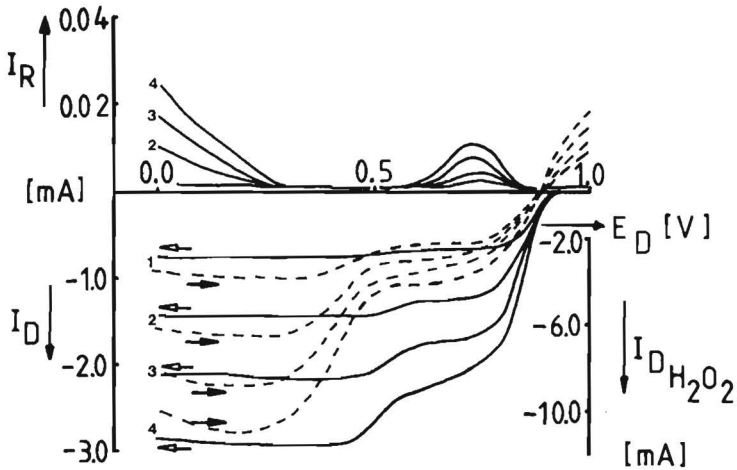


Fig. 5.5  $O_2$  reduction in 1 M KOH at a 2100 Å FePc film deposited on Au (solid lines); scan rate  $50 \text{ mV s}^{-1}$ , rotation frequencies 4 (1), 16 (2), 36 (3) and  $64 \text{ s}^{-1}$  (4). Reduction of  $H_2O_2$  in  $O_2$ -free 7 mM  $H_2O_2$  solution in 1 M KOH (dashed lines) at the same scan rate and rotation frequencies.



first wave is the reduction of  $O_2$  to  $H_2O_2$ ; during the second wave the diffusion-limited current for reduction of  $O_2$  to  $H_2O$  is reached. The results in  $O_2$ -free 4 mM  $H_2O_2$  solution (dashed lines) show that the second wave can be attributed to the subsequent reduction of the formed  $H_2O_2$  to  $H_2O$ . This conclusion is corroborated by the behaviour of the ring current. This  $O_2$  reduction in two waves is also observed on a bare Au electrode, except that the first wave is not so steep as with a CoPc film, deposited on Au. Since a second wave does not occur on a Cp substrate, and the  $H_2O_2$  reduction starts at the same potential as on bare Au, the subsequent reduction of the formed  $H_2O_2$  at the CoPc/Au electrode probably takes place at the gold substrate.

The results for a 2100 Å FePc film on Au are given in figure 5.5. The behaviour in dioxygen-free 7 mM  $H_2O_2$  solutions is again presented by the dashed lines. With Cp as substrate virtually the same results were obtained. Though the reduction seems to proceed in two waves, both waves correspond with  $O_2$  reduction to  $H_2O$  since only very small ring currents are observed. Below 0.5 V vs. RHE the diffusion-limited currents for  $O_2$  reduction to  $H_2O$  are reached; the first wave is somewhat kinetically limited.

The characterization of the films in  $O_2$ -free electrolyte was not possible. In most cases featureless cyclic voltammograms were obtained. As an example the results of CoPc films in 1 M KOH on three different substrates are given in figure 5.6. For films deposited on Au or Cp, no clear peaks can be observed at all. This is different on a Pt substrate, but here the peaks are obviously characteristic for the platinum itself. Nevertheless, two conclusions can be

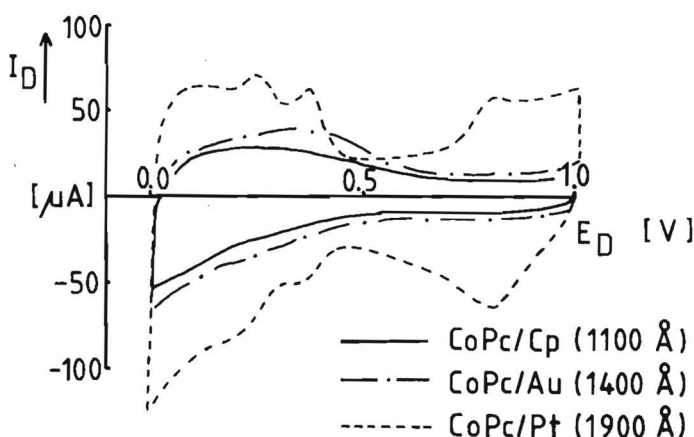


Fig. 5.6 Cyclic voltammetry in  $O_2$ -free 1 M KOH at CoPc films, deposited on three different substrates; scan rate 100 mV s<sup>-1</sup>.

drawn from these measurements, First, the electrolyte can penetrate into the film, otherwise the platinum peaks in figure 5.6 would not be visible. Secondly, the major part of the deposited catalyst is not detected electrochemically. Results obtained with irreversibly adsorbed phthalocyanines (see later in this section) show that both CoPc and FePc have redox peaks in the studied potential region. A Pc film of  $2000 \text{ \AA}$  thick corresponds to  $5.10^{-8}$  mol, assuming that the volume of a Pc molecule is about  $360 \text{ \AA}^3$ . This equals a charge of  $5.10^{-3} \text{ C}$  ( $n = 1$ ), a quantity that is clearly not seen in figure 5.6. This indicates that the major part of the molecules present is not in electrical contact with the substrate.

## 2. Irreversibly adsorbed phthalocyanines.

In figure 5.7 the results in  $\text{O}_2$ -free 1 M KOH are depicted. The Cp electrode was dipped for one minute in  $10^{-5}$ ,  $10^{-4}$  or  $10^{-3}$  M solutions of CoPc in pyridine. Though the obtained cyclic voltammograms were independent of the dipping time, with fresh dipping solutions the highest surface coverages are obtained. As compared to the Cp background a clear redox peak is present at 0.5 V vs. RHE. The peak is probably not related to the  $\text{Co}^{\text{II}}/\text{Co}^{\text{III}}$  but to the  $\text{Co}^{\text{I}}/\text{Co}^{\text{II}}$  redox couple, or to the ligand itself, because the  $\text{Co}^{\text{II}}/\text{Co}^{\text{III}}$  redox peak is situated at 1.2 V vs. RHE<sup>3</sup> at pH = 0. In 1 M KOH this potential with respect to RHE shifts to even higher values, if the redox process is pH-independent, because the potential of the reference electrode shifts 60 mV in cathodic direction compared to a pH-independent reference electrode. The peak surface i.e. the catalyst loading depends on the concentration of the dipping solution, so the adsorption seems to represent a fast equilibrium process. From the surface area under the peaks a catalyst loading of  $6.0 \cdot 10^{-11}$ ,  $1.6 \cdot 10^{-10}$  and  $2.6 \cdot 10^{-10} \text{ mol cm}^{-2}$  can be calculated for the  $10^{-5}$ ,  $10^{-4}$  and  $10^{-3}$  M dipping solutions respectively. One monolayer of adsorbed CoPc corresponds to  $1.4 \cdot 10^{-10} \text{ mol cm}^{-2}$  geometric surface area, assuming that the molecules lie flat on the surface and occupy an area of  $120 \text{ \AA}^2$ . Since even a polished Cp electrode will exhibit considerable surface roughness, the surface coverage ranges from about monolayer adsorption in the case of the  $10^{-3}$  M dipping solution, to submonolayer coverage with more dilute solutions. The measured  $\text{O}_2$  reduction on these electrodes (figure 5.7b) and the obtained ring currents (not displayed) show that all electrodes reduce  $\text{O}_2$  to  $\text{H}_2\text{O}_2$ . The  $E_{1/2}$  depends on the catalyst loading so the reaction is not yet reversible<sup>8</sup>. For comparison the results at  $16 \text{ s}^{-1}$  of a vacuum-

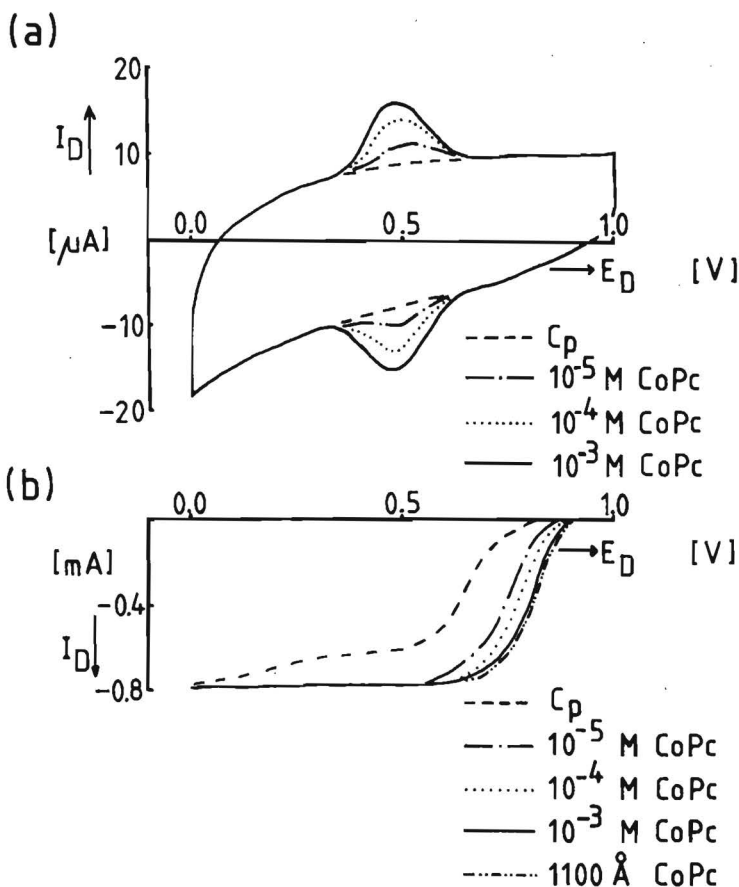


Fig. 5.7 Cyclic voltammetry in  $O_2$ -free 1 M KOH at CoPc, irreversibly adsorbed on Cp from pyridine solutions of different concentrations; scan rate  $100 \text{ mV s}^{-1}$  (5.7a);  $O_2$  reduction at the same electrodes in 1 M KOH; scan rate  $50 \text{ mV s}^{-1}$ , rotation frequency  $16 \text{ s}^{-1}$ ; for comparison the results for a  $1100 \text{ \AA}$  CoPc film under the same conditions are also presented (5.7b).

deposited CoPc film on Cp ( $1100 \text{ \AA}$ ) are also given in figure 5.7b: it has the same activity as an adsorbed monolayer of CoPc.

The same experiments were performed using FePc (figure 5.8). The characterization yields two redox peaks. The peak at  $850 \text{ mV}$  is probably due to the reaction:  $\text{Fe}^{\text{III}}\text{OH}^- + e^- \rightarrow \text{Fe}^{\text{II}} + \text{OH}^-$ . To which process the peak at  $450 \text{ mV}$  has to be ascribed is yet uncertain. The peak area strongly depends on the concentration of the dipping solutions: no peaks are detected using a  $10^{-5} \text{ M}$  FePc solution. The electrode prepared out of a  $10^{-3} \text{ M}$  FePc solution ( $1.6 \cdot 10^{-10} \text{ mol cm}^{-2}$ )

is very active for the  $O_2$  reduction in 1 M KOH (figure 5.8b). Dioxygen is reduced to water in virtually one wave, starting at 950 mV vs. RHE. With a lower catalyst loading ( $10^{-4}$  M FePc,  $2.10^{-11}$  mol  $cm^{-2}$ ) two waves are visible. The first one is kinetically limited; at higher overpotential the diffusion limited current for the reduction to  $H_2O$  is reached. The reason that the current drops again at still higher overpotential is probably the incomplete coverage with FePc. At such a high overpotential,  $O_2$  is also

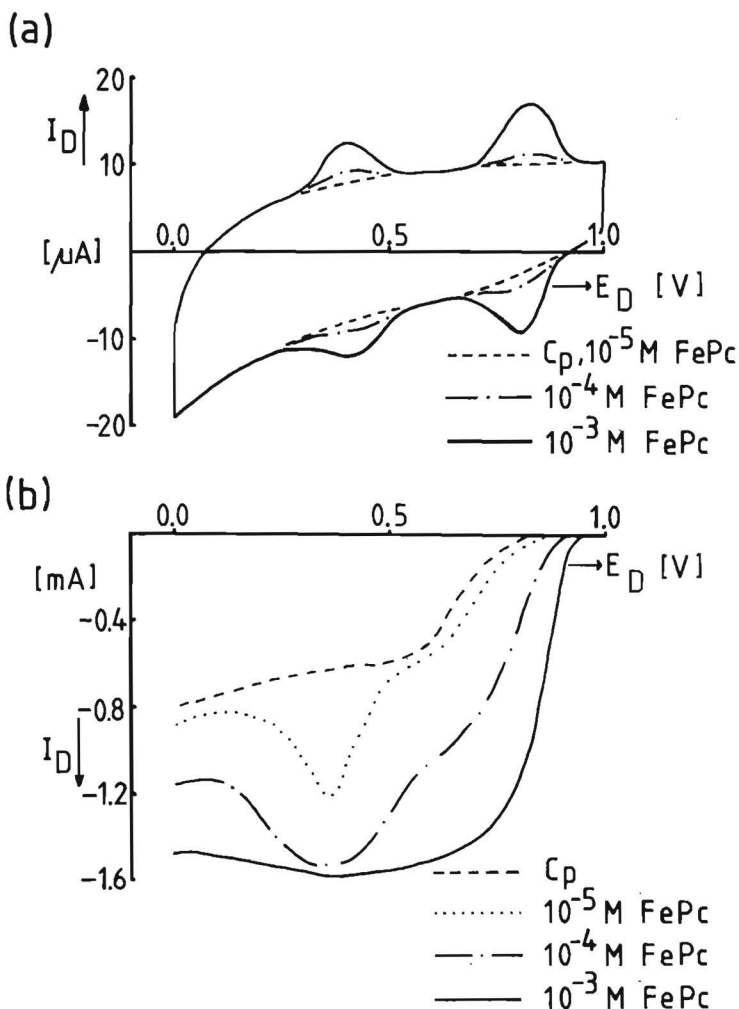


Fig. 5.8 Characterization in  $O_2$ -free 1 M KOH of FePc, irreversibly adsorbed on Cp from pyridine solutions of different concentrations; scan rate  $100 \text{ mV s}^{-1}$  (5.8a);  $O_2$  reduction on these electrodes in 1 M KOH; scan rate  $50 \text{ mV s}^{-1}$ , rotation frequency  $16 \text{ s}^{-1}$  (5.8b).

easily reduced on the uncovered substrate, leading, however, to the production of peroxide. Although no FePc can be detected on the surface in the case of a  $10^{-5}$  M dipping solution, it is clear from figure 5.8b that FePc is present: the disc current reaches values exceeding the diffusion-limited current for  $O_2$  to  $H_2O_2$ .

The electrodes prepared with the  $10^{-3}$  M CoPc or FePc solutions were also tested in  $O_2$ -saturated 0.5 M  $H_2SO_4$ . Results of an irreversibly adsorbed

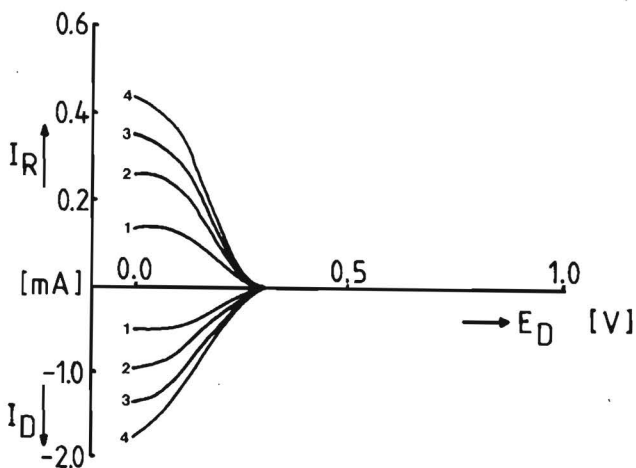


Fig. 5.9  $O_2$  reduction in 0.5 M  $H_2SO_4$  at CoPc, irreversibly adsorbed on Cp from a  $10^{-3}$  M pyridine solution; scan rate  $50 \text{ mV s}^{-1}$ , rotation frequencies 4 (1), 16 (2), 36 (3) and  $64 \text{ s}^{-1}$  (4).

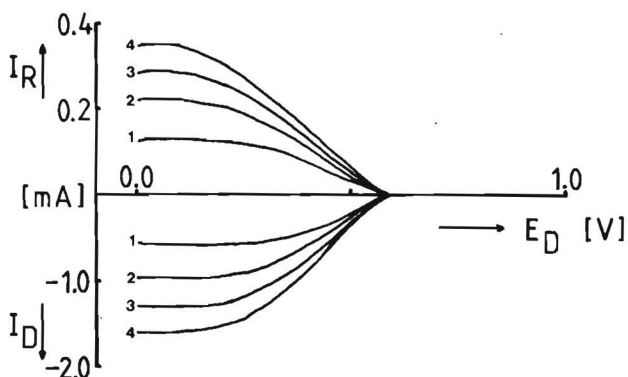


Fig.5.10  $O_2$  reduction in 0.5 M  $H_2SO_4$  at FePc, irreversibly adsorbed on Cp from a  $10^{-3}$  M pyridine solution; scan rate  $50 \text{ mV s}^{-1}$ , rotation frequencies 4 (1), 16 (2), 36 (3) and  $64 \text{ s}^{-1}$  (4).

monolayer CoPc are presented in figure 5.9. Comparison with figure 5.1 shows that the same result is obtained as with a vacuum-deposited CoPc film; the  $E_{1/2}$  in the case of an adsorbed monolayer is, however, somewhat shifted in anodic direction indicating the presence of a higher number of active sites <sup>8</sup>. An irreversibly adsorbed monolayer of FePc (figure 5.10) is more active than CoPc, but produces virtually only  $H_2O_2$  in this electrolyte. The stability was poor, but good enough to perform reliable RRDE-experiments.

#### 5.4 Discussion

The first question that arises from this work is in what part of the vacuum-deposited film the reaction takes place. As pointed out by Albery and Hillman <sup>9</sup> the reaction can take place in six different locations: at the electrode/film interface, at the electrolyte/film interface, throughout the whole film, or a reaction layer at the electrode surface, at the electrolyte interface or in the middle of the film. Which of the six possibilities represents the actual situation is to a large extent determined by physical properties of the film, such as permeability and electron conductivity. For instance, at a film with a low permeability and high conductivity the reaction proceeds at the electrolyte/film interface; in the case of a film with high permeability and low conductivity at the electrode/film interface. The figures 5.3, 5.4 and 5.6 show that the substrate is accessible for the electrolyte and the dissolved reactant. From the figures 5.1 and 5.9 one can conclude that only a small part (in the order of a monolayer) of the vacuum-deposited film is electrochemically active. If the whole film was active, a considerable shift of the  $E_{1/2}$  in anodic direction should have been observed in acid solution, as compared to an adsorbed monolayer, since the reaction is irreversible in this electrolyte. Such a shift has indeed been observed with cobalt chelates, directly incorporated into a porous conducting polymer <sup>8</sup>. The fact that the  $E_{1/2}$  of a vacuum deposited film has somewhat shifted in cathodic direction, indicates that even less than a monolayer is active. Since the electrolyte can penetrate into the film, this behaviour must be attributed to a very low conductivity of the film. Therefore, the  $O_2$  reduction on vacuum-deposited film takes place at the electrode/film interface. The layers on top are not in electrical contact with the substrate and therefore not active. Moreover, they hinder the diffusion of  $O_2$  to the electrode interface, resulting in somewhat inferior catalytic properties of the vacuum-deposited films. This conclusion was verified by a study of electrodes in  $O_2$ -saturated 1 M KOH, consisting of

both a CoPc and a FePc film of about  $1000 \text{ \AA}$ , deposited on Au (figure 5.11). If the FePc film is situated directly on the Au substrate and the CoPc film on top of it (solid line), the electrode should exhibit FePc behaviour i.e. reduction to water, if the above described model is correct. In the reverse

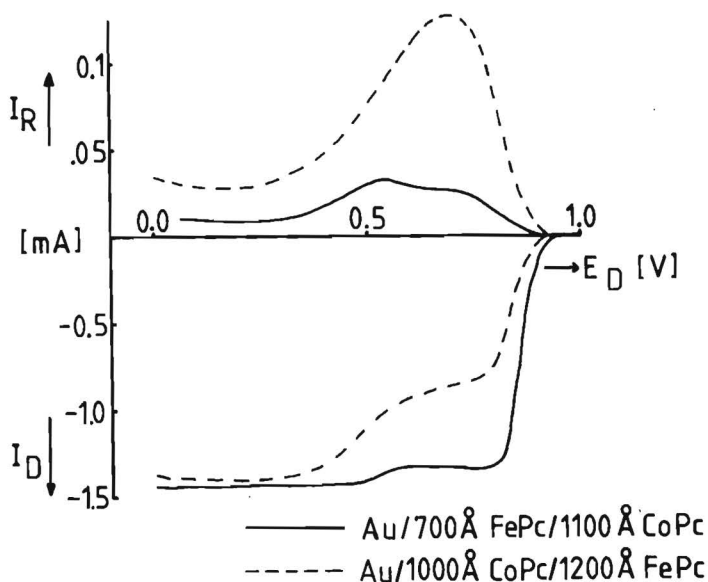


Fig.5.11  $\text{O}_2$  reduction in 1 M KOH at a Au electrode covered with both a CoPc and a FePc film; scan rate  $50 \text{ mV s}^{-1}$ , rotation frequency  $16 \text{ s}^{-1}$ . Dashed line: the CoPc film directly on the gold and the FePc film on top. Solid line: the FePc film directly on the Au and the CoPc film on top.

case (CoPc directly on the Au, FePc on top, dashed line) the  $\text{O}_2$  should at least initially be reduced to  $\text{H}_2\text{O}_2$  which can subsequently be reduced at the Au substrate at higher overpotential. Figure 5.11 shows that indeed this is found experimentally. Only the second wave of the dashed curve has somewhat shifted in anodic direction as compared to figure 5.5, perhaps caused by chemical decomposition (but not electrochemical reduction) of the formed  $\text{H}_2\text{O}_2$  at the FePc film on top. The latter phenomenon is probably also responsible for the increased production of water at the vacuum-deposited FePc film as compared to irreversibly adsorbed FePc (figures 5.2 and 5.10 respectively). If the FePc is present as a monolayer, the formed  $\text{H}_2\text{O}_2$  can easily diffuse into the solution; if the electrode is covered with a FePc film, a relatively high peroxide concentration can be build up inside the film, resulting in an increased chemical decomposition of this peroxide. The formed

O<sub>2</sub> can again be reduced at the electrode/film interface.

What remains to be explained is the difference between Fe and Co as the central metal atom. Cobalt phthalocyanine reduces O<sub>2</sub> to H<sub>2</sub>O<sub>2</sub> only, both in acid and alkaline electrolyte. The dependence of the E<sub>1/2</sub> of the O<sub>2</sub> reduction versus RHE, as a function of the pH, shows that this reduction is pH independent: the potential of the RHE itself namely shifts 60 mV per pH unit versus a pH-independent reference electrode. The rate determining step is most likely the pH-independent formation of superoxide<sup>10</sup>: O<sub>2</sub> + e<sup>-</sup> → O<sub>2</sub><sup>-</sup>. The behaviour of FePc is more complex. The O<sub>2</sub> reduction seems to proceed in two waves. The second wave coincides with the potential where H<sub>2</sub>O<sub>2</sub> is reduced to H<sub>2</sub>O quantitatively. Therefore, in this potential region reduction of O<sub>2</sub> to H<sub>2</sub>O<sub>2</sub> and subsequent reduction of the formed H<sub>2</sub>O<sub>2</sub> is possible. The first wave, however, is more interesting, since this wave also virtually corresponds with reduction of O<sub>2</sub> to H<sub>2</sub>O, while H<sub>2</sub>O<sub>2</sub> is quite stable on the electrode at these low overpotentials. In the beginning of this wave oxygen is even reduced to water without the production of H<sub>2</sub>O<sub>2</sub> as an intermediate, i.e. the so-called direct 4e<sup>-</sup> reduction. A survey of the literature shows that direct reduction of O<sub>2</sub> occurs on noble metals as platinum and silver<sup>11</sup>, electrodes prepared by under potential deposition (UPD) of metals<sup>12</sup>, and dicofacial dicobalt porphyrins<sup>13</sup>. In all cases the unique selectivity is explained by assuming bridging adsorption. In our view the first wave at FePc is also due to bridging adsorption: the formation of dimeric μ-peroxo oxygen adducts on iron containing chelates has been well documented<sup>14</sup>.

Since it is most likely that the adsorbed molecules lie parallel to the surface, these dimeric species will be very few in number: probably they can only be formed at places on the surface where the surface roughness enables the adsorption of two adjacent molecules with the iron centres properly spaced (ca. 4 Å) for the formation of dimeric O<sub>2</sub> adducts. Their relative low number explains the observation that the first wave is kinetically limited.

So in fact a monolayer of adsorbed FePc contains two different active species: monomeric and dimeric O<sub>2</sub> adducts. At very low overpotential only the dimers are able to reduce dioxygen, so no H<sub>2</sub>O<sub>2</sub> is formed. At higher overpotential also the monomers start to reduce O<sub>2</sub> with H<sub>2</sub>O<sub>2</sub> as the intermediate product: the ring current increases. The lower activity of the monomeric species is compensated by a much higher concentration of these sites at the surface. At even higher overpotential the reduction of the peroxide proceeds quantitatively: the ring current drops to zero and the limiting current for the reduction of O<sub>2</sub> to H<sub>2</sub>O is reached.



It is interesting to compare the results of FePc, irreversibly adsorbed on ordinary pyrolytic graphite, with the results of Zagal with tetrasulfonated iron phthalocyanine (FeTSPc), adsorbed on the basal plane of "stress annealed" pyrolytic graphite<sup>3</sup>. The latter substrate approximates a perfectly smooth surface. If the adsorbed molecules lie flat on the surface, the formation of dimeric O<sub>2</sub> adducts is very unlikely due to the absence of surface roughness. Indeed the first wave of the O<sub>2</sub> reduction on FeTSPc has almost vanished completely if the basal plane is used as a substrate.

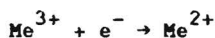
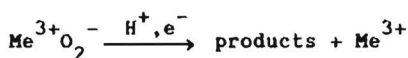
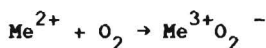
### 5.5 References

1. R. Jasinski, J. Electrochem. Soc. 112 (1965) 526.
2. H. Jahnke, M. Schönborn and G. Zimmermann, Topics in current chemistry 61 (1976) 133.
3. J. Zagal-Moya, Ph.D. Thesis, Case Western Reserve University, Cleveland (1978).
4. H. Behrel, W. Clauberg and G. Sandstede, Ber. Bunsenges. Phys. Chem. 81 (1977) 54.
5. M. Savy, C. Bernard and G. Magner, Electrochim. Acta 20 (1975) 383.
6. R.A. Bull, F.R. Fan and A.J. Bard, J. Electrochem. Soc. 130 (1983) 1636.
7. F. van den Brink, W. Visscher and E. Barendrecht, J. Electroanal. Chem. 157 (1983) 283; idem 157 (1983) 305; idem 172 (1984) 301; idem 175 (1984) 279.
8. A. Elzing, A. van der Putten, W. Visscher and E. Barendrecht, J. Electroanal. Chem. 200 (1986) 313 (chapter 4 of this thesis).
9. W.J. Albery and A.R. Hillman, J. Electroanal. Chem. 170 (1984) 27.
10. E. Yeager, Electrochim. Acta 29 (1984) 1527.
11. P. Fischer and J. Heitbaum, J. Electroanal. Chem. 112 (1980) 231.
12. K. Jüttner, Electrochim. Acta 29 (1984) 1597.
13. J.P. Collman, M. Marocco, P. Denisevich, C. Koval and F.C. Anson, J. Electroanal. Chem. 101 (1979) 117
14. G. McLendon and A.E. Martell, Coord. Chem. Rev. 19 (1976) 1.

## Chapter 6 Redox potential and electrocatalysis of dioxygen reduction on transition metal chelates

### 6.1 Introduction

Since the introduction of cobalt phthalocyanine (CoPc) as electrocatalyst for cathodic  $O_2$  reduction by Jasinski <sup>1</sup> in 1965, transition metal chelates have been studied for this purpose <sup>2</sup>. In figure 2.1, the molecular structures of the most extensively investigated chelates are given. For the qualitative explanation of their activity, different concepts were developed. Application of the MO theory <sup>2</sup> to these systems has shown that the highest interaction of  $O_2$  with the central metal ion will be obtained with Fe(II) and Co(II). The higher this interaction, the more the O-O bond is weakened, the more easily the molecule is reduced. Another approach has been given by Ulstrup <sup>3</sup>. If the electronic levels of electrode and reactant lie too far apart, the transition of electrons is improbable. The catalyst then should act as a mediator, supplying intermediate levels, increasing the probability of electron transport. A third concept is that of redox catalysis, developed by Beck <sup>4</sup>. In this concept the redox potential of the central metal ion is crucial. During the adsorption of  $O_2$ , the metal ion is oxidized, thereby reducing the  $O_2$  molecule. The simplest representation is as follows:



In order to account for supplementary experimental evidence, a somewhat modified model was developed <sup>4</sup> in which the central metal ion could also be partly oxidized.

From this scheme it is clear that the potential where  $O_2$  is reduced should be closely related to the  $Me^{II}/Me^{III}$  redox potential of the central metal ion. Nevertheless, in relatively few cases these redox potentials have actually been measured in the same electrolyte in which the  $O_2$  reduction is studied. In most cases, if measured at all, these redox potentials were determined in water-free media, since this results in sharp peaks. The effect of

the pH on the redox potential in such water free media is rather difficult to translate to that of the pH in water as a solvent. Moreover, it is questionable whether or not it is allowed to identify values for the redox potential found in solution to that adsorbed on the electrode substrate. Recently, Ni and Anson<sup>5</sup> have shown a 340 mV difference between a dissolved and an adsorbed cobalt porphyrin. A meaningful correlation between O<sub>2</sub> reduction and redox potential, however, is only possible if both processes are studied in the same electrolyte. A good example of such an approach is the work of Zagal<sup>6</sup> who investigated both redox potentials and O<sub>2</sub> reduction of the water soluble cobalt and iron tetrasulphonated phthalocyanines (TSPc), adsorbed on pyrolytic graphite, as a function of pH. From previous work in our laboratory<sup>7,8</sup> (chapters 4 and 5), it has become clear that irreversibly adsorbed monolayers of FePc, CoPc and CoTAA can be prepared by dipping a pyrolytic graphite (Cp) disc into pyridine solutions of the corresponding chelates. These phenomena gave rise to a more detailed study of pH effects on the adsorbed macrocycles. The objective of this research is to measure the redox potentials of the different chelates as a function of the solution pH, and to establish the correlation between these values and the observed E<sub>1/2</sub>'s for O<sub>2</sub> reduction in the same electrolytes.

## 6.2 pH and thermodynamics of O<sub>2</sub> reduction

The study of O<sub>2</sub> reduction is complicated by the fact that different products can be formed: O<sub>2</sub> can be either reduced directly to water, or to H<sub>2</sub>O<sub>2</sub> which can be the stable endproduct or is subsequently reduced to H<sub>2</sub>O. The first step in the reduction mechanism is most likely the formation of the superoxide<sup>10,11</sup>:  

$$O_2 + e^- \rightarrow O_2^-$$
The equilibrium potential of this couple is -0.33 V vs. NHE and is independent of the solution pH. The equilibrium potentials of both the O<sub>2</sub>/H<sub>2</sub>O couple and the O<sub>2</sub>/H<sub>2</sub>O<sub>2</sub> couple decrease 60 mV per increase in pH unit (figure 6.1). The driving force for superoxide formation increases rapidly with increasing pH. In fact, at Hg, the reduction of O<sub>2</sub> to H<sub>2</sub>O<sub>2</sub> at high pH is a reversible reaction<sup>12</sup>. Therefore, if the reduction of O<sub>2</sub> on transition metal chelates is investigated as a function of pH, two simultaneously occurring effects have to be accounted for:

- the stability of superoxide changes as a function of pH;
- the redox potential of the central metal ion can change, and thus influence the kinetics of the reaction.

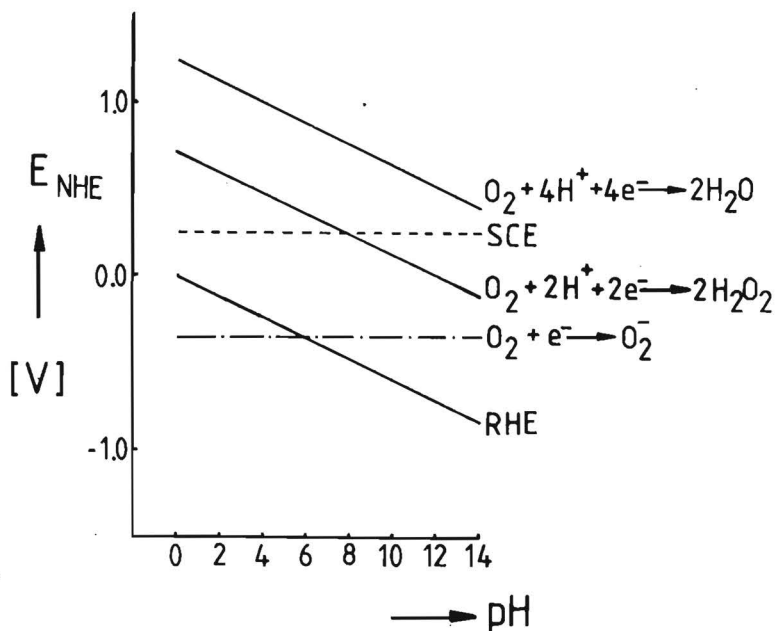


Fig. 6.1: Pourbaix diagram for  $\text{O}_2$  reduction.

### 6.3 Experimental

In order to eliminate mass-transport problems, the rotating disc electrode technique was used<sup>13</sup>. The chelates were applied onto a polished ( $0.3 \mu\text{m Al}_2\text{O}_3$ , Buehler) Cp disc ( $A = 0.5 \text{ cm}^2$ ) via irreversible adsorption during one minute out of  $10^{-3} \text{ M}$  pyridine solutions. Three chelates were studied: CoPc and FePc (Eastman Kodak), and CoTAA, kindly provided by Professor K. Wiesener (Technische Universität, Dresden, DDR). The electrodes were studied in the following buffer solutions: pH = 0:  $\text{HClO}_4$ , pH = 2:  $\text{KCl}/\text{HCl}$ , pH = 4:  $\text{KH Phthalate}/\text{HCl}$ , pH = 6:  $\text{KH}_2\text{PO}_4/\text{NaOH}$ , pH = 8:  $\text{HCl}/\text{H}_3\text{BO}_3/\text{NaOH}$ , pH = 10,12:  $\text{NaOH}/\text{glycine}/\text{NaCl}$ , pH = 14:  $\text{NaOH}$ . All electrochemical experiments were performed in a standard three-compartment electrochemical cell. A Pt foil is used as a counter electrode; a reversible hydrogen electrode (RHE) as a reference. All measured potentials are given with respect to RHE. Redox potentials were determined by scanning the disc potential in  $\text{O}_2$ -free solution ( $\text{N}_2$ ) from 1.0 V to 0.0 V and back again with  $100 \text{ mV s}^{-1}$ . In some cases (pH = 0-4), the upper scan limit was 1.2 V, since there is a CoPc redox peak present in that region.

The  $\text{O}_2$  reduction was measured by scanning the disc potential with  $50 \text{ mV s}^{-1}$  in  $\text{O}_2$ -saturated solutions from 1.0 V to 0.0 V and vice versa, at a

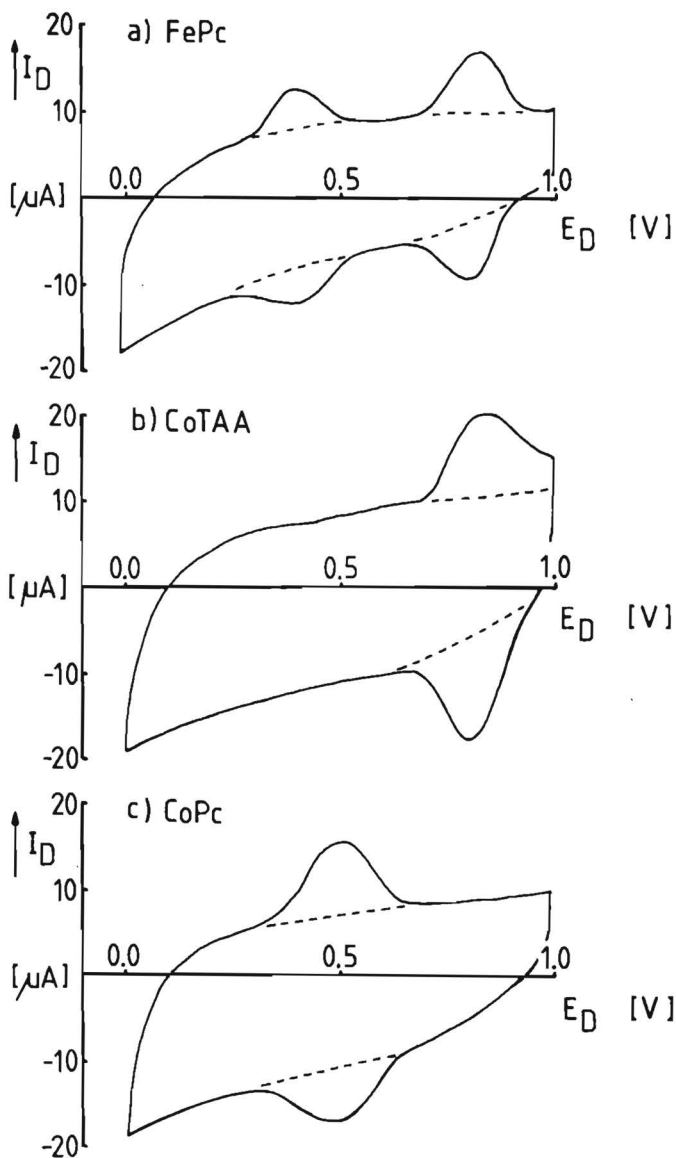


Fig. 6.2: Determination of the redox potentials of FePc (a), CoTAA (b) and CoPc (c), irreversibly adsorbed on Cp. The dashed curves represent the Cp background. Electrolyte:  $O_2$ -free 1 M NaOH; scan rate  $100 \text{ mV s}^{-1}$ .

rotation frequency of  $16 \text{ s}^{-1}$ . Since the conductivity of the solutions of  $\text{pH} = 2-6$  was insufficient, during  $O_2$  reduction experiments one mol  $\text{KNO}_3$  per litre electrolyte was added. This addition had no effect on the measured redox potentials.

## 6.4 Results

An example of the cyclic voltammograms of the different adsorbed chelates in 1 M NaOH is given in figure 6.2. Compared to the Cp background (dashed curves), the adsorbed molecules give rise to one or more redox peaks. In the case of a reversible electron transfer to adsorbed species, the redox potential is equal to the peak potential and the peak area proportional to the catalyst loading.

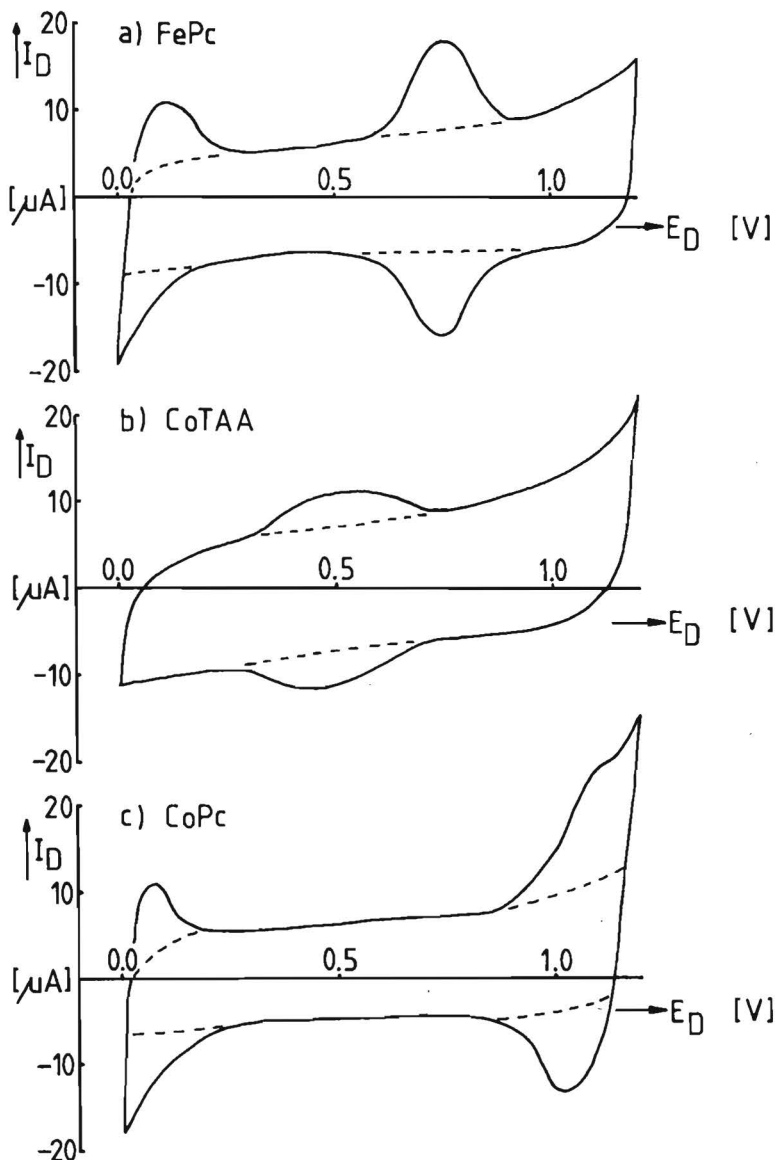


Fig. 6.3: The same as figure 6.2, but now at pH = 2.

Although a difference in the number of active sites affects the location of the  $O_2$ -reduction wave <sup>7</sup>, this difference is only small ( $1.6 \cdot 10^{-10} \text{ mol cm}^{-2}$  for FePc;  $2.3 \cdot 10^{-10} \text{ mol cm}^{-2}$  for CoTAA and  $2.6 \cdot 10^{-10} \text{ mol cm}^{-2}$  for CoPc) and will therefore only have a small effect. The peaks in the cyclovoltammograms in acid media were somewhat less resolved (figure 6.3). The peak potential of CoTAA at these pH's was difficult to determine due to peak broadening. The reason for this peak broadening is unclear but was not further investigated. At pH = 0, no accurate determination of the CoTAA redox potential was possible. The redox potentials as a function of the pH are summarized in figure 6.4.

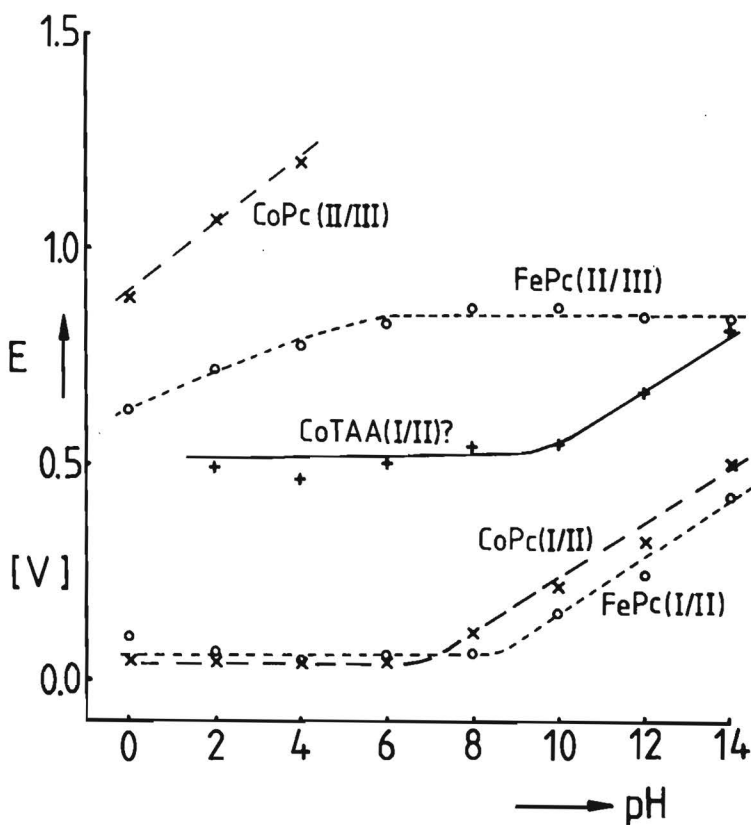


Fig. 6.4: Redox potentials of FePc, CoTAA and CoPc as a function of the solution pH.

The results of the  $O_2$ -reduction experiments are depicted in the figures 6.5-6.7. Since the diffusion-limited currents depend on the electrolyte under consideration, mainly due to differences in  $O_2$  solubility, the disc current

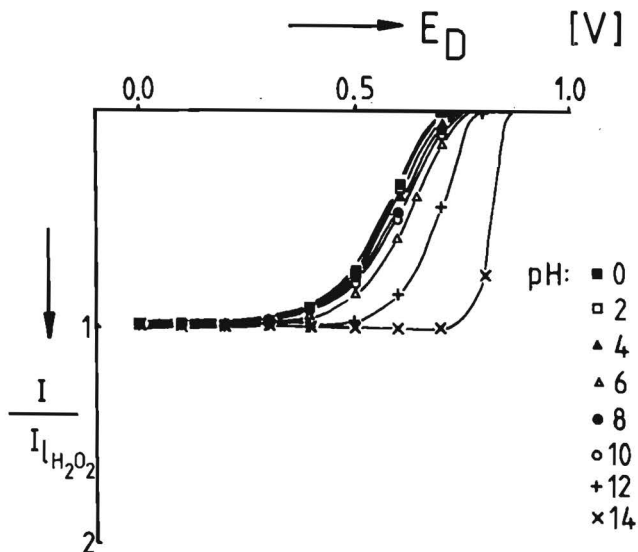


Fig. 6.5:  $O_2$  reduction on CoTAA, irreversibly adsorbed on Cp, as a function of the solution pH. Rotation frequency  $16 \text{ s}^{-1}$ . To compensate for different  $O_2$  solubilities in the various buffer solutions, the disc current  $I$  is divided by the diffusion limited current for  $O_2$  reduction to  $H_2O_2$  in the corresponding electrolyte,  $I_L$ .

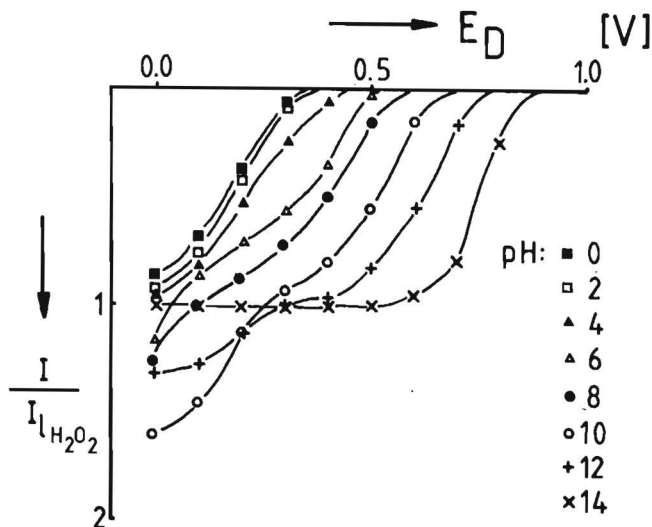


Fig. 6.6:  $O_2$  reduction on CoPc, irreversibly adsorbed on Cp, as a function of the solution pH.



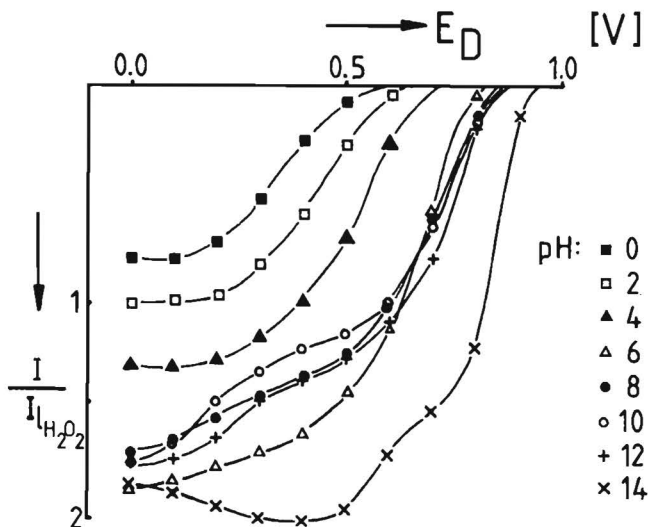


Fig. 6.7:  $O_2$  reduction on FePc, irreversibly adsorbed on Cp, as a function of the solution pH.

is plotted as  $I_D$  divided by  $I_L(H_2O_2)$ , the latter being the diffusion-limited current for  $O_2$  reduction to  $H_2O_2$  ( $n = 2$ ). Since CoTAA reduces  $O_2$  to  $H_2O_2$  exclusively<sup>9</sup>, the obtained limiting current at CoTAA in the corresponding electrolyte was taken as  $I_L(H_2O_2)$ .

### 6.5 Discussion

The assignment of the different redox peaks is not completely straightforward. Both CoPc and FePc behave similarly to the water-soluble CoTSPc and FeTSPc, only the values of the different redox potentials are somewhat shifted<sup>7,14</sup>. The high potential of CoPc at low pH is related to the  $Co^{II}/Co^{III}$  redox couple. As already established by Zagal<sup>6</sup>, this redox process is pH independent; its peak, measured vs. RHE therefore shifts ca. 60 mV in a positive direction per increase in pH unit. The CoPc peak, observed at high pH (figure 6.2c) is probably related to the  $Co^I/Co^{II}$  redox couple<sup>14</sup>. Below  $pH = 7$ , this redox process becomes pH dependent: the potential vs. the pH dependent RHE reaches a constant value. The most anodic peak of FePc (figure 6.2a) is related to the  $Fe^{II}/Fe^{III}$  redox process<sup>6</sup>. This redox couple is pH dependent for  $6 < pH < 14$ . The other FePc peak is probably related to the  $Fe^I/Fe^{II}$  redox couple. This peak is pH dependent from  $pH = 0-8$ ; at higher pH this process becomes pH independent. This redox process will not be discussed any further since for the first wave of the  $O_2$  reduction, the  $Fe^{II}/Fe^{III}$  peak is involved.

The only available information about the redox behaviour of CoTAA is obtained with a slurry electrode<sup>4</sup> in 4.5 N H<sub>2</sub>SO<sub>4</sub>. A redox process was observed at ca. 0.5 V vs. RHE, which was attributed to either the two-electron oxidation of the ring system, or to the Co<sup>II</sup>/Co<sup>III</sup> redox couple. In our view, however, the CoTAA redox process more likely represents the Co<sup>I</sup>/Co<sup>II</sup> redox couple; for a Co<sup>II</sup>/Co<sup>III</sup> system, the potential would be very low. Compared to CoPc, the Co<sup>I</sup>/Co<sup>II</sup> peak of CoTAA shows the same pH dependence, however, the values of the CoTAA redox potentials are several hundreds of millivolts higher.

Before entering into the relation between the redox potentials and the observed O<sub>2</sub> reduction, some general features of the figures 6.5-6.7 will be discussed. As stated before, with CoTAA only H<sub>2</sub>O<sub>2</sub> is produced (figure 6.5). With CoPc (figure 6.6) initially H<sub>2</sub>O<sub>2</sub> is formed which is to some extent further reduced to H<sub>2</sub>O at pH = 6-12. At pH = 14 only H<sub>2</sub>O<sub>2</sub> is formed. In the case of FePc (figure 6.7), the main product is H<sub>2</sub>O at high pH. This difference in selectivity of FePc compared to the cobalt-containing chelates has been discussed elsewhere<sup>8,15</sup>. Even at pH 14, the reduction to water is occurring at potentials which are far away from the theoretically obtainable 1.23 V. Contrary to the reduction of O<sub>2</sub> to H<sub>2</sub>O<sub>2</sub>, the reduction to H<sub>2</sub>O is still slow at this pH.

For the comparison of CoTAA with CoPc, for both complexes both the redox potentials E<sub>p</sub> and half-wave potentials E<sub>1/2</sub> for O<sub>2</sub> reduction to H<sub>2</sub>O<sub>2</sub> are presented in figure 6.8. The CoTAA redox potential decreases 60 mV per pH unit going from pH = 14 to pH = 10. The same applies to the E<sub>1/2</sub> for the O<sub>2</sub> reduction at CoTAA. Below pH = 10, the redox potential remains constant. Figure 6.8 shows that the same is true for E<sub>1/2</sub>. With CoPc similar behaviour is obtained, only the values are deviating.

Especially in acid media, the difference in redox potential between CoPc and CoTAA is also reflected in the E<sub>1/2</sub>'s. At pH = 0, E<sub>1/2</sub> of CoTAA is 400 mV more anodic than E<sub>1/2</sub> of CoPc. At higher pH, this difference becomes less; at pH = 14 it is 70 mV, despite a 300 mV difference in redox potential. Similar values for E<sub>1/2</sub> at pH = 14 have been found on other peroxide-producing substrates like Au and Hg<sup>8,12</sup>. This shows that at this pH, the reduction to H<sub>2</sub>O<sub>2</sub> has become so reversible that the actual redox state of the catalyst is less important. An interesting observation is that despite the inferior results in acid as compared to alkaline solution, from the fuel cell point of view, the O<sub>2</sub> reduction to H<sub>2</sub>O<sub>2</sub> as such is more catalyzed in acid than in alkaline media. At pH = 14, E<sub>1/2</sub> for O<sub>2</sub> reduction is shifted ca. 300 mV in anodic

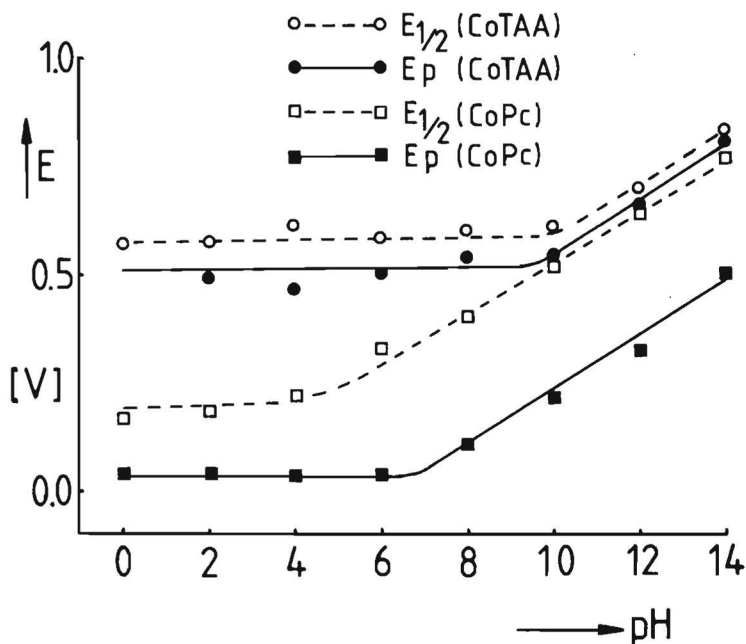


Fig. 6.8: pH dependence of the redox potentials  $E_p$  of CoPc and CoTAA, and the  $E_{1/2}$  of the  $O_2$  reduction to  $H_2O_2$ .

direction, compared to the standard potential of superoxide formation; at pH = 0 this shift is ca. 900 mV with CoTAA.

In the case of FePc, the  $Fe^{II}/Fe^{III}$  redox peak is constant from pH = 6 to pH = 14. In general this is also true for the measured  $O_2$  reduction, only at high pH there is some deviation. A measurement at pH = 13 (not displayed) resulted in a wave that virtually coincided with the wave of pH = 14. Whether this behaviour is due to a drastic increase in conductivity, going from pH = 12 to pH = 13, or that Fe chelates are more influenced by complexing anions of the buffer solutions, is unclear.

### 6.6 Concluding remarks

Summarizing, this work has shown that in the case of an irreversible  $O_2$  reduction, there is a clear correlation between the redox potential of the central metal ion and the observed  $O_2$ -reduction behaviour. With increasing reversibility of the reaction, the actual redox state of the catalyst becomes less important.

A comparison between CoPc and CoTAA in acid media shows that differences in redox potential severely influence the activity. In our view this influence is

underestimated so far, probably because most of the work published has been performed with gas-diffusion electrodes. The presence of a vast amount of catalyst molecules and the nature of this electrode (wetting properties) overshadow the performance of the individual molecules. With gas-diffusion electrodes only small differences in activity are found<sup>2</sup>, contrary to the results of rotating disc experiments. This work demonstrates that changes in the macrocyclic ring structures have a profound effect on the catalytic activity (400 mV increase in  $E_{1/2}$  going from Pc to TAA), due to differences in ligand strength. Especially the size and form of the conjugated  $\pi$ -system and the  $N_4$  cage (square in the case of CoPc, rectangular for CoTAA) deserve more attention.

### 6.7 References

1. R. Jasinski, J. Electrochem. Soc. 112 (1965) 526.
2. For a review of the early work: H. Jahnke, M. Schönborn and G. Zimmermann, Topics in current chemistry 61 (1976) 133.
3. J. Ulstrup, J. Electroanal. Chem. 79 (1977) 191.
4. F. Beck, J. Appl. Electrochem. 7 (1977) 239.
5. C.L. Ni and F.C. Anson, Inorg. Chem. 24 (1985) 4754.
6. J. Zagal-Moya, Ph.D. Thesis, Case Western Reserve University, Cleveland (1978).
7. A. Elzing, A. van der Putten, W. Visscher and E. Barendrecht, J. Electroanal. Chem. 200 (1986) 313 (chapter 4 of this thesis).
8. A. van der Putten, A. Elzing, W. Visscher and E. Barendrecht, J. Electroanal. Chem., accepted for publication (chapter 5 of this thesis).
9. A. van der Putten, A. Elzing, W. Visscher and E. Barendrecht, J. Electroanal. Chem. 205 (1986) 233 (chapter 10 of this thesis).
10. D.T. Sawyer and E.T. Seo, Inorg. Chem. 16 (1977) 499.
11. E. Yeager, Electrochim. Acta 29 (1984) 1527.
12. C.J. van Velzen, M. Sluyters-Rehbach, A.G. Remijnse, G.J. Brug and J.H. Sluyters, J. Electroanal. Chem. 134 (1982) 87.
13. J. Albery, 'Electrode kinetics', Clarendon Press, Oxford (1975).
14. S. Zecevic, B. Simic-Glavaski and E. Yeager, J. Electroanal. Chem. 196 (1985) 339.
15. A. Elzing, A. van der Putten, W. Visscher and E. Barendrecht, to be published.

**Chapter 7** The four-electron reduction of dioxygen to water on a planar dicobalt chelate

For almost two decades, 3d transition metal chelates have been studied as electrocatalysts for the cathodic reduction of dioxygen. The best activities were obtained with the  $N_4$  chelates of Fe and Co <sup>1</sup>. It was also shown that mononuclear Co chelates reduce dioxygen to hydrogen peroxide; only with Fe as a central metal ion was reduction of dioxygen to water observed. In 1979 Collman, Anson, and collaborators <sup>2</sup>, however, reported the reduction of dioxygen to water on the cofacial dicobaltporphyrin (fig. 7.1a). The two por-

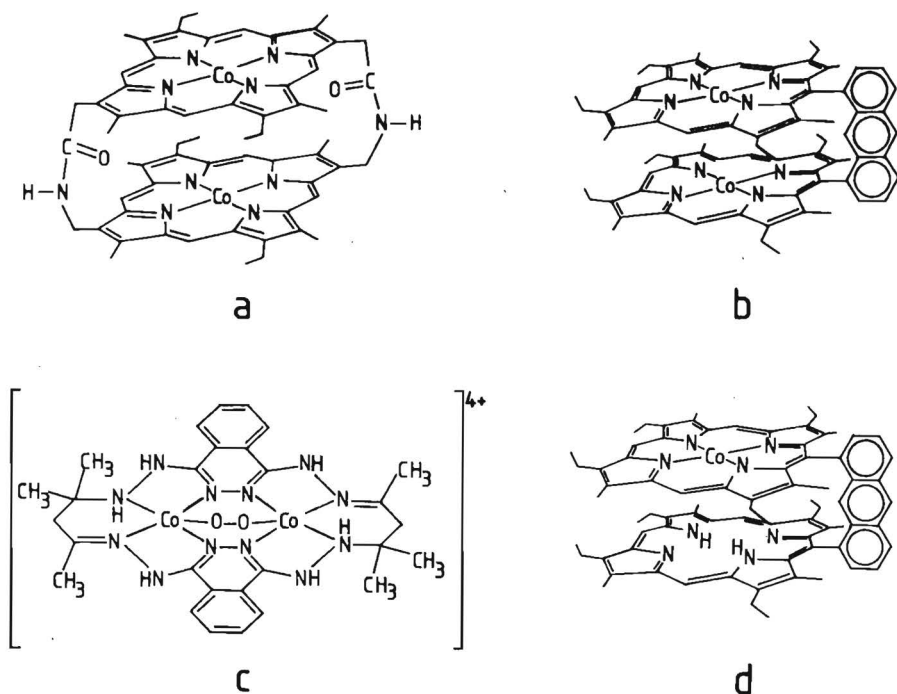


Fig. 7.1 Molecular structure of some dinuclear cobalt chelates:  
 (a) amide bridged dicofacial dicobalt porphyrine  $Co_2FTF_4$  (ref. 2)  
 (b) planar dicobalt chelate  $Co_2TAPH^{4+}$  (ref. 3)  
 (c) anthracene linked dicofacial dicobalt porphyrin (ref. 4)  
 (d) idem, containing only one Co atom (ref. 5)

phyrin rings are so spaced that bridging coordination of  $O_2$  becomes possible. Clearly, this bridging coordination, requiring the presence of two Co centres at the appropriate distance, is a crucial condition for the occurrence of  $4e^-$  reduction. In principle, this condition can also be fulfilled by planar chelates, containing two Co ions. Indeed,  $4e^-$  reduction of dioxygen on the planar cobalt complex, depicted in fig. 7.1b, was reported recently by Yeager and Sarangapani<sup>3</sup>.

We now report our results with a different planar dinuclear Co complex, namely diaqua-dichloro-bis(3,5-di-2-pyridyl-1,2,4-triazolato)dicobalt(II)

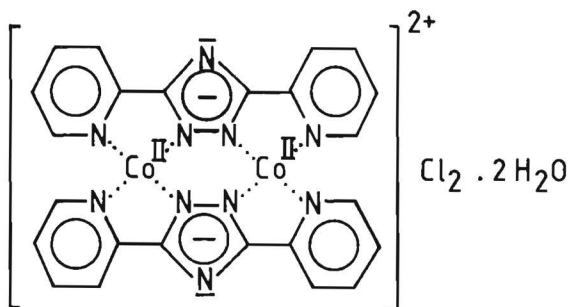


Fig. 7.2 Molecular structure of  $Co_2dpt_2Cl_2$

$(Co_2(dpt)_2Cl_2, \text{ fig. 7.2})$ , kindly provided by Mr. R. Prins, State University of Leiden. The electrochemical measurements were performed with a rotating ring (Pt)-pyrolytic graphite disc electrode ( $S = 0.5 \text{ cm}^2$ ;  $M = 0.27$ ), in a standard three-compartment electrochemical cell. All potentials are given with respect to the reversible hydrogen electrode (RHE). The ring was slightly platinumized to ensure quantitative  $H_2O_2$  detection; the ring potential was set at 1.2 V vs. RHE. Before each experiment, the ring was activated by periodic evolution of hydrogen and oxygen for 1 min. The catalyst was applied to the disc (previously polished with  $0.3 \mu\text{m } Al_2O_3$ , Buehler) via irreversible adsorption from a  $5 \times 10^{-3} \text{ M}$  solution of  $Co_2(dpt)_2Cl_2$  in warm ( $\sim 40^\circ\text{C}$ ) dimethyl sulfoxide. Since the adsorption process appeared to be slow, an adsorption time of 2 h was used. The reduction of  $O_2$  was measured both in alkaline and acidic  $O_2$ -saturated solutions (1 M KOH and 0.5 M  $H_2SO_4$ , respectively), by scanning the disc potential from 1.0 to 0.2 V vs. RHE at  $50 \text{ mV s}^{-1}$ . Moreover, an attempt was made to characterize the disc electrode in  $O_2$ -free 1 M KOH. The results for the  $O_2$  reduction in alkaline solution are given in fig. 7.3, the curves for which were taken after ca. 5 scans at  $64 \text{ s}^{-1}$ . During the first scans, qualitatively the same results were obtained; however, somewhat

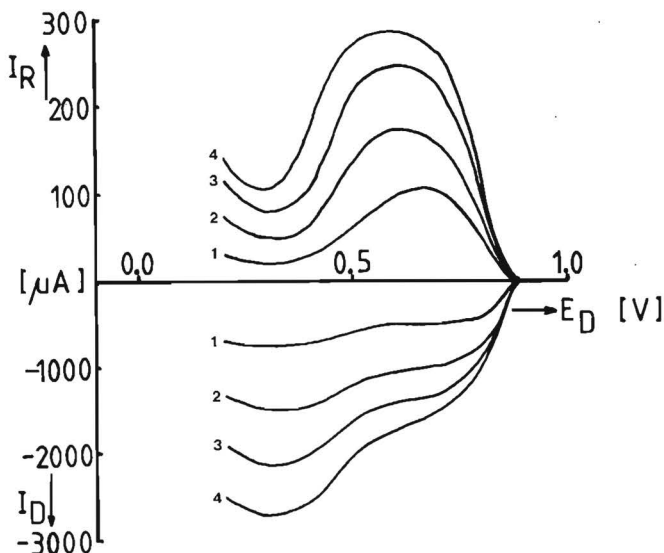


Fig. 7.3  $O_2$  reduction in 1 M KOH at  $Co_2(dpt)_2Cl_2$ , adsorbed on pyrolytic graphite. Rotation freq. 4 (1), 16 (2), 36 (3) and  $64\ s^{-1}$  (4).

less  $H_2O_2$  was produced. Since the diffusion-limited current for  $O_2$  into  $H_2O$  conversion at  $64\ s^{-1}$  is 3 mA in this electrolyte, it is clear from both disc current and ring current that  $O_2$  is reduced to water in two waves; in the first wave, the main product is  $H_2O_2$ . During the second wave, the limiting current for the  $4e^-$  reduction of water is virtually reached.

The results in acid solution are presented in fig. 7.4. Since the complex is unstable in acid solution, only the first scans at  $16\ s^{-1}$  are given. The diffusion-limited current for the reduction of  $O_2$  to  $H_2O$  at  $16\ s^{-1}$  is 2 mA under these conditions, it is therefore clear that virtually only  $H_2O_2$  is formed. Owing to the lack of stability in acid solution the characterization of the disc electrode was only performed in  $O_2$ -free 1 M KOH. In this case the disc potential was varied from 1 to 0 V vs. RHE at  $100\ mV\ s^{-1}$ , and vice versa. The results (fig. 7.5) show that although the cyclic voltammogram of the modified disc electrode significantly differs from that of the unmodified electrode background, no distinct redox couples can be detected, as was also reported by Sarangapani<sup>3</sup>. If nevertheless the observed humps are considered to correspond to one-electron redox processes, one can conclude from fig. 7.5 that the complex is adsorbed on a monolayer level. Summarizing, the conclusion of this study is that  $Co_2(dpt)_2Cl_2$  is able to reduce  $O_2$  to  $H_2O$  in alkaline solution.

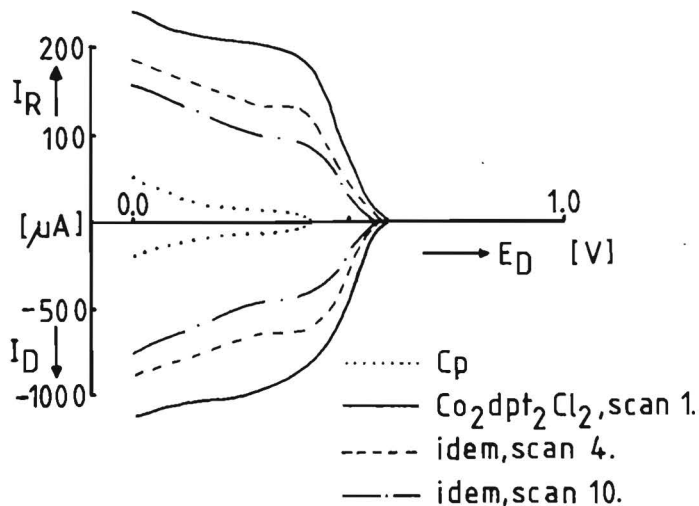


Fig. 7.4  $\text{O}_2$  reduction in 0.5 M  $\text{H}_2\text{SO}_4$  at  $\text{Co}_2\text{dpt}_2\text{Cl}_2$ , adsorbed on pyrolytic graphite. Results of the first scans at a rotation frequency of  $16 \text{ s}^{-1}$ .

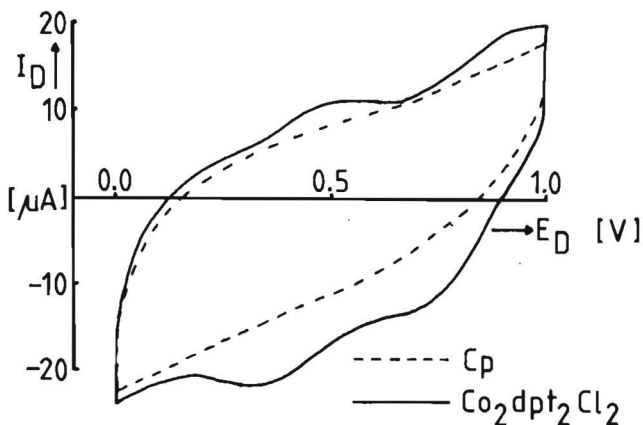


Fig. 7.5 Characterization in  $\text{O}_2$ -free 1 M KOH of  $\text{Co}_2\text{dpt}_2\text{Cl}_2$ , adsorbed on pyrolytic graphite. Scanrate  $100 \text{ mV s}^{-1}$ .

If we now compare the properties of the dinuclear cobalt chelates reported so far, two groups can be distinguished: planar complexes, reducing  $\text{O}_2$  to  $\text{H}_2\text{O}$  in alkaline solution, and 'sandwich' complexes, either amide<sup>2</sup> (fig. 7.1a), or anthracene<sup>4</sup> bridged (fig. 7.1c,d), giving reduction to  $\text{H}_2\text{O}$  in



acid solution. Both groups allow the formation of  $\mu$ -peroxo adducts so this cannot explain the reversed selectivity. In our view this phenomenon is related to the formal redox potentials of the Co centres;  $4e^-$  reduction seems only to occur if these potentials have values in the range 0.6-0.7 V vs. RHE. The sandwich complexes fulfill this condition in acid solution. If it is assumed that the  $\text{Co}^{\text{II}}-\text{Co}^{\text{III}}$  redox processes are pH-independent, the potentials with respect to RHE in the same solution can shift 60 mV in the anodic direction per unit increase in pH. As a consequence, the potentials of the sandwich complexes will be too high in alkaline solution, leading to  $\text{H}_2\text{O}_2$  production. Unfortunately, neither we nor Sarangapani and Yeager<sup>3</sup> were able to detect distinct redox peaks at the planar complexes in alkaline solution, but the experimental results indicate that these potentials have the appropriate values in this electrolyte. Likewise, these potentials will be too low in acid solution, leading, again, to  $\text{H}_2\text{O}_2$  as end product. If this model is correct, it also implies that it is impossible to develop cobalt-containing catalysts that give  $4e^-$  reduction both in acid and in alkaline solution since the reduction of  $\text{O}_2$  and  $\text{H}_2\text{O}_2$  can only occur in a limited pH range.

The observation that the sandwich complexes produce virtually no  $\text{H}_2\text{O}_2$ , while the planar complexes yield considerable amounts, can be explained by the fact that the activity of the corresponding monomeric adducts differ in acid and alkaline solution. If  $\text{O}_2$  is attached to one Co atom, the most probable rate-determining step is the formation of superoxide:  $\text{O}_2 + e^- \rightarrow \text{O}_2^-$ , leading to  $\text{H}_2\text{O}_2$  as end product. This reduction to  $\text{H}_2\text{O}_2$  is more reversible in alkaline solution because its rate-determining step is pH-independent. At high pH the monomeric and dimeric pathways proceed at comparable rates, leading to mixed production of  $\text{H}_2\text{O}$  and  $\text{H}_2\text{O}_2$ . The dimeric pathway, however, seems to be pH-dependent. The  $E_{1/2}$  of this pathway with respect to RHE remains therefore unchanged at different pH values. The  $E_{1/2}$  of the monomeric pathway is pH-independent and this  $E_{1/2}$  vs. RHE shifts 60 mV in the anodic direction per unit increase in pH. In acid solution, the dimeric pathway is therefore much more favourable, so at low overpotential, there will be no competition between the two pathways, and only  $\text{H}_2\text{O}$  is formed. At potentials where the monomers also start to reduce dioxygen,  $\text{H}_2\text{O}_2$  can be formed. This indeed is observed experimentally<sup>2b</sup>.

Finally, we discuss a striking result of Liu et al.<sup>5</sup>, namely the fact that an anthracene-linked diporphyrin, containing only one cobalt atom (fig. 7.1d), was also able to reduce  $\text{O}_2$  to  $\text{H}_2\text{O}$ , but at lower rates than the corresponding dicobalt complex. Although the second porphyrin ring does not

contain a Co ion, the potential of the remaining Co has shifted to 0.6 V vs. RHE<sup>5</sup>. Nevertheless, the formation of an intramolecular adduct seems unlikely since the molecule contains only one catalytic centre. Perhaps in this case intermolecular  $\mu$ -peroxo adducts have been formed. The lower activity of the monocobalt diporphyrin is easily explained by a lower number of active sites, since only relatively few dimeric species will be present on the surface. Such a decrease in the number of active sites shifts  $E_{1/2}$  in the cathodic direction, but does not prevent the attainment of the limiting current<sup>6</sup>. This hypothesis could be checked by repeating the experiment on 'stress annealed' pyrolytic graphite<sup>7</sup>. This approximates to a perfectly smooth surface. Assuming that the porphyrin rings of adsorbed molecules lie parallel to the surface, intermolecular Co-O-O-Co binding will be absent on this substrate, and consequently no  $4e^-$  reduction should occur.

#### References

1. H. Jahnke, M. Schönborn and G. Zimmermann, Topics in current chemistry 61 (1976) 133.
2. J.P. Collman, M. Marocco, P. Denisevich, C. Koval and F.C. Anson, J. Electroanal. Chem. 101 (1979) 117; J.P. Collman, P. Denisevich, Y. Konai, M. Marocco, C. Koval and F.C. Anson, J. Am. Chem. Soc. 102 (1980) 6027; R.R. Durand jr., C.S. Bencosme, J.P. Collman and F.C. Anson, J. Am. Chem. Soc. 105 (1983) 2710.
3. S. Sarangapani, Ph.D. Thesis, Case Western Reserve University, Cleveland (1983); E. Yeager, Electrochim. Acta 29 (1984) 1527.
4. C.K. Chang, H.Y. Liu and I. Abdalmuhdi, J. Am. Chem. Soc. 106 (1984) 2725.
5. H.Y. Liu, I. Abdalmuhdi, C.K. Chang and F.C. Anson, J. Phys. Chem. 89 (1985) 665.
6. A. Elzing, A. van der Putten, W. Visscher and E. Barendrecht, J. Electroanal. Chem. 200 (1986) 313 (chapter 4 of this thesis).
7. J.H. Zagal-Moya, Ph.D. Thesis, Case Western Reserve University, Cleveland (1978).

## Chapter 8 Increased valence theory and the four electron reduction of dioxygen to water

### 8.1. Introduction

The electrochemical reduction of  $O_2$  on transition metal  $N_4$  chelates has been extensively studied<sup>1,2</sup>, not only for a better understanding of the way nature reduces  $O_2$ , but also for application in oxygen electrodes for fuel cells and metal-air batteries. These studies have shown that  $O_2$  can be reduced in two ways:

- $4e^-$  reduction of  $O_2$  to  $H_2O$  without hydrogen peroxide as an intermediate, the so-called direct reduction.
- $2e^-$  reduction of  $O_2$  to  $H_2O_2$  which can be the stable end product or can be subsequently reduced to  $H_2O$ .

In biological systems the formation of  $H_2O_2$  is usually avoided;  $O_2$  is exclusively reduced to  $H_2O$ . Model substances for these systems like the porphyrins and phthalocyanines of Fe and Co do not display such a high selectivity. In monomeric form,  $O_2$  is reduced via the intermediate production of  $H_2O_2$  which is the stable product with Co as the central metal atom, or is partly reduced to  $H_2O$  in the case of Fe.

In 1979 Collman and Anson reported the  $4e^-$  reduction of  $O_2$  on a dicofacial dicobalt porphyrin<sup>3,4</sup> (fig. 7.1a). As long as the two porphyrin rings are properly spaced (ca. 4 Å) to allow intramolecular bridging coordination of the  $O_2$ , reduction to  $H_2O$  was observed in acid solution. In alkaline solution, however, only  $H_2O_2$  was formed. Based on the same principle, other dicofacial dicobalt porphyrins were synthesized like the anthracene-bridged dicobalt diporphyrin of Liu et al.<sup>5</sup> (fig. 7.1c), giving, identical results as the Collman complexes.

This bridge adsorption should also be possible on two  $CoN_4$  centres lying in the plane of the molecule. Indeed Yeager and Sarangapani<sup>6</sup> reported the reduction of  $O_2$  to  $H_2O$  on  $Co_2TAPH(NO_3)_4$  (fig. 7.2b) in alkaline solution. Our own results with  $Co_2(dpt_2)Cl_2$  (fig. 7.2d)<sup>7</sup> showed that in acid solution  $O_2$  is reduced to  $H_2O_2$ ; in alkaline solution a mixed production of  $H_2O$  and  $H_2O_2$  was achieved. That the cofacial complexes yield virtually no  $H_2O_2$  while the planar chelates give considerable amounts, is caused by the fact that the activity of the corresponding monomeric  $O_2$  adducts differ in acid and alkaline solution<sup>7</sup>. If  $O_2$  is only attached to one Co centre, the reduction to

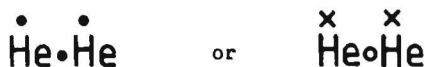
$\text{H}_2\text{O}_2$  probably proceeds via  $\text{O}_2^-$  as an intermediate: This pathway is thermodynamically much more unfavourable in acid than in alkaline solution. In other words, in alkaline solution the direct pathway and the reduction to  $\text{H}_2\text{O}_2$  proceed at comparable rates with low overpotential; in acid solution only the direct reduction can proceed at low overpotential. For the reduction to  $\text{H}_2\text{O}_2$  a much higher overpotential is necessary. Summarizing, one can conclude that dicofacial dicobalt porphyrins reduce  $\text{O}_2$  to  $\text{H}_2\text{O}$  in acid solution and to  $\text{H}_2\text{O}_2$  in alkaline solution. Planar dicobalt porphyrins are able to reduce  $\text{O}_2$  to  $\text{H}_2\text{O}$  in alkaline solution and to  $\text{H}_2\text{O}_2$  in acid solution. This reversed behaviour with respect to the solution pH has not been recognized so far. The increased valence theory developed by Harcourt<sup>8</sup> has been successful in explaining a number of solution phase properties of these complexes in the presence of dioxygen<sup>9</sup>. In this chapter we want to apply this increased valence theory to the reduction behaviour of the different dicobalt chelates.

## 8.2. Increased-valence theory

For the description of the chemical binding between two atoms, often the concept introduced by Lewis in 1916 is used. The binding occurs via spin pairing into a so-called "shared pair of electrons". The increased electron density in the region between two nuclei reduces the kinetic energy of the system. The Lewis concept does not mean that only electron-pair binding can occur; studies of the  $\text{H}_2^+$  ion show that its dissociation energy is of the same order of magnitude as of  $\text{H}_2$ <sup>10</sup>. Also in  $\text{H}_2^+$  the kinetic energy and hence the total energy of the system is lowered when electron density accumulates in the internuclear region; in fact the introduction of a second electron into the region between the nuclei further decreases this kinetic energy with only about 10% as compared to the introduction of the first electron. Nevertheless, the energy has decreased and therefore the electron-pair bond is in most cases more important than the one-electron bond. Another interesting species is the  $\text{He}_2^+$  ion. Two electrons with parallel spins occupy 1S orbitals on the two atoms; the third electron can be shared between these orbitals and thus a bond is formed. This type of bond was first described by Pauling as



He called it a "three-electron bond". As was pointed out by Linnett,<sup>10</sup> this description is misleading since it suggests that three electrons take part in the binding. In fact it is a one electron bond. Linnett suggested a different representation:



(x is an electron of one spin; o an electron of the other spin, ● means that the spin is not specified). This representation shows much more clearly<sup>11</sup> that two electrons are associated with each He atom. The Pauli principle prohibits the participation of the two electrons with parallel spins to take part in the binding: they are essentially located on the separate atoms.

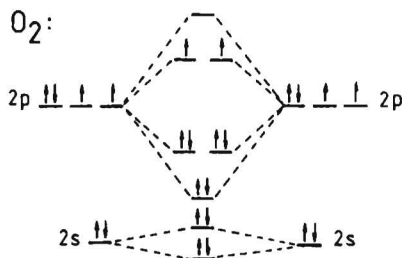
There are circumstances in which two one-electron bonds are energetically more favourable than one electron pair bond. A nice example is the O<sub>2</sub> molecule<sup>10</sup>. According to the Lewis concept the ground state can be depicted as



The ground state of O<sub>2</sub> however has a magnetic moment, indicating that it contains more electrons of one spin than of the other and this observation is not compatible with structure (A). A different arrangement can be constructed with seven electrons of one spin and five of the other:



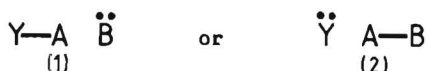
The seven x electrons are favourably oriented on the corners of two tetrahedra with a common apex; the five o electrons on the corners of two tetrahedra with a common face. Every oxygen atom has an octet of electrons consisting of four electrons of one spin and four of the other. The advantage of structure (B) compared to (A) is that the electrons are not associated in close pairs: The interelectronic repulsion energy is reduced. Structure (B) therefore represents the ground state; (A) is an excited state. In molecular orbital theory this can be represented as follows:



This MO scheme corresponds with groundstate B; for the construction of structure A, the two unpaired electrons have to be paired, which costs energy.

The one-electron bond is also essential for the increased valence theory. This theory originated from studies of  $N_2H_4$  and  $N_2O_4$ <sup>12</sup>. According to valence bond formulae, in both molecules the N-N bond should be single; the N-O bond in  $N_2O_4$  should contain an average of three bonding electrons. The N-N distance in  $N_2O_4$  however, is much longer than in  $N_2H_4$ . Moreover, the N-O distance in  $N_2O_4$  is even somewhat smaller than in HNO, which has four bonding electrons. As will be shown later in this section the increased valence theory successfully accounts for these experimental observations.

The theory is most easily explained on a system consisting of three atoms A, B and Y, containing four electrons<sup>8</sup>. The valence bond formulae are



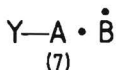
So-called increased valence formulae can be constructed by delocalizing a B electron of (1) into an AB bonding orbital or an Y electron of (2) into an AB antibonding orbital:



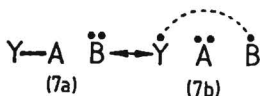
Starting from (4), the electron distributions (5) and (6) are generated:



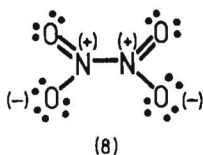
The extent of delocalization in (4) is appreciable if the formal charge of Y in (2) is negative, that on B positive and on A zero or positive. If the atomic orbitals of Y and A show sufficient overlap, a fractional two electron bond is formed:



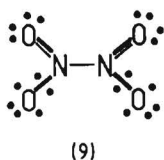
In fact structure (7) summarizes resonance between the structures (7a) and (7b):



The Y-A bond in (7) is weaker than in (1) and is therefore expressed as a thin line. Calculations have shown that in structure (7) more electrons can participate in the binding than in structure (1). The driving force to form (7) out of (2) is the reduction of the formal charges on the atoms, accompanied by an increase in the number of bonding electrons. How large this increase will be, depends on the energy level of the different orbitals. More bonding electrons result in an increase in the valence of the atoms which explains the name of this theory. For  $N_2O_4$ , the standard valence bond representation is (8) and three other resonance structures which differ in the locations of the N=O double bonds:



The increased valence theory yields (9):

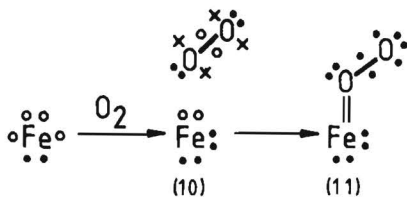


Structure (9) indicates quite easily that the N-N bond number in  $N_2O_4$  is less than unity and that the N-O bond contains four bonding electrons as in HNO.

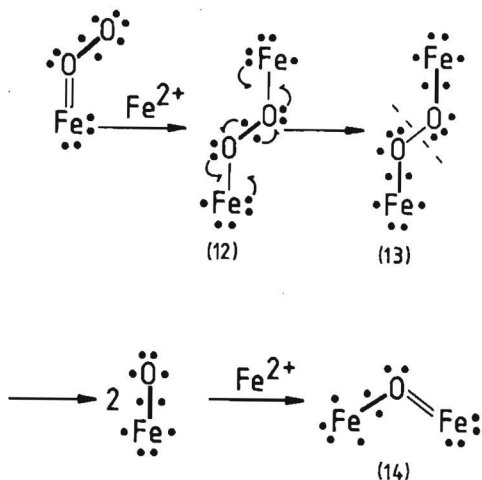
### 8.3. Increased valence theory and $O_2$ adducts

The increased valence theory has already been used to explain experimental observations regarding  $O_2$  adducts of haemoglobin<sup>13</sup>, a number of dissolved Fe and Co porphyrins and phthalocyanines<sup>9</sup>, and the reduction of  $O_2$  on cytochrome c oxidase<sup>13</sup>. In haemoglobin, each  $Fe^{2+}$  is surrounded by five nitrogen atoms, four of the porphyrin itself and one of a histidine group which axially coordinates to the  $Fe^{2+}$ . In the ground state the  $Fe^{2+}$  has four unpaired electrons ( $S = 2$ ) and therefore the molecule is paramagnetic. The  $O_2$  adduct however is diamagnetic ( $S = 0$ ). To account for this, the Fe(II) ( $S = 2$ ) is promoted to the intermediate spin state Fe(II) ( $S = 1$ ) which

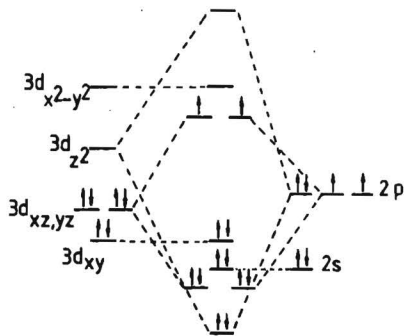
reacts via spin-pairing with ground state  $O_2$  to afford increased valence structure (11).



Another interesting reaction is the formation of  $\mu$ -oxo complexes of Fe(II) porphyrins in  $O_2$  saturated solutions<sup>9</sup>. These  $\mu$ -oxo complexes have not been observed with Co(II) porphyrins. Increased valence structure (11) reacts with a second intermediate spin Fe(II) ( $S = 1$ ) to generate structure (12). In (12), two O-O bonding electrons delocalize, together with four Fe and O-O non-bonding electrons, to afford (13), in which the O-O bond number is even less than unity. O-O bond breaking occurs and the formed Fe(II)O species reacts with Fe(II) ( $S = 1$ ) to  $\mu$ -oxo species (14):

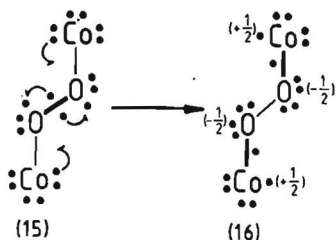


The corresponding MO scheme for the Fe(II)O intermediate can be represented as follows:



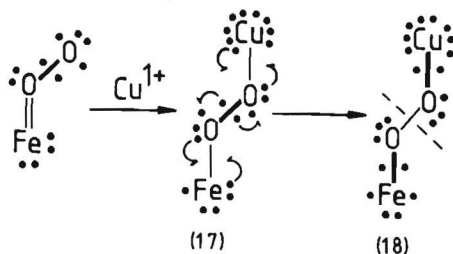


The similarity between the MO scheme of Fe(II)O and O<sub>2</sub> is striking: the Fe(II)O species therefore will be relatively stable. For O<sub>2</sub>-bridged dimeric cobalt compounds a similar reaction scheme can be set up leading to structure (15). The same delocalizations as in structure (12), however, cannot take place. The only way of weakening the O-O bond is by the construction of (16):



The formation of (16), however, involves formal charge separation; moreover, the number of binding electrons does not increase. Therefore the O-O bond will not split and indeed no  $\mu$ -oxo Co dimers have been observed experimentally in solution.

The reduction of O<sub>2</sub> as performed in nature by cytochrome c oxidase has also been described<sup>13,2</sup>. It has a high resemblance with the O-O bond breaking at the Fe-O-O-Fe adduct except that one Fe(II) is replaced by a Cu(I):

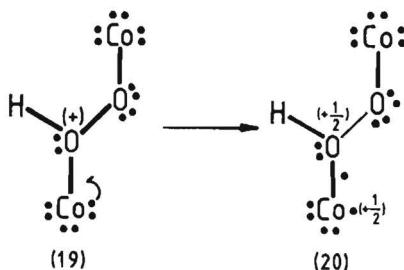


After the bond breaking both species finally react with two protons and one electron to produce two H<sub>2</sub>O, Fe(III) and Cu(II). The latter two species are regenerated with two electrons to the initial Fe(II) and Cu(I).

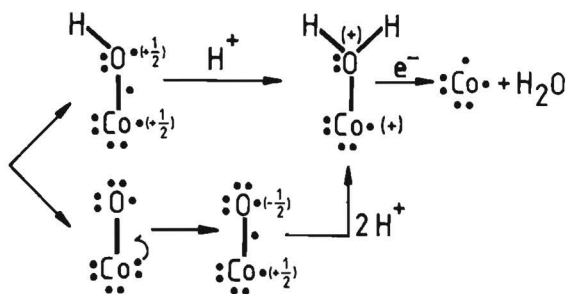
#### 8.4. Application of the increased valence theory to O<sub>2</sub> reduction on dimeric O<sub>2</sub> adducts

For the above described increased-valence formulae, the solution pH is not taken into consideration. These formulae, however, are not protonated and can therefore be used to explain the results, obtained in alkaline solution. Since

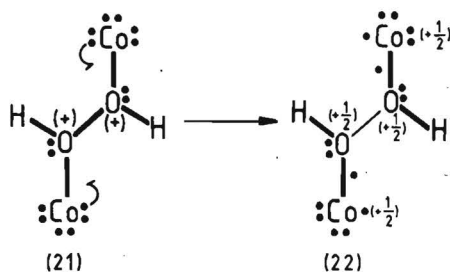
structure (15) does not allow splitting of the O-O bond, it is not surprising that the dicofacial dicobalt porphyrins yield only  $H_2O_2$  in alkaline solution. If we follow the mechanism of Collman et al. in acid solution<sup>4</sup>, the  $O_2$  adduct (15) is protonated. The relatively increased electronegativity of the O-atom in (19) allows the delocalization of a cobalt non-bonding electron into a Co-O bonding orbital:



In species (20), the O-O bond is weakened. This bond is now able to split, giving reduction to water according to the following scheme:

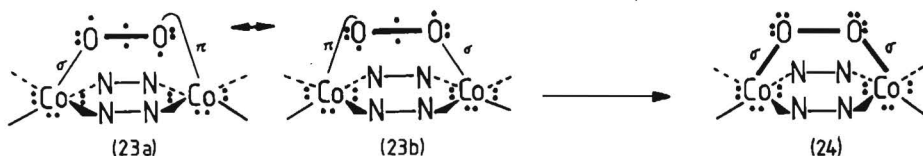


The Co(III), at least initially formed as intermediate spin  $S = 1$  can be regenerated to the initial Co(II) ( $S = \frac{1}{2}$ ). Perhaps even diprotonation is possible, leading to (22). The bond number for the O-O  $\sigma$ -bond will be smaller than in structure (20):



Although this mechanism explains the observed behaviour of the Collman complexes in acid solution, a number of problems remain:

- Since protonation is unlikely in alkaline solution, the  $O_2$  adduct of the planar dicobalt chelates can be represented in this electrolyte, initially by resonance between the increased-valence structures (23a) and (23b), each of which has a fractional Co-O  $\sigma$ -bond and a fractional Co-O  $\pi$ -bond. There would then be a strong tendency to form two Co-O  $\sigma$ -bonds, as occurs in (24) with a strained peroxide linkage. This would proceed via the  $\pi$ -electron shifts that are indicated in (23a) and (23b), and would be accompanied by orbital rehybridization for both cobalt and oxygen:

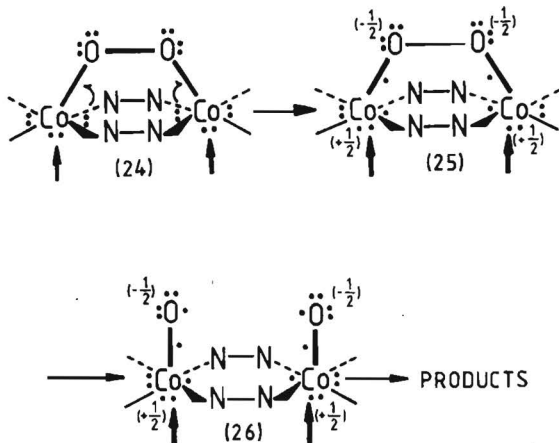


Based on similar arguments as for structure (15), this species should not be able to break the O-O bond in the solution phase. Nevertheless, these complexes reduce  $O_2$  to  $H_2O$  in alkaline solution if they are adsorbed on an electrode <sup>6,7</sup>.

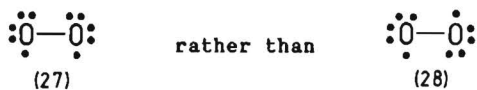
- Consequently, if planar dicobalt chelates are able to split the O-O bond, why do the Collman complexes only give  $H_2O_2$  in alkaline solution?
- The same mechanism as for the dicofacial dicobalt chelates in acid solution can be constructed for the dicofacial diiron chelates in acid solution. In fact they should be able to split the O-O bond even more easily. Nevertheless the latter complexes do not display an enhanced activity and selectivity as compared to monomeric iron porphyrin <sup>4</sup>.

These considerations show that the possibility of dimeric adsorption is not the only precondition for the occurrence of direct reduction of  $O_2$ . In our view, a second precondition is that the redox potentials of the metal ion centres must have appropriate values. As shown by Collman and Anson, the  $Co^{III}/Co^{II}$  redox potentials of the Co centres in acid solution are closely related to the  $O_2$  reduction onset potential. This indicates that the redox potentials have the appropriate values in this case. Since  $Fe^{III}/Fe^{II}$  porphyrin redox potentials in general have lower values than  $Co^{III}/Co^{II}$ , the redox potentials of the dicofacial diiron chelates are probably too low: no improved performance is obtained as compared to the monomeric Fe porphyrin.

If we now go to alkaline solution, the potential of the reversible hydrogen reference electrode has shifted 840 mV in cathodic direction (60 mV per unit increase in pH from 0 to 14). If the potentials of the  $\text{Co}^{\text{III}}/\text{Co}^{\text{II}}$  redox couples are pH independent, as with  $\text{CoPc}^{14}$ , then they will be too high (ca. 1.5 V versus RHE at pH = 14) in alkaline solution. Of course, the same applies to the planar dicobalt chelates. Since the  $\text{Co}^{\text{III}}/\text{Co}^{\text{II}}$  redox couples are probably not involved in alkaline solution, a possible explanation would be that in that case the  $\text{Co}^{\text{II}}/\text{Co}^{\text{I}}$  couples are involved, leading to the following model:



The two arrows in structure (24) indicate the injection of negative charge onto the cobalt atoms, increasing the relative electronegativity of the oxygen atoms, facilitating the delocalization of a cobalt non bonding electron into a Co-O bonding orbital. That the  $\text{O}_2$  is adsorbed in a cis configuration is advantageous for the splitting of the O-O bond. The  $\text{O}_2$  valence state is



In (27), the interelectronic repulsion will be higher than in (28), weakening the O-O bond. Perhaps this phenomenon also explains the results of Liu et al.<sup>15</sup>, who synthesized a dicofacial dicobalt porphyrin onto which the  $\text{O}_2$  has to be adsorbed in a cis configuration. These authors attributed the improved activity of the latter molecule to a better accessibility of protons to the adsorbed  $\text{O}_2$  molecule.

Summarizing, for the direct reduction of  $O_2$  on dicobalt chelates two preconditions seem to be necessary: bridge adsorption of the  $O_2$ , and appropriate values for the cobalt redox potentials. According to the increased valence formulae, O-O bond breaking is possible if the relative electronegativity of the oxygen atoms is increased, facilitating the delocalization of a cobalt non-bonding electron into a Co-O bonding orbital, thereby weakening the O-O bond. In acid solution this is realized by the protonation of either one or both oxygen atoms; in alkaline solution probably by injection of negative charge onto the cobalt atoms.

### 8.5. Concluding remarks

Although dicofacial diiron porphyrins did not give improved results in acid solution, this could change in alkaline solutions. In acid solution their redox potentials are too low: they should have appropriate values, i.e. in the vicinity of 0.8 V versus RHE. Our own results with  $FePc^{14}$  show that this molecule has a  $Fe^{III}/Fe^{II}$  redox peak at 0.85 V versus RHE at pH = 14. The behaviour of dicofacial diiron phthalocyanine would therefore be interesting, since this molecule could fulfil both preconditions for the occurrence of direct reduction in alkaline solution. Moreover, since this redox peak is pH dependent from pH = 6 upto pH = 14, the catalyst could also be active in this pH range.

### 8.6. References

1. H. Jahnke, M. Schönborn, G. Zimmermann, Topics in current chemistry 61 (1976) 133.
2. M. Tarasevich, A. Sadkowski and E. Yeager, Oxygen Electrochemistry, in Comprehensive Treatise of Electrochemistry, Vol. 7: Kinetics and Mechanisms of Electrode Processes (Edited by B. Conway, J. Bockris, E. Yeager, S. Khan and R. White), Chapter 6, pp.301-398, Plenum Press, New York (1983).
3. J.P. Collman, M. Marocco, P. Denisevich, C. Koval and F.C. Anson, J. Electroanal. Chem. 101 (1979) 117.
4. J.P. Collman, P. Denisevich, Y. Konai, M. Marocco, C. Koval and F.C. Anson, J. Am. Chem. Soc. 102 (1980) 6027.

5. C.K. Chang, H.Y. Liu and I. Abdalmuhdi, *J. Am. Chem. Soc.* 106 (1984) 2725; H.Y. Liu, I. Abdalmuhdi, C.K. Chang and F.C. Anson, *J. Phys. Chem.* 89 (1985) 665.
6. S. Sarangapani, Ph.D. Thesis, Case Western Reserve University, Cleveland (1983); E. Yeager, *Electrochim. Acta* 29 (1984) 1527.
7. A. van der Putten, A. Elzing, W. Visscher and E. Barendrecht, *J. Chem. Soc., Chem. Comm.* (1986) 477 (chapter 7 of this thesis).
8. R.D. Harcourt, *J. Chem. Educ.* 45 (1968) 779; 46 (1969) 856.
9. R.D. Harcourt, *J. Inorg. Nucl. Chem.* 39 (1977) 243 and references therein.
10. J.W. Linnett, "The Electronic Structures of Molecules", Methuen, London (1964).
11. R.D. Harcourt, *J. Chem. Educ.* 62 (1985) 99.
12. R.D. Harcourt, *J. Mol. Struct.* 9 (1971) 221; *J. Am. Chem. Soc.* 102 (1980) 5195, 103 (1981) 5623; and Ref. 13, chapter 7, 11 and 13.
13. R.D. Harcourt, "Qualitative Valence Bond Descriptions of Electron-Rich Molecules: Pauling "3-Electron Bonds" and "Increased Valence" Theory in Lecture Notes in Chemistry, edited by G. Berthier, M.J.S. Dewar, H. Fischer, K. Fukui, G.G. Hall, H. Hartmann, H.H. Jaffé, J. Jortner, W. Kutzelnigg, K. Ruedenberg and E. Scrocco, Springer Verlag, Berlin-Heidelberg-New York (1982).
14. A. van der Putten, A. Elzing, W. Visscher and E. Barendrecht, to be published (chapter 6 of this thesis).
15. H.Y. Liu, M.J. Weaver, C.-B. Hang and C.K. Chang, *J. Electroanal. Chem.* 145 (1983) 439.

## Chapter 9 A new method of preparing a rotating ring-disc electrode (RRDE) for the study of carbon-supported catalysts.

### 9.1 Introduction

In order to produce fuel-cell electrodes with a very high surface area, suitable catalysts are dispersed on carbon, mixed with a binder such as teflon, and pressed onto a metal screen<sup>1</sup> to form a gas-diffusion electrode. The electrocatalytic properties of such electrodes are determined by recording their voltammetric behaviour. This method, however, has some disadvantages. Firstly, the transport of the fuel and the dioxygen is very ill-defined: the *i*-E curve is determined by the electrocatalytic as well as the microgeometric properties determining transport of the electrode, and is therefore not a good measure for the catalytic properties as such. Secondly, these measurements do not reveal any information about the selectivity of the electrode reactions. Information of this kind can be obtained with more sophisticated hydrodynamic methods such as with the RRDE. Therefore, it would be convenient if the carbon-supported catalyst could be applied as a very thin layer to the disc of such an electrode. This modified electrode has to fulfill a number of conditions:

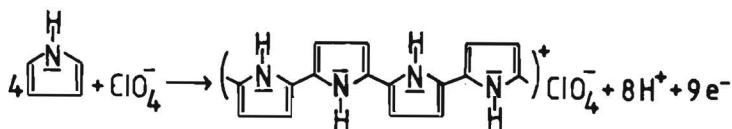
- the layer must be very thin so that the hydrodynamic behaviour of the RRDE is not disturbed
- the layer must be accessible to electrons and reactants. The use of paste electrodes is less appropriate since the pasting liquid causes wetting problems of the catalyst<sup>2</sup>.

Another way of manufacturing such an electrode, without the use of a pasting liquid, was by electrophoretic deposition, as described by Savy et al.<sup>3</sup>, but we were unable to reproduce their results. The adherence of the carbon to the disc appeared to be insufficient. Therefore, we investigated the possibility to incorporate the carbon in a polymeric film. Polypyrrole was chosen since we had already some experience in preparing this polymer. Moreover, it satisfies the conditions of conductivity and high porosity.

### 9.2 Preparation technique

Polypyrrole (PP) can be deposited at an electrode by electropolymerization of pyrrole<sup>5</sup>. The electrolyte composition for which the best results are obtained is the following: 0.1 M LiClO<sub>4</sub>, 1 vol.% pyrrole, 0.5 vol.% H<sub>2</sub>O in

acetonitril; (however, also other solvents e.g. water or ethanol can be used). Polymeric units are formed according to:



The polymer itself is electroactive. In the potential range of interest for fuel cell reactions (0-1 V vs. RHE), the polymer is in the oxidized, conducting state. The stability is good in acidic solutions but too low to perform reliable experiments in alkaline solution. In order to prepare the carbon modified electrodes, suspensions of carbon (Norit BRX) of different concentrations (250-1250 mg/liter formation solution) were made. As a carrier RRDE we used one with an Au disc (0.5 cm<sup>2</sup>) and a Pt-ring (N = 0.27). At first, the following technique was tried. The electrode was rotated (faced down) in the carbon suspension. (Rotation was necessary since the suspensions are unstable due to coagulation of the carbon particles). Rotation of the RRDE not only causes a flow in the electrolyte which keeps the particles in solution, but also constantly supplies particles to the disc of the RRDE. The PP was formed potentiostatically at ca. 800 mV versus a saturated calomel electrode (SCE). The counter electrode was a platinum foil. The amount of polymer and the rate of its formation was monitored by recording the amount of charge that passed through the circuit, 24 mC.cm<sup>-2</sup> being equivalent to 0.1 μm PP<sup>6</sup>. After the formation the electrode was flushed with ethanol, dried and inspected microscopically.

This method gave irreproducible results: virtually no carbon was incorporated in the PP film. The addition of a surfactant to the electrolyte (10<sup>-3</sup> M sodiumtoluene sulphonate) to charge the carbon particles negatively so that they can be incorporated as large anions, did not give any improvement. Hence, the following technique was developed. On top of the RRDE (faced upwards!) a tight-fitting KEL F hood was placed in which a hole was drilled with exactly the same diameter as the disc (figure 9.1). This cell was filled with 500 μl carbon/electrolyte/monomer suspension, which had previously been agitated in an ultrasonic bath for 5 minutes. A cylindrical Pt electrode was placed in the convex meniscus at the top of the cell. In the cell, the carbon particles will precipitate on the disc surface. When the current is switched on, the



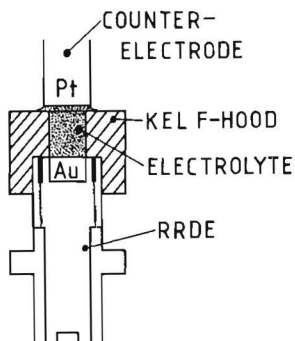


Fig. 9.1: Cross-section of the electrochemical cell.

polymerization of the pyrrole starts both on the gold electrode and the carbon. The polymer chains will grow into a three-dimensional network which attaches the carbon to the electrode. Visual inspection after flushing with ethanol showed that indeed the carbon was incorporated in the polymer film. The adherence of the particles and the stability of the film was good enough to perform RRDE experiments. Although the distribution of the carbon over the disc surface was very fine and regular, some spots on the surface were only covered with PP. More concentrated suspensions resulted in irregular deposits. The use of acetylene black which has a smaller particle size than Norit BRX did not give any improvement since it formed aggregates on a very short time scale, also resulting in irregular deposits. The best results were obtained with a Norit BRX suspension of 500 mg/liter, and PP formation during 10 minutes with a current of 1 mA.

### 9.3 The hydrodynamic behaviour

The introduction of carbon particles in a PP layer results in an electrode with a certain surface roughness, which will influence the hydrodynamic behaviour of the RRDE. Especially at high rotation frequencies, the thickness of the diffusion layer will become of the same order of magnitude as the surface roughness, resulting in deviations of the equations derived by Levich<sup>7</sup>. This effect was verified in a  $5 \cdot 10^{-2}$  M  $K_3Fe(CN)_6$  solution in 1 M KCl. The disc current was measured at -200 mV vs. SCE where the reduction of the ferri complex is diffusion limited; the ring was held at +800 mV vs. SCE. The reduction of ferricyanide also proceeds at the PP itself. The results of the disc

current and the calculated collection efficiency ( $-I_R/I_D$ ) as a function of the rotation frequency are presented in figure 9.2. The dashed lines represent the theoretical values for  $I_D$  and  $N$  according to the Levich equations. From figure 9.2 it follows that such behaviour is obeyed upto a rotation frequency of  $16 \text{ s}^{-1}$ . At higher frequencies the disc current deviates in the positive direction, as expected; the measured collection efficiency then decreases. Therefore, our experiments were carried out in the frequency range of  $0-16 \text{ s}^{-1}$ .

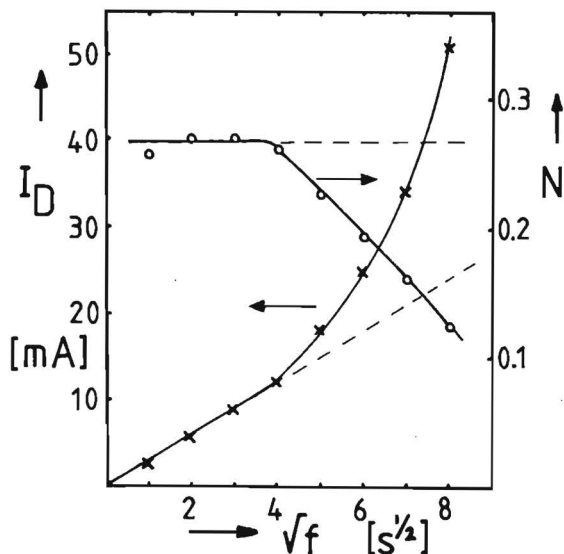


Fig. 9.2: Limiting disc current (x) and measured collection efficiency (o) of the reduction of ferricyanide ( $5.10^{-2} \text{ M}$ ) at a carbon-modified electrode, as a function of the square root of the rotation frequency. The dashed lines represent the values according to the Levich equations.

#### 9.4 Results of some preliminary experiments

In order to show the possibilities of this new method, dioxygen reduction was studied in  $0.5 \text{ M H}_2\text{SO}_4$  at electrodes with four different types of carbon: Norit BRX (0.2 mg) and Norit BRX, impregnated with respectively 20 weight % metalfree, cobalt- and iron phthalocyanine ( $\text{H}_2\text{Pc}$ ,  $\text{CoPc}$  and  $\text{FePc}$ , 0.25 mg). The impregnation was realized by dissolving 10 mg of the corresponding Pc in 20 ml THF, adding 40 mg Norit BRX, and refluxing and stirring for 30 minutes. Thereafter an equal volume of water was added, the carbon was filtrated (GA

glass filter), washed with water and ethanol, dried at 100°C and ground for 5 minutes in an agate mortar. The results with these electrodes can be compared with those obtained at gas-diffusion electrodes<sup>8</sup>. The reduction of dioxygen can proceed along two pathways: the direct reduction to water, and the reduction to hydrogen peroxide which can subsequently be reduced to water. The ring electrode was slightly platinized to ensure quantitative detection of hydrogen peroxide. This was done before the modification of the disc to avoid platinum adsorption on the carbon. After the modification, the electrode was transferred to an O<sub>2</sub>-saturated 0.5 M H<sub>2</sub>SO<sub>4</sub>. After activation of the ring by periodical evolution of H<sub>2</sub> and O<sub>2</sub> for 1 minute, the net dioxygen reduction current was measured at a rotation frequency of 9 s<sup>-1</sup>. The disc potential was varied from +1000 mV to +200 mV vs. RHE. At the ring (+1200 mV vs. RHE) the peroxide production was monitored. All measurements were performed at room temperature.

Figure 9.3 gives a characterization of the disc electrode. The dotted curve represents a gold electrode in an dioxygen-free 0.5 M H<sub>2</sub>SO<sub>4</sub> solution,

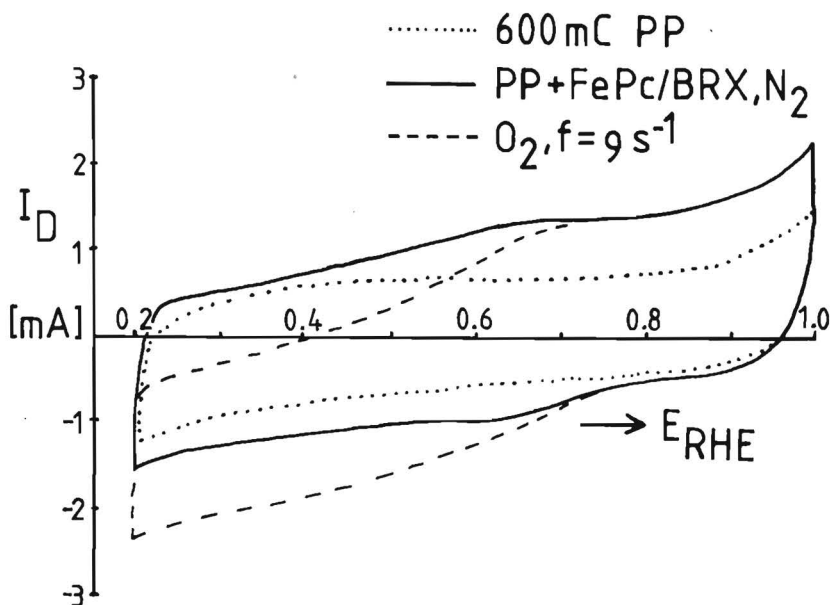


Fig. 9.3: Cyclic voltammetric characterization in 0.5 M H<sub>2</sub>SO<sub>4</sub> of a 600 mC PP film on gold (.....), a 20 weight % FePc/Norit BRX modified stagnant PP electrode in N<sub>2</sub>-saturated solution (—), and in O<sub>2</sub>-saturated solution at f = 9 s<sup>-1</sup> (- - -). Scanrate 10 mV s<sup>-1</sup>; disc surface 0.5 cm<sup>2</sup>.

covered with 600 mC PP, without carbon; the solid curve denotes the incorporation of the Norit BRX carbon particles, impregnated with 20 weight % FePc. The dashed curve was obtained with the latter electrode after saturation of the electrolyte with dioxygen and at a rotation frequency of  $9 \text{ s}^{-1}$ . It is clear that dioxygen is reduced at this electrode, starting at about 800 mV vs. RHE. If the electrode was not rotated in the dioxygen-saturated solution, about the same cyclic voltammogram was obtained as in the nitrogen-saturated solution. Therefore, the net dioxygen-reduction current at a certain rotation frequency was taken as the difference between the current at this rotation frequency and the current response of the stagnant electrode.

A gold electrode which is only covered with 600 mC PP does not reduce dioxygen in this potential range, neither does an electrode from which the carbon was removed with a tissue. This proves that the catalysis of the dioxygen reduction is exclusively caused by the modified carbon itself.

The results with the four modified Au disc electrodes are presented in figure 9.4, together with the resulting ring currents. It must be remarked that Norit BRX itself is a very poor catalyst for the reduction of dioxygen; the reduction proceeds to  $\text{H}_2\text{O}_2$  exclusively ( $N = 0.27$ ). Impregnation with  $\text{H}_2\text{Pc}$  shows no improvement, contrary to the use of CoPc and FePc, which both give a significant catalytic improvement. Clearly, the metal ion is the centre of the electrocatalytic activity. The CoPc modified carbon catalyses the reduction of dioxygen to  $\text{H}_2\text{O}_2$ . The FePc/carbon electrode shows the highest activity; moreover, the reduction also proceeds partly to water.

With respect to the selectivity, this behaviour is the same as that of vacuum-deposited CoPc and FePc films in alkaline solution<sup>9,10</sup>, although the FePc/BRX electrode in this case produces relatively more  $\text{H}_2\text{O}_2$ ; the activity in alkaline solution is higher.

Comparison of our results with those of van Veen and Visser<sup>8</sup> for gas-diffusion electrodes prepared from the same carbons, shows a similar increase in activity due to impregnation of the Norit BRX.

The fact that the electrodes are not totally covered with carbon is also reflected in the value of the limiting currents. In the case of CoPc, where the reduction proceeds entirely to  $\text{H}_2\text{O}_2$ , the theoretical value of this current is  $750 \mu\text{A}$  ( $S = 0,5 \text{ cm}^2$ ,  $D = 2.1 \times 10^{-5} \text{ cm}^2 \text{ s}^{-1}$ ,  $v = 10^{-2} \text{ cm s}^{-1}$ <sup>12</sup>,  $C(\text{O}_2) = 1,03 \cdot 10^{-3} \text{ M}$ <sup>13</sup>). This means that about two thirds of the electrode is covered. It was observed that this fraction is determined mainly by the interaction between the separate particles which will depend on their properties such as average particle size, surface charge, etc.

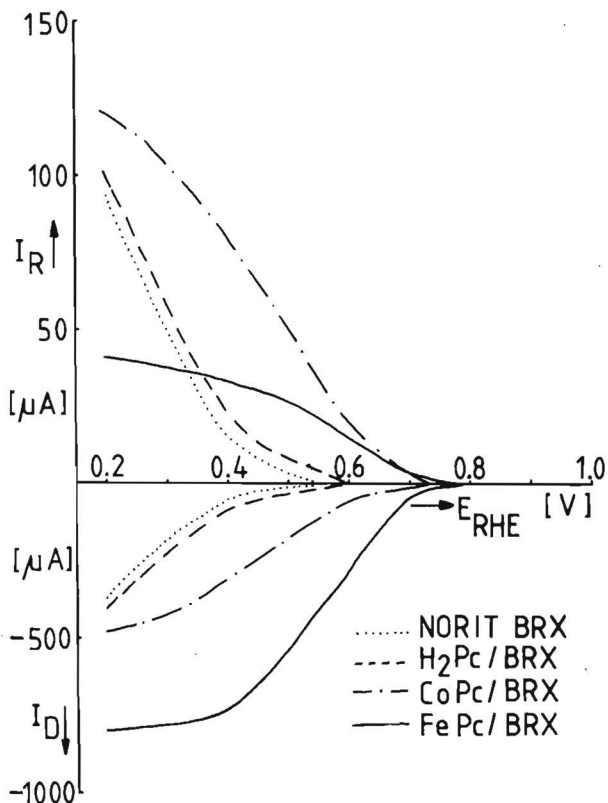


Fig. 9.4:  $O_2$  reduction in  $0.5\text{ M H}_2\text{SO}_4$  at  $f = 9\text{ s}^{-1}$  at Norit BRX, and Norit BRX impregnated with 20%  $H_2Pc$ ,  $CoPc$  and  $FePc$  respectively.

### 9.5 Concluding remarks

The catalytic properties of carbon-supported catalysts in acid solution can be measured by incorporation of carbon particles in a polypyrrole film. The transport of reactants to the electrode is much better defined than in the case of gas-diffusion electrodes. The preparation of the electrodes is fast and easy, contrary to the preparation of gas-diffusion electrodes. The selectivity can also be determined since a RRDE can be prepared. Because the formation of the polymer is an electrochemical process, it is very easy to cover only the disc of the RRDE with the catalyst. With this method, all kinds of carbons can be investigated, impregnated with different catalysts or subjected to other treatments, such as pyrolysis.

## 9.6 References

1. H. Jahnke, M. Schönborn, G. Zimmermann, Topics in current chemistry 61 (1976) 133.
2. J.A.R. van Veen, Electrochim. Acta 27 (1982) 1403.
3. M. Savy, P. Andro, C. Bernard, Electrochim. Acta 19 (1974) 403.
4. L.J.J. Janssen and A.M.T.P. van der Putten, Neth. Pat. No. 8500335 (1985).
5. A.F. Diaz, J.I. Castillo, J.A. Logan and W.-Y. Lee, J. Electroanal. Chem. 129 (1981) 115.
6. A.F. Diaz, J.I. Castillo, J. Chem. Soc. Comm. (1980) 397.
7. V.G. Levich, Physicochemical Hydrodynamics, Prentice Hall (1962).
8. J.A.R. van Veen, C. Visser, Electrochim. Acta 24 (1979) 921.
9. F. van den Brink, W. Visscher, E. Barendrecht, J. Electroanal. Chem. 157 (1983) 283.
10. F. van den Brink, W. Visscher, E. Barendrecht, J. Electroanal. Chem. 172 (1984) 301.
11. R.J. Millington, Science 122 (1955) 1090.
12. R.C. Weast (Ed.), Handbook of Chemistry and Physics, CRC Press, Boca Raton, FA, 62nd ed., 1981-1982, p. D-242.
13. K.E. Gubbins, R.D. Walker, J. Electrochem. Soc. 112 (1965) 469.

## Chapter 10 Dioxygen reduction on pyrolyzed carbon supported transition metal chelates

### 10.1 Introduction

Transition metal chelates have been studied for  $O_2$  reduction, both in alkaline and acid solution. Usually, the chelate is dispersed onto a carbon support and applied as a gas-diffusion electrode. It was already established by Jahnke et al.<sup>1</sup> in 1973 that heat treatment in an inert atmosphere (pyrolysis) favourably effects the activity and stability towards  $O_2$  reduction. A survey of the literature, published so far<sup>2-19</sup> shows that the obtained results hardly can be compared with each other, due to great differences in experimental conditions, of which the most important are:

- the chelate under consideration,
- the pyrolysis temperature,
- the carbon support and the method of chelate dispersion on this carbon,
- the electrolyte in which the  $O_2$  reduction has been measured.

Most of the work has been performed on the tetraphenylporphyrins (TPP), tetramethoxyphenylporphyrins (TMPP), dibenzotetraazaannulenes (TAA) and phthalocyanines (Pc) of Fe and Co; also the metal-free compounds have been used to study the effect of the central metal atom. In addition, the pyrolysis conditions widely differ. Most authors carry out the pyrolysis in an inert atmosphere (Ar,  $N_2$ ) at different temperatures. An overview of the investigated chelates and corresponding pyrolysis temperatures can be found in table 10.1. It is striking that in most cases no temperature program is given, though this program can influence the ultimate results.

Another important parameter is the carbon support and the applied impregnation method. Properties such as the chemical nature of the carbon, pore size and pore-size distribution, specific surface area etc. determine, together with the catalyst loading, whether the catalyst is present as (sub)monolayer coverage or in the form of aggregates. This is also influenced by the preparation method, and properties of the chelate itself: mechanical mixing for instance<sup>9</sup> will give aggregates; precipitation from a solution gives a more uniform coverage. A number of different carbons and some of their properties are presented in table 10.2.

Finally the results are influenced by the electrolyte in which the  $O_2$  reduction has been studied. Most authors use  $H_2SO_4$  at room temperature, however, also  $H_3PO_4$ <sup>2,10</sup>,  $NaCl$ <sup>16</sup>,  $NaOH$ <sup>9</sup> and  $KOH$ <sup>15</sup> are used. In our view,

Table 10.1: Overview of the investigated chelates and corresponding pyrolysis temperatures.

chelate	T <sub>p</sub> (°C)	reference
H <sub>2</sub> , CoTMPP	800	2
Fe, CoTPP/Fe, CoPc	600-800	3
CoTPP	500-700	4
CoTPP/CoTMPP/CoTBP	800-900	5
CoTMPP	300-1200	6
H <sub>2</sub> , CoTMPP	830	7
CoTPP	700	8
CoTMPP	800-900	9
CoTAA	950	10
H <sub>2</sub> , CoTAA	300-1200	11
H <sub>2</sub> , CoTMPP	830	12
H <sub>2</sub> , CoTAA	650	13
CoTMPP	300-1200	14
Co, FeTMPP	700, 800	15
H <sub>2</sub> , CoPc/FeTPP	950	16
FeTPP.Cl	200-1000	17
CoTAA/CoTAA.Br <sub>2</sub>	500	18
CoTAA	700	19

results obtained in alkaline solution are not so revealing since the reduction of O<sub>2</sub> to H<sub>2</sub>O<sub>2</sub> in this electrolyte is quasi-reversible; only slight differences in activity between the different chelates exist and even carbon itself has a high activity towards dioxygen reduction. Therefore, the results are more determined by physical texture of the catalyst/carbon support than by chemical composition of the catalyst itself.

Virtually all electrochemical measurements have been performed on gas-diffusion electrodes. With this type of electrode only i-E curves can be measured, as a function of time. Major drawbacks are that no information about the selectivity can be obtained and that the transport of O<sub>2</sub> is ill-defined. The fraction of the electrode surface which is active for the O<sub>2</sub> reduction is mainly determined by the wetting of the carbon. In general, impregnation of



Table 10.2. Some properties of frequently used carbon supports.

carbon	chemical nature	$S_{\text{BET}}$ ( $\text{m}^2 \text{g}^{-1}$ )	catalyst loading (weight %)	authors
Norit BRX	active carbon	1800	20	van Veen et al. <sup>3</sup>
P 33	active carbon	1020	10-20	Wiesener et al. <sup>6,7, 11-14</sup>
Vulcan XC72	acetylene black	250	5	Yeager et al. <sup>9</sup>

the support with a catalyst and the pyrolysis will change the wetting degree and thus also the electrochemical behaviour.

Also some results with rotating ring-pasted disc electrodes (RRDE) have been published<sup>5,9,17</sup>. Bagotskii et al.<sup>5</sup> and Scherson et al.<sup>9</sup> used teflon to attach the carbon to the disc, retaining the wetting problem; Ikeda et al.<sup>17</sup> applied FeTPP.Cl onto glassy carbon, but in the absence of a porous carbon support. For the chemical and physical characterization of the carbon-supported chelates before, and after pyrolysis, a spectrum of different techniques was used such as DTA/TG, chemical analysis, conductivity, magnetic susceptibility, BET surface determination, and spectroscopy such as X-ray, IR, TEM, MS, ESR, XPS, ESCA and EXAFS.

Summarizing, it must be concluded that each chelate has its characteristic pyrolysis behaviour which depends on the carbon support, the temperature program and the pyrolysis temperature. However, there is no unambiguous opinion why pyrolysis has a beneficial effect on the activity.

## 10.2 Developed theories for activity enhancement

It is generally agreed that the improved stability is caused by the reaction of the chelate with the carbon support. The most reactive parts of the molecule are then no longer susceptible for irreversible oxidation due to the formation of hydrogen peroxide. Moreover, the pyrolyzed catalysts are better  $\text{H}_2\text{O}_2$  decomposers, resulting in a lower  $\text{H}_2\text{O}_2$  concentration in the pores of the catalyst.

With regard to the improvement in activity, different opinions are presented. An important factor here is the role of the central metal atom. With unpyrolyzed catalysts the central metal ion is the active site. The question is whether this is also the case after pyrolysis. According to Wiesener et al.

6,7,11-14 the cobalt is no longer the active site after pyrolysis. During pyrolysis a new catalyst is formed consisting of nitrogen and carbon. The cobalt acts as a promotor for these pyrolysis reactions. The most convincing evidence for this theory should be the measured activity of  $H_2$ TAA and CoTAA as a function of pyrolysis temperature. In both cases the same bell-shaped curve was obtained<sup>11</sup>, only shifted with respect to the temperature. Measurements of the  $H_2O_2$  decomposition and the BET surface showed the same behaviour, indicating that both with  $H_2$ TAA and CoTAA the same catalyst is formed, only at different temperatures. The presence of cobalt accelerates the pyrolysis reactions so that the maximum is already obtained at lower temperatures. The authors reported the same behaviour with catalysts in which Co and  $H_2$ TAA were added separately: after pyrolysis the same activity was obtained as with pyrolyzed CoTAA.

This theory is contradicted by Yeager et al.<sup>9</sup>. They also conclude that cobalt accelerates the pyrolysis reactions, but in their view the increased activity is not caused by the pyrolysis product of the organic skeleton, i.e. a nitrogen carbon compound. Their conclusion is based on the result that pyrolyzed  $H_2$ TMPP (800°C) did not show an improved activity. Unfortunately these authors did not measure the activity at different pyrolysis temperatures; it could be that for the improvement of  $H_2$ TMPP a higher temperature is necessary. Mössbauer spectroscopy of pyrolyzed CoTMPP showed the presence of cobalt oxide. In their opinion some sort of cobalt species is responsible for the improved activity, but their explanation remains a bit vague. In their view, the results of Wiesener et al. with  $H_2$ TAA are a consequence of the presence of impurities in the P33 carbon. However, according to Gruenig<sup>20</sup>, extensive purification of the carbon had no effect.

A third explanation was offered by van Veen et al.<sup>3</sup>, based on the concept of redox catalysis. Their results should prove that the chelate indeed reacts with the carbon support; however, the  $MeN_4$  units remain intact ( $T \leq 800^\circ C$ ) according to EXAFS measurements. In their view two kinds of catalysts can be discerned: metal chelates for which the redox potential is too positive (Co) or too negative (Fe). With Co complexes, saturation of the organic skeleton due to pyrolysis leads to an increased electron density on the metal ion, resulting in a more cathodic redox potential. With Fe complexes also a bond is formed between the Fe and the substrate, lowering the electron density on the metal ion; the net effect of these processes shifts the redox potential in anodic direction. Therefore, the activity of both Co and Fe complexes increases after pyrolysis, irrespective whether the redox potential at room

temperature is too positive or too negative. This explanation seems very unlikely, since the  $\pi$ -system of the organic skeleton will become larger due to polymerization with the support. Electrons that took part in the Co-N bond will become more delocalized, resulting in a weakened ligand field. The Co complex will change from a low into a high-spin complex with a higher electron density on the  $3d_{z^2}$  orbital, facilitating  $O_2$  adsorption<sup>4</sup>.

Summarizing, it can be stated that the different opinions regarding the increased catalytic activity after pyrolysis are not necessarily caused by conflicting experimental results. A meaningful comparison between different chelates can only be made if the chelates are compared over the whole temperature range 300-1200°C. Comparison at only one temperature has no meaning; some chelates will not have reacted at all while others are already totally decomposed. Another requirement is a good discrimination between physical and chemical effects. With gas-diffusion electrodes this is impossible since modification of the carbon support influences both catalytic, transport and wetting properties. It is therefore risky to draw conclusions about what happens with the transition metal macrocycles themselves. In this paper the activity and selectivity of some chelates will be compared as a function of pyrolysis temperature. Furthermore, the effect of the carbon support will be investigated.

As stated above, the transport of  $O_2$  in gas-diffusion electrodes is ill-defined. Moreover, the actual surface area where the electrochemical processes are taking place is not exactly known and depends on the wetting properties of the catalyst system. Therefore, a different type of electrode was used<sup>21</sup>, described in chapter 9.

### 10.3 Experimental

The (modified) carbon particles are attached to the disc of a RRDE via incorporation in a conducting polypyrrole film. With this more sophisticated hydrodynamic technique, the transport of  $O_2$  to the electrode is well defined; at the ring electrode the  $H_2O_2$  production can be monitored, and so the selectivity be determined. Moreover, since the whole pore system can be filled with electrolyte, and the  $O_2$  is transported to the catalyst via the liquid phase, the wetting problem does not occur. This enables a better distinction between physical and chemical parameters.

Experiments were conducted with 20 weight %,  $H_2Pc$ ,  $CoPc$ , and  $FePc$  (Eastman Kodak), and  $H_2TAA$  and  $CoTAA$ , kindly provided by Professor Wiesener (Technische

Universität, Dresden). Two supports were used: Norit BRX and P33, the latter also provided by Professor Wiesener. The impregnation of the carbon was realized by dissolving 10 mg of the corresponding chelate in 20 ml tetrahydrofuran (THF), adding 40 mg of carbon support, followed by refluxing and stirring for 30 minutes. Thereafter, the catalysts were pyrolyzed in  $N_2$  at temperatures ranging from 400–1200°C. In general, the catalysts were heated to the desired pyrolysis temperature in one hour, maintained at this temperature for four hours and slowly cooled to room temperature. In a few cases, the pyrolysis was done in Ar. The pyrolyzed catalysts were ground in an agate mortar and 0.25 mg was attached to the gold disc ( $0.5 \text{ cm}^2$ ) of a RRDE (Au disc, Pt ring,  $N = 0.23$ ) via incorporation in a polypyrrole film according to the described procedure. The electrochemical experiments were conducted in a standard three-compartment electrochemical cell, filled with 150 ml  $O_2$  saturated  $0.5 \text{ M H}_2\text{SO}_4$ . The  $O_2$  reduction was measured at 20°C by scanning the potential from 1000 to 200 mV versus RHE with  $10 \text{ mV s}^{-1}$ , at a rotation frequency of  $9 \text{ s}^{-1}$ . The disc current was corrected for the high capacitive polypyrrole background current<sup>21</sup>.

Since the number of active sites is perhaps the most important parameter determining the reduction capability, Norit BRX electrodes were prepared containing 1–50 weight % CoPc. Finally, to allow a reasonable comparison, the "intrinsic catalytic activity" (turnover number) was measured of both CoPc and CoTAA, adsorbed on a pyrolytic graphite (Cp) disc ( $S = 0.5 \text{ cm}^2$ ,  $N = 0.27$ ) at monolayer coverage.

#### 10.4 Results

In the figures 10.1 and 10.2 results in  $0.5 \text{ M H}_2\text{SO}_4$  for 20% CoPc, FePc and  $H_2$ Pc supported on Norit BRX are depicted as a function of pyrolysis temperature. As previously reported<sup>21</sup>, the pure diffusion-limited currents ( $750 \mu\text{A}$  at  $9 \text{ s}^{-1}$  for  $O_2 \rightarrow H_2O_2$ ) are not reached since a fraction of the electrode is not covered with carbon particles. The activity of CoPc increases up to a treating temperature of 600°C; at higher temperatures, however, degradation of the catalyst occurs with loss of performance. This activity increase is accompanied by a decrease in the amount of peroxide formed, caused by electrochemical reduction or chemical decomposition of the  $H_2O_2$ . The activity of FePc increases slightly up to 600°C; at higher temperatures a very rapid degradation occurs, so FePc seems to be less resistant against heat treatment

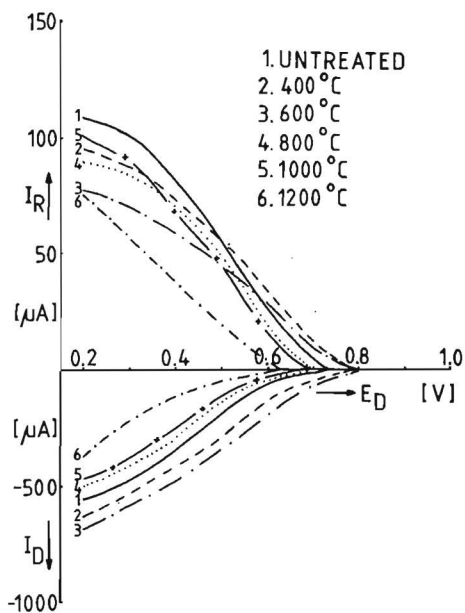


Fig. 10.1.  $O_2$  reduction in  $0.5\text{ M H}_2\text{SO}_4$  at  $f = 9\text{ s}^{-1}$  on  $20\%$   $\text{CoPc/BRX}$ , as a function of pyrolysis temperature.

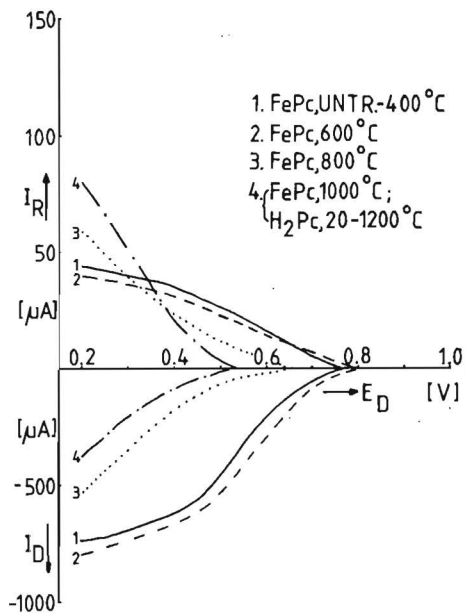


Fig. 10.2.  $O_2$  reduction in  $0.5\text{ M H}_2\text{SO}_4$  at  $f = 9\text{ s}^{-1}$  on  $20\%$   $\text{FePc/BRX}$  and  $20\%$   $\text{H}_2\text{Pc/BRX}$  as a function of pyrolysis temperature.

than  $\text{CoPc}$ . Another conclusion that can be drawn from Fig. 10.2 is that the activity of  $\text{H}_2\text{Pc}$  does not increase after pyrolysis, not even at high temperature. This is in contrast with results of Wiesener et al., who claim that with  $\text{H}_2\text{TAA}$ , pyrolyzed at  $950^\circ\text{C}$  the same catalyst is formed as with  $\text{CoTAA}$  at  $650^\circ\text{C}$ . To investigate this discrepancy, catalysts were prepared ( $20$  weight %) of  $\text{CoTAA}$ ,  $\text{CoPc}$ ,  $\text{H}_2\text{TAA}$  and  $\text{H}_2\text{Pc}$ , both on P33 carbon and Norit BRX. The cobalt-containing catalysts were pyrolyzed at  $650^\circ\text{C}$ , the metal-free ones at  $950^\circ\text{C}$ . The pyrolysis was carried out both in  $\text{N}_2$  and  $\text{Ar}$ , but no differences were observed within the error of the measurement. The results for  $\text{CoTAA}$  are presented in figure 10.3. It is clear that unpyrolyzed  $\text{CoTAA}$  is already very active; contrary to  $\text{CoPc}$  the reduction also proceeds to water in the studied potential range. Both activity and selectivity are influenced by the carbon support: especially the peroxide elimination is improved with Norit BRX as compared to P33. It is surprising that the disc current decreases after pyrolysis, probably caused by a decrease in the number of active sites. The

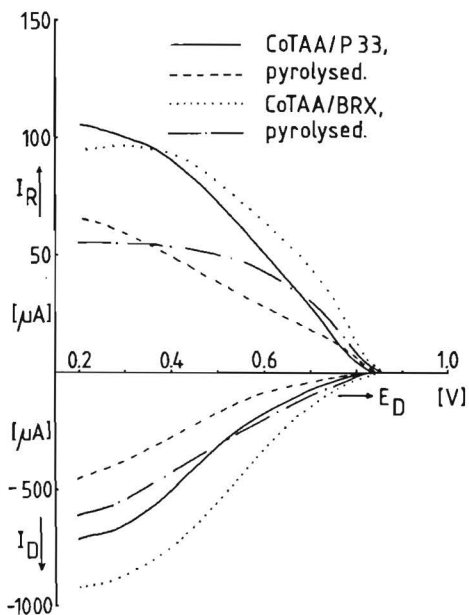


Fig. 10.3.  $O_2$  reduction in  $0.5\text{ M H}_2\text{SO}_4$  at  $f = 9\text{ s}^{-1}$  on 20% CoTAA/P33 and 20% CoTAA/BRX, both unpyrolyzed and pyrolyzed at  $650^\circ\text{C}$ .

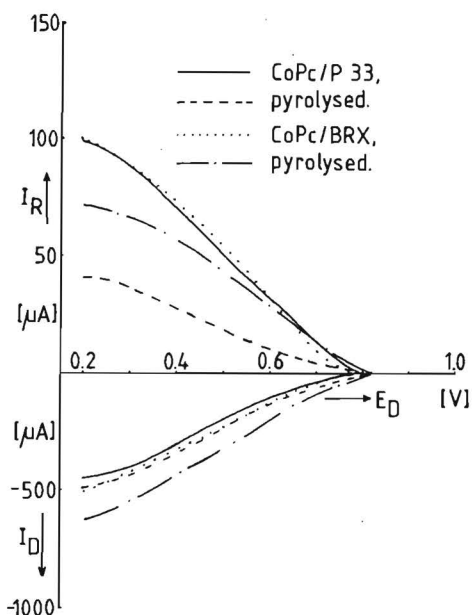


Fig. 10.4.  $O_2$  reduction in  $0.5\text{ M H}_2\text{SO}_4$  at  $f = 9\text{ s}^{-1}$  on 20% CoPc/P33 and 20% CoPc/BRX, both unpyrolyzed and pyrolyzed at  $650^\circ\text{C}$ .

ring current, however, indicates that the selectivity has increased. The behaviour of CoPc on these carbons is quite different (Fig. 10.4). On both supports disc and ring currents, respectively increase and decrease, showing an increased activity and selectivity after pyrolysis.

The results with  $H_2TAA$  (Fig. 10.5) show that although a slight increase in activity has occurred, by no means the same catalyst is formed as with pyrolyzed CoTAA.

The better performance of carbon-supported CoTAA as compared with CoPc can be attributed to a higher intrinsic catalytic activity of CoTAA. This is illustrated in Fig. 10.6. The reduction of  $O_2$  was measured in  $0.5\text{ M H}_2\text{SO}_4$  at CoTAA and CoPc, adsorbed as monolayer on pyrolytic graphite (Cp). The electrodes were prepared by dipping a freshly polished Cp electrode in a  $10^{-3}\text{ M}$  pyridine solution of CoTAA and CoPc, respectively. Electrochemical characterization in dioxygen-free  $1\text{ M KOH}$  yielded redox peaks corresponding with

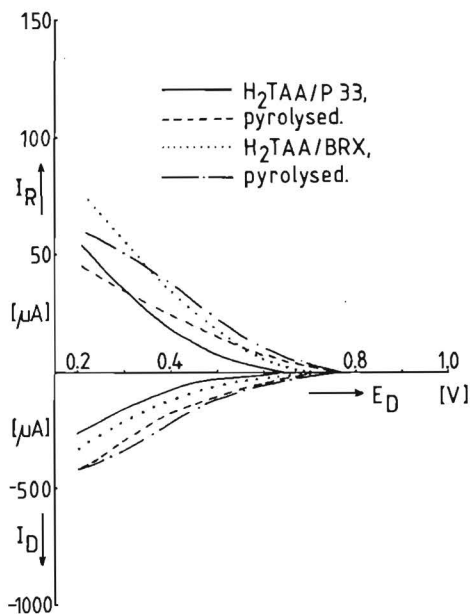


Fig. 10.5.  $O_2$  reduction in  $0.5\text{ M H}_2\text{SO}_4$  at  $f = 9\text{ s}^{-1}$  on 20%  $H_2TAA/P33$  and 20%  $H_2TAA/BRX$ , both unpyrolyzed and pyrolyzed at  $950^\circ\text{C}$ .

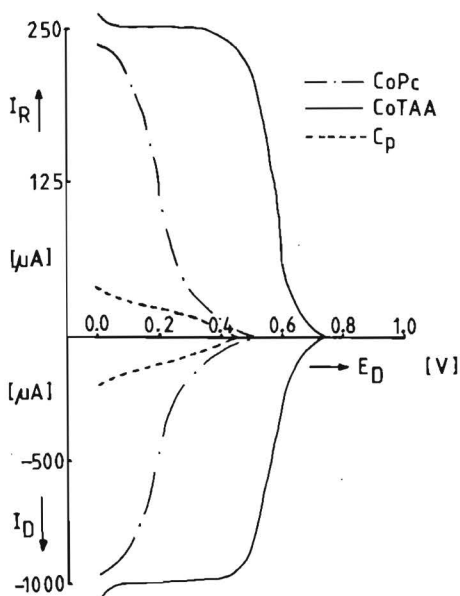


Fig. 10.6.  $O_2$  reduction in  $0.5\text{ M H}_2\text{SO}_4$  at  $f = 16\text{ s}^{-1}$  on CoPc and CoTAA, adsorbed at monolayer coverage on pyrolytic graphite Cp.

$2.3 \cdot 10^{-10}$  and  $2.6 \cdot 10^{-10}\text{ mol cm}^{-2}$  for CoTAA and CoPc, respectively<sup>21</sup> (chapter 6). The  $E_{1/2}$  for the  $O_2$  reduction is about 370 mV more anodic for CoTAA. Both at CoTAA and CoPc the reduction proceeds to  $H_2O_2$  exclusively, since  $N = 0.27$ . In this case pure diffusion-limited currents ( $1000\text{ }\mu\text{A}$  at  $16\text{ s}^{-1}$  for  $O_2 \rightarrow H_2O_2$ ) are obtained since the whole surface is electrochemically active. Figure 10.6 proves again that results with different chelates, supported on different carbons are difficult to compare with each other due to differences in intrinsic catalytic activities themselves.

The effect of the total amount of catalyst present on the disc on the obtained disc and ring current was investigated by varying the weight % CoPc on Norit BRX from 1-50. The results (Fig. 10.7) show that increasing the number of sites, shifts the  $E_{1/2}$  in anodic direction. In fact this behaviour looks similar to the observed improvement of CoPc/BRX due to pyrolysis, i.e. the increase in the disc current after pyrolysis can be caused by an increment in

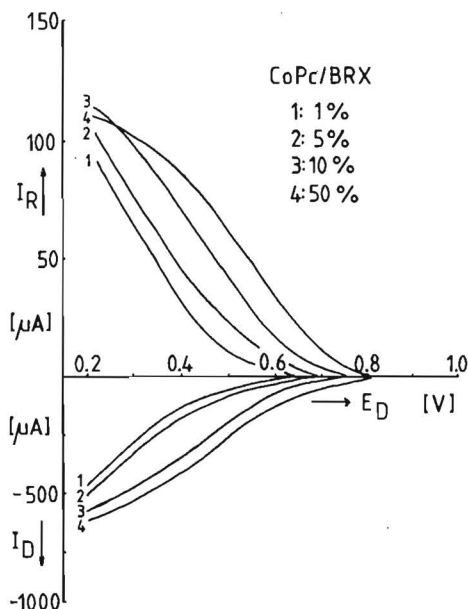


Fig. 10.7.  $O_2$  reduction in  $0.5\text{ M H}_2\text{SO}_4$  at  $f = 9\text{ s}^{-1}$  on CoPc/BRX as a function of the CoPc loading (weight %).

the number of available active sites. Another phenomenon is the fact that at high loadings the peroxide elimination is accelerated. From figure 10.6 it can be seen that CoPc and CoTAA, adsorbed on monolayer level do not reduce or decompose  $H_2O_2$ ; however, porous systems with high loadings in good electrical contact are indeed able to accomplish this in the studied potential range.

### 10.5 Discussion

A literature survey, and our own results indicate that the activity and the pyrolysis behaviour of carbon-supported transition metal chelates is determined by various factors, such as the chelate under consideration, the texture of the carbon support, the dispersion of the catalyst over the support, the kinetics of the pyrolysis reactions, etc. These factors are both of chemical and physical nature. Relevant conclusions about what happens with the catalyst itself can only be drawn if this distinction can be made. Gas-diffusion electrodes are not suited for this purpose; the modified RRDE electrode described in this paper is better in this respect, however, the distinction remains difficult. Nevertheless, some general conclusions can be drawn: The central metal atom is the active site with unpyrolyzed catalysts. This is also the case after pyrolysis since the activity of metal-free chelates hardly



increases. Our measurements do not confirm the theory of Wiesener et al.: at 950°C, pyrolyzed H<sub>2</sub>TAA/P33 did by no means approach the activity of CoTAA/P33, pyrolyzed at 650°C. All pyrolyzed catalysts show an increased peroxide elimination; the changes in activity are more difficult to interpret.

During the heat treatment, the following processes can take place:

- migration of chelates over the carbon surface<sup>22</sup>,
- reaction of the outer fringes of the organic skeleton of the chelate with the support, the central metal-N<sub>4</sub> unit remaining intact,
- decomposition of the chelate giving β-Co or cobalt oxides after contact with air. It is unlikely that these metal-only species are the new active sites in acid medium since the pyrolysis of carbon, impregnated with cobalt acetate only, does not lead to an enhanced activity.

All these processes have their own kinetics with their own temperature dependence and the condition of the pyrolyzed catalyst is determined by the relative rate of these processes at the given pyrolysis temperature. At high temperature the decomposition dominates, but this decomposition also seems to occur at lower temperatures, where the pyrolysis still has a beneficial effect on the activity. Based on the above described arguments, we come to the following model: Starting with the unmodified carbon support, a large available surface area is present which, however, has a very low activity towards O<sub>2</sub> reduction. Impregnation with chelates has two opposing effects regarding the activity. The O<sub>2</sub> reduction is enhanced due to the presence of the catalyst, but also the pore system is partially blocked resulting in a lower effective surface area. To which amount the pores are blocked depends on the catalyst loading, the size of the molecules themselves, and the impregnation method, i.e. whether the catalyst is already dispersed or present in the form of aggregates. With increasing pyrolysis temperature diffusion of the chelates and (partial) decomposition starts to occur. These processes again have an opposing effect on the activity: a more random dispersion will increase the number of available active sites; moreover, the accessibility of the pore system as compared to the unmodified carbon is restored. Of course, decomposition decreases the activity. The actual pyrolysis temperature determines which effect predominates. If the temperature is too high, decomposition overrides the improved dispersion: the number of active sites even decreases compared to the unpyrolyzed material.

Another effect is the reaction of the outer fringes of the organic skeleton with the support. As long as the Me-N<sub>4</sub> unit remains intact, the activity is

preserved: by this reaction, the improved dispersion obtained during the heat treatment is retained after cooling to room temperature. This reaction is probably responsible for the improved peroxide elimination, lowering the  $H_2O_2$  concentration in the pore system. Also, since the most reactive parts of the molecule have already reacted, the catalyst is less sensitive for irreversible oxidation caused by (peroxide) intermediates, formed during the  $O_2$  reduction.

With this model, the observed results can be explained: pyrolysis of FePc virtually does not enhance the activity since the stability of FePc is relatively low: degradation already occurs at relatively low temperature. CoPc is better in this respect, leading to an increased activity.  $H_2Pc$  remains unactive since a transition metal ion is essential for the catalysis. The high activity of CoTAA compared to CoPc is due to the higher intrinsic activity of CoTAA itself and, for a smaller part, to the fact that with the same loading in weight % more catalyst molecules are present in the case of CoTAA due to the difference in molecular weight (345 vs. 572). Moreover we expect CoTAA to yield better dispersions than CoPc since the molecule is much smaller, penetrating more easily in the pore system of the support. This also provides an explanation for the decrease in the disc current after pyrolysis of CoTAA. Already at room temperature an excellent dispersion is obtained: pyrolysis does not improve this dispersion. Some molecules react with the support, increasing the peroxide elimination; other decompose and loose their activity. The net effect is a decrease in disc current accompanied by an increase in selectivity. Perhaps some molecules sublime from the carbon support due to the relatively high vapour pressure of CoTAA compared to CoPc. This possibility was checked by performing the pyrolysis in a small sealed quartz tube filled with  $N_2$  at atmospheric pressure. Sublimation should, if not prevented at all, at least be reduced. These experiments, however, gave virtually the same results for both CoTAA and  $H_2TAA$  on P33 carbon, as when the pyrolysis was carried out in a flowing  $N_2$  stream. It should be noted that also the measurements of Gruenig<sup>20</sup>, showing the change in BET surface area as a function of pyrolysis temperature are inexplicable if sublimation is occurring. After pyrolysis, the original BET surface area of the P33 carbon is restored. This happens at a lower temperature for CoTAA than for the more volatile  $H_2TAA$ . If sublimation was occurring, the reverse behaviour would have been observed.

## 10.6 References

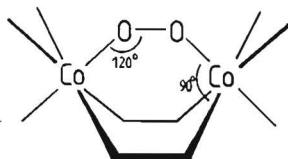
1. H. Jahnke, M. Schönborn, G. Zimmermann, *Katalyse an Phthalocyaninen*. Ed. H. Kropf, F. Steinbach. Georg Thieme Verlag, Stuttgart (1973) p.71.
2. R. Holze, D. Scherson, D. Tryk, S. Gupta and E. Yeager, *ISE Meeting 1984, Berkeley USA (1984)* 399.
3. J.A.R. van Veen, J.F. van Baar, K.J. Kroese, *J. Chem. Soc., Faraday Trans. 1*, 77 (1981) 2827.
4. K. Okabayashi, O. Ikeda, H. Tamura, *Chem. Lett.* (1982) 1659.
5. V.S. Bagotskii, M.R. Tarasevich, O.A. Levina, K.A. Radyushkina and S.I. Andruseva, *Dokl. Akad. Nauk SSSR* 233 (1977) 889.
6. A. Fuhrmann, K. Wiesener, I. Iliev, S. Gamburtsev and A. Kaisheva, *J. Power Sources* 6 (1981) 69.
7. A. Kaisheva, S. Gamburtsev, I. Iliev, *Elektrokhimiya* 18 (1982) 139.
8. R.W. Joyner, J.A.R. van Veen, W.H.M. Sachtler, *J. Chem. Soc., Faraday Trans. 1*, 78 (1982) 1021.
9. D.A. Scherson, S.L. Gupta, C. Fierro, E.B. Yeager, M.E. Kordesch, J. Eldridge, R.W. Hoffman and J. Blue, *Electrochim. Acta* 28 (1983) 1205.
10. A. Abelleira, F. Kulik, F. Walsh, *ISE Meeting 1984, Berkeley USA (1984)* 396.
11. G. Gruenig, K. Wiesener, S. Gamburtsev, I. Iliev and A. Kaisheva, *J. Electroanal. Chem.* 159 (1983) 155.
12. S. Gamburtsev, I. Iliev, A. Kaisheva, *Elektrokhimiya* 19 (1983) 1261.
13. G. Gruenig, K. Wiesener, A. Kaisheva, S. Gamburtsev and I. Iliev, *Elektrokhimiya* 19 (1983) 1571.
14. K. Wiesener, *Elektrokhimiya* 18 (1982) 758.
15. J.A.R. van Veen, H.A. Colijn, *Ber. Bunsenges. Phys Chem.* 85 (1981) 700.
16. D.M. Drazic, Z.V. Ledinski, S.K. Zecevic, *J. Appl. Electrochem.* 13 (1983) 337.
17. O. Ikeda, H. Fukuda, H. Tamura, *J. Chem. Soc., Chem. Comm.* (1984) 567.
18. H.P. Dhar, R. Darby, V.Y. Young and R.E. White, *Electrochim. Acta* 30 (1985) 423.
19. S. Gamburtsev, G. Gruenig, A. Kaisheva, I. Iliev and K. Wiesener, *Elektrokhimiya* 20 (1984) 500.
20. G. Gruenig, *Thesis, Dresden (1983)*.
21. A. van der Putten, W. Visscher, E. Barendrecht, *J. Electroanal. Chem.* 195 (1985) 63 (chapter 9 of this thesis).
22. A. Mongilardi-Mativet, *These, Université de Haute-Alsace (1981)*.

## Chapter 11 Concluding remarks and outlines for future research

The work described in this thesis has shown that the determination of the activity of transition metal chelates for the reduction of  $O_2$  should be performed on electrode systems which allow a characterization in both qualitative and quantitative sense, and for which the mass-transport properties are well defined. In that way, the catalytic activity per site (turnover number) can be calculated, which is the best indication for the activity of an electrocatalyst. This can be done with a pyrolytic graphite (Cp) rotating disc electrode onto which the macrocycles are irreversibly adsorbed. The Cp is inert towards  $O_2$  reduction, has a low double-layer current which facilitates the characterization of the electrode, and very well resembles the carbon support which is used for the production of commercial gas-diffusion electrodes. The redox potentials of the chelates can be measured in the same solution in which the  $O_2$  reduction is studied.

Chapter 6 has shown that a clear relation exists between these redox potentials as a function of the pH, and the obtained activity. In practice, however, the pH of the fuel-cell electrolyte is set and the "fine-tuning" of the redox potential has to be achieved in another way. A comparison between CoPc and CoTAA has shown that a change in the ligand can shift the redox potential of the Co as much as 400 mV. An interesting study would be the effect of size and shape of the  $N_4$  cage on the redox potential. In this respect also the effect of electron-donating or electron-accepting side groups on the redox potential would be of interest. These results might lead to the construction of Hammett plots<sup>1</sup>, with which the effect of different side groups on the redox potential can be predicted. Work of this kind has been done in the early seventies using gas-diffusion electrodes. As pointed out in chapter 6, this electrode system is not suitable for studies of this type. Also with respect to the selectivity of the reaction, it is of interest to investigate the possibility of synthesizing dinuclear planar Co chelates with different Co-Co distances, allowing the optimization of this distance. Since also the value of the redox potential of the Co atoms seems to be crucial in order to get  $4e^-$  reduction of  $O_2$  to water, the effect of electron-donating or electron-accepting side groups is also relevant. Another interesting point in this connection is the rigidity of the ligand. The cobalt atoms will try to achieve an octahedral configuration, while the Co-O-O bond angles should be  $120^\circ$ <sup>2</sup>. In the case of  $Co_2(dpt)_2Cl_2$ , where the ligands are rigid,

these two conditions cannot be fulfilled simultaneously. The formed  $O_2$  adduct will therefore be somewhat distorted. How this affects the magnitude of the interaction of dioxygen with the electrocatalyst is yet unclear. In principle, both conditions can be fulfilled on a chelate with the following structure:



In this type of chelate the nitrogen atoms between the Co centres must have  $sp^3$  hybridization to allow the bending of the Co-N-N bond, leading to a high degree of saturation of the ligand. In the case of mononuclear chelates, however, saturation of the ligand results in a very low activity. More information about the proposed dimeric mechanism with FePc could be obtained by studying such Fe chelates, with which the formation of dimeric  $O_2$  adducts is impossible due to steric hindrance, e.g. the picket-fence porphyrins of Collman<sup>3</sup>. With such chelates the prewave that is observed in the case of FePc in alkaline solution should disappear. Also the construction of a Pt ring/basal plane of stress annealed pyrolytic graphite disc is of interest since the disc material approximates to a carbon single crystal surface, possibly preventing the formation of dimeric adducts on the surface. The question how the chelates are oriented on the graphite surface is still a matter of debate, despite a number of investigations with sophisticated spectroscopic techniques. Recently some evidence was presented that the molecules lie parallel to the surface<sup>4</sup>. Perhaps the application of new techniques such as electron tunnelling microscopy<sup>5</sup> might provide an answer. For the application of transition metal chelates as  $O_2$  reduction catalysts, the dispersion of the catalyst over the carbon support is very important. Most chelates which have a strong tendency to aggregate which leads to poor dispersions of the catalyst and a correspondingly low number of active sites. Therefore solvent properties of chelates should be considered as well, and also properties such as the size of the catalyst molecules. The higher the solubility of a catalyst and the smaller the size of the molecule, the better is the dispersion that can be obtained. This will also depend on the texture of the used carbon support. Unfortunately, a reliable method for the determination of the catalyst dispersion is still lacking. With respect to the effect of pyrolysis on carbon-supported transition metal chelates, the crucial question is whether the  $CoN_4$  units are retained after

the pyrolysis. Although the electrochemical results, described in this thesis provide some evidence that this is indeed the case, the real proof should be spectroscopic. The ideal method to solve this question seems to be EXAFS which, however, is not a routine technique yet. The activity enhancement due to pyrolysis is also related to the formation of a better dispersion, but during this process also some decomposition of the catalyst occurs. Perhaps the optimum catalyst is a carbon support whose entire pore system is covered with a monolayer of  $\text{CoN}_4$  units, chemically bonded to this support. Such a system will have a maximum number of active sites with a minimum decline in mass-transport properties, as compared to the unmodified support. Whether transition metal chelates will be used for the production of commercial electrodes is yet uncertain. Compared with the commonly applied Pt, the activity of transition metal chelates is high enough in alkaline solution. The turnover number and selectivity of FePc in alkaline solution is even superior to those of Pt. This changes going to acid solution, since the reduction of  $\text{O}_2$  on Pt is pH dependent, contrary to most chelates. This leads to poorer results for macrocycles in acid solution.

An important advantage of chelates, besides their low price and high availability, is their insensitivity to (organic) electrolyte impurities. Contrary to Pt<sup>6</sup>, the presence of these impurities does not lead to poisoning of the electrocatalyst in the case of transition metal chelates.

Although in this work the stability of transition metal chelates was not tested under practical conditions (i.e. in a gas-diffusion electrode configuration), also RRDE data provide some information about this stability. This is caused by the high turnover numbers that are achieved in the case of irreversibly adsorbed monolayers (in the order of  $100 \text{ s}^{-1}$ , compared to ca.  $10^{-4} \text{ s}^{-1}$  with gas-diffusion electrodes). The results indicate that cobalt chelates are much more stable than their corresponding iron analogues. The stability of both compounds rapidly goes down with decreasing pH.

Based on these considerations, cobalt-containing chelates certainly have possibilities as electrocatalysts for the reduction of dioxygen in alkaline fuel cells. In this electrolyte, a performance comparable to Pt can be obtained. Application in acid fuel cells might be possible if organic fuels are considered. Compared to Pt, however, a considerable decrease in performance has to be taken into account.

## References

1. L.P. Hammett, Chem. Revs. 17 (1935) 225.
2. Professor J. Reedijk, personal communication.
3. J.P. Collman, T.R. Halpert and K.S. Suslick in "Metal ion activation of dioxygen", edited by T.G. Spiro, Wiley (1980).
4. J.J. McMahon, S. Baer and C.A. Melendres, J. Phys. Chem. 90 (1986) 1572.
5. H.Y. Liu, F.R. Fan, C.W. Lin and A.J. Bard, J. Am. Chem. Soc. 108 (1986) 3838.
6. "Assessment of Research Needs for Advanced Fuel Cells", U.S. Department of Energy Advanced Fuel Cell Working Group, 1984-85, edited by S.S. Penner. Also published as Energy 11 (1986) 1.

### Acknowledgements

The author wishes to thank Prof. Wiesener (Technische Universität Dresden) for providing CoTAA, H<sub>2</sub>TAA and P33 carbon; Rob Prins (State University of Leiden) for providing the planar dicobalt chelate; Norit Research NV for providing samples of different active carbons, and the Department of Physical Chemistry for the use of their ovens.



## Symbols

C	concentration	$\text{mol l}^{-1}$
D	diffusion coefficient	$\text{cm}^2 \text{s}^{-1}$
E	potential	V
F	Faraday constant	$\text{C mol}^{-1}$
f	frequency	$\text{s}^{-1}$
I	current	A
i	current density	$\text{A cm}^{-2}$
k	rate constant	$\text{cm s}^{-1}$
N	collection efficiency	-
n	number of electrons	-
S	spin quantum number	-
R	gas constant	$\text{J K}^{-1} \text{mol}^{-1}$
T	temperature	K
$\alpha$	transfer coefficient	-
$\eta$	overvoltage ( $E - E_{\text{eq}}$ )	V
$\nu$	kinematic viscosity	$\text{cm}^2 \text{s}^{-1}$
$\omega$	rotation frequency	$\text{rad s}^{-1}$

## Superscripts

s	bulk
$\sigma$	surface

## Subscripts

a	anodic
c	cathodic
D	disc
d	diffusion
eq	equilibrium
L	diffusion limited
ox	oxidized form
p	peak
R	ring
red	reduced form
o	under standard conditions
$\frac{1}{2}$	half-wave

## Abbreviations

BET	Brunauer Emmett Teller
CE	counter electrode
C <sub>P</sub>	pyrolytic graphite
DTA/TG	differential thermal/thermogravimetric analysis
ESCA	electron spectroscopy for chemical analysis
ESR	electron spin resonance
EXAFS	extended X-ray absorption fine structure
IR	infrared
MS	mass spectroscopy
NHE	normal hydrogen electrode
PP	polypyrrole
Pc	phthalocyanine
RE	reference electrode
RHE	reversible hydrogen electrode
RRDE	rotating ring-disc electrode
SCE	saturated calomel electrode
TAA	tetraazaannulene
TBP	tetrabenzoporphyrin
TEM	transmission electron microscopy
THF	tetrahydrofuran
TMPP	tetramethoxyphenylporphyrin
TPP	tetraphenylporphyrin
TRPP	tetra(p-substituent)phenylporphyrin
TSPc	tetrasulfonated phthalocyanine
UV-VIS	ultra-violet/visable
WE	working electrode
XPS	X-ray photoelectron spectroscopy

## Summary

The reduction of dioxygen is of interest for the development of fuel cells. Since this reduction is a slow reaction, its rate has to be increased using suitable electrocatalysts. Transition metal chelates are efficient alternatives for the commonly applied platinum.

A study of the literature (chapter 2) showed that the reported results are to a large extent influenced by the applied electrode-preparation method, and their corresponding mass-transport behaviour. In the present work, the electrocatalytic properties such as activity, selectivity and stability of a number of chelates are investigated under well-defined mass-transport conditions. This can be realized with the rotating ring-disc electrode technique (chapter 3). A number of different electrode preparation methods such as irreversible adsorption, vacuum deposition, impregnation of porous carbon, evaporation of the solvent and incorporation into a conducting polymer film, were compared. All electrode systems are characterized with cyclic voltammetry in  $O_2$ -free solution. It is found that the number of active sites can widely differ from the number of catalyst molecules present. An equation was derived for the relation between the halfwave potential  $E_{1/2}$  and the number of active sites (chapter 4).

A comparison between vacuum-deposited films and irreversibly adsorbed monolayers of iron- and cobalt phthalocyanine (FePc and CoPc) indicates that with vacuum-deposited films only a very small fraction of the film is electrochemically active (chapter 5). For the study of the electrocatalytic properties of chelates, irreversibly adsorbed monolayers are recommended since their characterization results in distinct redox peaks. With this system the redox potentials  $E_p$  of FePc, CoPc and CoTAA (cobalt tetraazaannulene) were measured as a function of the solution pH, as well as  $E_{1/2}$  for the reduction of dioxygen under the same conditions (chapter 6). In acid solution there is a clear correlation between  $E_p$  and  $E_{1/2}$ . This changes going to alkaline solution. In this electrolyte, the reduction is highly reversible so the value of  $E_p$  is less important.

The selectivity of the reaction has been investigated by studying the reduction of  $O_2$  on a planar dicobalt chelate (chapter 7). Like dicofacial dicobalt porphyrins, this chelate allows the bridging coordination of  $O_2$ . Compared to the dicofacial dicobalt porphyrins, however, the planar chelate displays reversed selectivity with respect to the solution pH. In alkaline

solution,  $O_2$  is reduced to water; in acid solution hydrogen peroxide is formed. A qualitative explanation for this observation with the aid of the "increased valence theory" is presented in chapter 8. Besides bridging coordination, the electronegativity of the adsorbed dioxygen molecule has to be increased in order to split the O-O bond. In acid solution this is achieved via protonation of the adsorbed  $O_2$  molecule; in alkaline solution via reduction of the cobalt centres.

The research for improving the stability has been focussed on the effect of pyrolysis on carbon-supported transition metal chelates. There is no consensus in the literature why this treatment not only improves the stability but also the activity. In order to study the  $O_2$  reduction on carbon-supported transition metal chelates with the rotating ring-disc technique, a method was developed to attach the carbon particles to the disc of such an electrode. This was achieved by incorporating the carbon particles into a conductive polypyrrole film (chapter 9). With this method, the effect of pyrolysis was studied on CoPc, FePc and CoTAA and their metal-free analogues, deposited on Norit BRX (chapter 10). Both activity and selectivity pass through a maximum as a function of pyrolysis temperature. This behaviour is explained with a model in which the migration of the chelate molecules over the support, reaction of the outer fringes of the organic skeleton with the support, and total degradation of the catalyst, with loss of activity, has been taken into account.

Finally, in chapter 11 some concluding remarks and suggestions for future research are presented. It is concluded that there is still room for improving the electrocatalytic properties of transition metal chelates. An advantage of these catalysts is their insensitivity to solution impurities. For stability reasons, as yet their application seems to be limited to cobalt chelates in alkaline solution.

## Samenvatting

De reductie van zuurstof is een belangrijke reactie voor de ontwikkeling van brandstofcellen. Aangezien deze reductie in het algemeen traag verloopt, moet de snelheid van deze reactie met behulp van elektrokatalysatoren worden verhoogd. Overgangsmetaalchelaten zijn geschikte alternatieven voor het gewoonlijk hiervoor toegepaste platina.

Een kritische studie van de literatuur (hoofdstuk 2) laat zien dat de gepubliceerde resultaten voor een belangrijk deel worden bepaald door de gebruikte bereidingswijze van de elektroden, en de daarmee samenhangende massatransporteigenschappen. In dit proefschrift wordt een onderzoek beschreven naar de activiteit, selectiviteit en stabiliteit van een aantal chelaten, waarbij het massatransport goed is gedefinieerd. Dit is gerealiseerd door gebruik te maken van de roterende ring-schijf-elektrodeteknik (hoofdstuk 3). Een aantal verschillende bereidingswijzen van de elektroden, zoals irreversibele adsorptie, opdampen, impregneren van poreuze kool, verdampen van het oplosmiddel en inbouw in een geleidend polymeer, is met elkaar vergeleken. Alle elektrodesystemen zijn gekarakteriseerd met behulp van cyclische voltammetrie in zuurstofvrije oplossing. Gevonden is dat het aantal actieve sites sterk kan afwijken van het aantal aanwezige katalysatormolekulen. Er is een relatie afgeleid tussen de halfwaarde potentiaal  $E_{1/2}$  en het aantal actieve sites (hoofdstuk 4).

Uit een vergelijking tussen dikke opgedampte lagen van ijzer- en kobaltftalocyanine (FePc en CoPc), en irreversibel geadsorbeerde monolagen van deze complexen, komt naar voren dat bij de opgedampte lagen slechts een zeer gering gedeelte van de film elektrochemisch actief is (hoofdstuk 5); voor de studie van de elektrokatalytische eigenschappen van chelaten zijn irreversibel geadsorbeerde monolagen het meest geschikt, omdat de karakterisering van deze elektroden resulteert in scherpe redoxpieken.

Met behulp van dit systeem zijn de redoxpotentialen  $E_p$  van FePc, CoPc en CoTAA (kobalttetraazaannuleen) gemeten als functie van de pH, alsmede  $E_{1/2}$  voor de zuurstofreductie onder dezelfde condities (hoofdstuk 6). In zuur milieu bestaat er een duidelijk korrelatie tussen  $E_p$  en  $E_{1/2}$ . Dit verandert bij hogere pH: onder die omstandigheden is de reductie dermate reversibel dat de waarde van  $E_p$  er minder toe doet.

De selectiviteit van de reactie is onderzocht aan een vlak dikobaltchelaat (hoofdstuk 7). Net als bij dicofaciale dikobaltporfyrienes, kan aan dit molekuul brugadsorptie van  $O_2$  optreden. Vergeleken met de dicofaciale dikobalt-

chelaten vertoont het vlakke dikobaltchelaat een omgekeerde selektiviteit met betrekking tot de pH van het elektrolyt. In alkalisch milieu treedt reductie tot water op; in zuur milieu wordt waterstofperoxyde gevormd. Een kwalitatieve verklaring voor deze waarnemingen met behulp van de "increased valence" theorie is weergegeven in hoofdstuk 8. Naast brugadsorptie moet de elektronegativiteit van het geadsorbeerde zuurstofmolekuul worden verhoogd om splitsing van de O-O binding mogelijk te maken. In zuur milieu gebeurt dit door protonering van het geadsorbeerde zuurstofmolekuul; in alkalisch milieu via reductie van de kobaltatomen.

Het onderzoek met betrekking tot de verbetering van de stabiliteit heeft zich de laatste jaren toegespitst op het effect van pyrolyse op koolgedragen overgangsmetaalchelaten. Tot op heden is er geen overeenstemming in de literatuur waarom deze behandeling niet alleen de stabiliteit, maar ook de activiteit verbetert. Om de zuurstofreductie aan koolgedragen chelaten te kunnen bestuderen met de roterende ring-schijf-elektrodeteknik, is eerst een methode ontwikkeld om de kooldeeltjes aan te brengen op de schijf van een dergelijke elektrode. Dit is verwezenlijkt door de kooldeeltjes in te bouwen in een geleidende polypyrroolfilm (hoofdstuk 9). Met behulp van deze techniek is het effect van de pyrolyse onderzocht op FePc, CoPc, CoTAA en hun metaalvrije derivaten, aangebracht op Norit BRX (hoofdstuk 10). Zowel de activiteit als de selektiviteit vertoont een maximum als functie van de pyrolysetemperatuur. Om dit gedrag te verklaren is een model ontwikkeld waarin rekening wordt gehouden met migratie van de chelaatmolekulen over de drager, reactie van het organische skelet met deze drager, en algehele ontleding van de katalysator onder verlies van de activiteit.

Dit proefschrift eindigt met een aantal slotopmerkingen en suggesties voor verder onderzoek (hoofdstuk 11). Hieruit blijkt dat er nog ruimte is voor verbetering van de elektrokatalytische eigenschappen van overgangsmetaalchelaten. Een voordeel van deze katalysatoren ten opzichte van platina is hun ongevoeligheid voor verontreinigingen in het elektrolyt. Vanwege stabiliteitsredenen lijken de mogelijkheden voor toepassing vooralsnog beperkt tot kobaltchelaten in alkalisch milieu.

## Curriculum vitae

De schrijver van dit proefschrift is geboren op 24 augustus 1958 te Helmond. Na het behalen van het diploma Gymnasium B aan het Pauluslyceum te Tilburg, is hij in september 1976 begonnen met de studie Scheikundige Technologie aan de Technische Hogeschool Eindhoven. Het afstudeeronderzoek werd verricht bij de vakgroep Elektrochemie onder leiding van Professor E. Barendrecht. In januari 1983 behaalde hij het ingenieursexamen (cum laude). Per 1 februari 1983 is hij begonnen met een promotieonderzoek bij de vakgroep Elektrochemie, waarvan dit proefschrift het resultaat is. In 1985 kreeg hij voor dit werk een prijs van het "Professor Gelissen Fonds".

## Dankwoord

In de eerste plaats wil ik hier kamergenoot en kollega Bert Elzing bedanken. Beste Bert, onze samenwerking heeft mij geleerd dat werken in teamverband veel meer oplevert dan de som van de afzonderlijke delen. Zonder deze kruisbestuiving had dit proefschrift er anders uitgezien.

Prof. Barendrecht wil ik bedanken voor het opstarten van het onderzoek en de vrijheid van handelen die ik bij het uitvoeren ervan heb gekregen. In mijn ogen is deze vrijheid essentieel voor het opleiden van zelfstandige onderzoekers.

Wil Visscher wil ik bedanken voor haar rol als "drager". In deze beeldspraak vervul ik de rol van katalysator. De katalysator doet weliswaar het werk, maar zonder drager levert dit geen bruikbaar resultaat op. Jouw vermogen tot relativeren is voor mij een grote steun geweest.

Professor Dr. J. Reedijk wil ik bedanken voor het nauwgezet nakijken van het proefschrift.

Professor Dick Harcourt for the stimulating correspondence which resulted in chapter 8.

Het "Professor Gelissen Fonds" voor het mogelijk maken van een studiereis naar de USA: Prof. E. Yeager (Cleveland, Ohio), Prof. A. Bard (Austin, Texas), Dr. N. Vanderborgh (Los Alamos, New Mexico), Dr. P. Ross and Prof. E. Cairns (Berkeley, California) and Prof. F. Anson (Pasadena, California) for being so kind to allow a visit to their institutes.

San de Beer voor zijn adviezen met betrekking tot het gebruik van kool.

Bert Boeringa voor maken van de beste ring-schijf-elektrodesystemen ter wereld (ik heb in ieder geval nog geen betere gezien).

De glasblazerij voor de hoogwaardige en vooral snelle dienstverlening.

Netty Rijkema-Hölscher voor het nauwgezet en snel omzetten van het manuscript tot een voor iedereen leesbaar geheel.

Riek Bossong voor het opruimen van mijn broodkruimels.

De studenten Johan Dijkstra, Coert van Lare en Sik Nin Tang voor de door hen geleverde bijdrage gedurende het praktikum Elektrochemie.

Mijn (ex-)kamergenoten en de overige leden van de vakgroep voor de prettige werksfeer.

Alle familie, vrienden en bekenden die ertoe hebben bijgedragen dat de afgelopen vier jaar ook op het sociale vlak een leerzame periode was.

Tenslotte mijn racefiets voor het zonder protesteren omzetten van frustratie in snelheid als het allemaal eens wat minder ging.



## STELLINGEN

1. Voor gemodificeerde elektroden zijn "turnover numbers" een betere maat voor de activiteit van een elektrokatalysator dan de uitwisselingsstroomdichtheid.

Hoofdstuk 4 van dit proefschrift.

2. Een belangrijk voordeel van overgangsmetaalchelaten als elektrokatalysatoren voor de reductie van zuurstof is hun ongevoeligheid voor verontreinigingen in het elektrolyt.
3. De informatieve waarde van Koutecky-Levich plots wordt overschat.

J. Koutecky, V.G. Levich, Zh. Fiz. Khim. 32(1958)1565.

4. De door Randin uitgewerkte korrelatie tussen de zuurstof-reductieactiviteit van overgangsmetaalchelaten in waterige oplossing en hun redoxpotentialen, gemeten in niet-waterige media, is niet toegestaan.

J.-P. Randin, Elektrochim. Acta 19(1974)83;

Hoofdstuk 6 van dit proefschrift.

5. De door Pound et al. berekende theoretische celspanning van de nikkeloxyde-zink akku is onjuist, omdat voor de activiteit van het zinkaat een veel te lage waarde is aangenomen.

B. G. Pound, R.P. Singh, D.D. MacDonald, J. Power Sources 18(1986)1.

6. Bij het bestuderen van de zuurstofreductie met behulp van een roterende ring-schijfelektrode is kwantitatieve detectie van de gevormde waterstofperoxyde slechts mogelijk, wanneer van een geplatineerde ring gebruik wordt gemaakt. Ten onrechte wordt dit platineren door veel onderzoekers achterwege gelaten.

S.-M. Park, S. Ho, S. Aruliah, M.F. Weber, C.A. Ward, R.D. Venter  
S. Srinivasan, J. Electrochem. Soc. 133(1986)1641.

7. De opvatting van Duffield et al. dat het amalgameren van een zinkelektrode de reversibiliteit van dit systeem verhoogt doordat de aanwezigheid van kwik op het oppervlak de vorming van "kink sites" overbodig maakt, wordt niet bevestigd door hun experimentele resultaten.

A. Duffield, P.J. Mitchell, N.A. Hampson, N. Kumar, D.W. Shield,  
J. Power Sources 15(1985)93.

8. Een goede bewegwijzering voor fietsers vereist een eigen, duidelijk herkenbaar bordensysteem.

9. Door de toenemende invloed van het bedrijfsleven op het universitaire onderzoek dreigt de wetenschappelijke vrijheid van deze instellingen in gevaar te komen.

10. Voor het opleiden tot zelfstandig onderzoeker is de studiedruk in de huidige eerste fase van het universitaire onderwijs te hoog.

11. In tegenstelling tot de zuurstofreduktie in een brandstofcel is dit proces bij het uitoefenen van duursporten meestal niet de limiterende faktor.

Eindhoven, 19 december 1986

André van der Putten.